AN EXTREMELY LARGE YET ULTRALIGHTWEIGHT SPACE TELESCOPE AND ARRAY

Feasibility assessment of a new concept

May 29, 1999

NIAC Grant # 07600-006

Ivan Bekey
Bekey Designs, Inc.
46245 Quarter Charge Dr.
Annandale, VA 22003

AN EXTREMELY LARGE YET ULTRALIGHTWEIGHT SPACE TELESCOPE AND ARRAY

PHASE I FEASIBILITY ASSESSMENT OF A NEW CONCEPT

EXECUTIVE SUMMARY

This study has established the feasibility of a new and revolutionary concept for space telescopes based on the principle of replacing structures with information. The basic telescope concept embodies a powerful new principle for space systems: substitute information webs for structural webs. This capitalizes on the fundamental attributes of space in which mass is expensive while information and its processing is lightweight and cheap.

The telescope concept thus employs a flimsy membrane primary mirror that is neither inflated nor edge supported, and no truss structure whatever. It substitutes information-intensive means to adaptively shape the membrane and to stationkeep all the elements with a virtual truss. This adaptive shaping and virtual truss function with a number of closed loop adaptive systems to compensate for errors and disturbances, and deliver quality optical instrument performance.

This allows the development and deployment of a 25 meter aperture telescope whose total on-orbit weight is less than 150 Kg. and that can be packaged for launch aboard a Pegasus or smaller launch vehicle. The main features of the concept are:

1. A membrane primary mirror which is fully adaptive across its entire surface so that its figure is shaped by software commands, is unsupported and unstretched, composed of three layers: two piezoelectric films in a bimorph configuration, and one Nitinol film. The piezoelectric layers are actuated by an external scanning electron beam responsive to a downstream figure sensor so that both gross scale curvature and fine scale errors are corrected in closed loop.

2. A second stage of correction consisting of a liquid crystal driven by a sensor that determines the residual errors of the primary mirror and imposes a 2-dimensional pattern of time delays on the light reaching the focal array so as to cancel those residual errors. The liquid crystal is actuated in a direct-laser addressed mode operating on the thermal gradient principle, attaining 1-2 orders of magnitude greater correction capability than current crystals, yet maintaining fast response and low scattering losses.

3. An architecture for the telescope that has no truss structure, but rather stationkeeps the primary membrane, the electron beam assembly, the figure sensor, and the focal assembly on an axial configuration in space, with maximum separation between elements of 500 meters for a 25 meter primary aperture.

4. A formation flying metrology and control system which establishes and maintains this configuration, enabling repointing the telescope ensemble, which attains and maintains accuracies of 100 microns and 10 arc seconds relative to each other, well within the correction range of the liquid crystal and adaptive membrane.

5. Use of many MEMS FEEP thruster units distributed along the peripheries of all the telescope elements for translational and rotational control, with micronewtons trust so as to mostly avoid creating dynamic disturbances.

6. A means to rapidly steer the field of view of the telescope by many degrees without moving any of the four main elements, avoiding introducing disturbances. This consists of two auxiliary small mirrors near the focal Assembly which are rotated and translated for fast disturbance-free steering.

7. Means to package and deploy the membrane without introducing surface artifacts that would seriously degrade the telescope's optical performance.

Any number of ensembles of such 25-100 meter diameter telescopes can be operated as a giant coherent super-ensemble in which they combine the light on a common focal array. This super-ensemble can be operated as a coherent imager with hundreds of meter separation, or as a pairwise interferometer with hundreds of kilometers dimensions.

The Phase I study has determined by analysis and some laboratory experimentation that all elements of this telescope are feasible, and that the telescope can indeed be made to function and operate as a coherent ensemble. In addition, techniques were identified that will allow the packaging and deployment of the large membrane so that the entire telescope can be launched in a Pegasus class or smaller launch vehicle.

A number of technologies were identified as necessary for the successful development and functioning of the concept. The most critical of these will require development and demonstration beyond those that are planned by other programs. In particular these are the fully adaptive self-deploying membrane, the large correction range liquid crystal, the means for packaging and deployment of the membrane, and the MEMS field effect electrostatic propulsion (FEEP) thrusters. In addition, the entire optical system must be system engineered to obtain confidence in its characterization, performance, and cost estimates. These areas are proposed to be pursued in Phase II of this investigation.

The performance, utility, and likely low cost obtainable with such telescopes using these technologies is nothing short of phenomenal, since the telescope techniques are applicable to filled apertures of 25-100 meters diameter, and to sparse apertures hundreds of kilometers diameter or more.

A 25 meter telescope would attain 10,000 times the sensitivity of Hubble and 100 times the sensitivity of NGST. It could detect stars of 8 stellar magnitudes fainter than Hubble at a distance of the very edge of the universe and the beginning of time. In addition an earth pointing telescope in GEO would be able to rapidly scan most of a hemisphere and dwell on any desired area indefinitely, both with 1 meter resolution for unprecedented climate, weather, and earth resources sensing.

A very rough estimate of the likely cost of a 25 meter diameter space telescope using this new concept is about $60 Mullion, launched. Contrast this with similar estimates of the cost of developing and launching a 25 meter telescope using NGST construction, which is about $4.5 Billion.

This concept is the first viable of attaining the Origins Programs' goals of fielding 25 clusters of four 12-25 meter telescopes, hundreds of Km apart, for imaging earth-sized planets around other stars.

No upper stage is needed to launch this telescope into GEO or Solar orbit, since the elements can place themselves into final orbit using their on-board MEMS high Isp thrusters. It is estimated that the added propellant would roughly double the telescope weight depending on the desired orbit. But even then the entire weight of the 100 telescopes would be about 25,000 Kg. and all could be launched in a single Space Shuttle flight.

The estimated cost of the 100 25 class telescopes needed for this mission is about $600 million, as contrasted with an estimated cost of $450 Billion if NGST techniques were used.

In view of the exceptional potential utility of this concept, and the assessment that all its technologies are feasible with appropriate design, technology development, and demonstration, it is proposed that a Phase II activity be funded to undertake these further investigations.

1. CONCEPT DESCRIPTION

The basic telescope concept embodies a powerful new principle for space systems: substitute information webs for structural webs. This capitalizes on the fundamental attributes of space in which mass is expensive while information and its processing is light-weight and cheap. The telescope concept thus employs a flimsy membrane primary mirror and no truss structure whatever. It substitutes information-intensive means to adaptively shape the membrane and to stationkeep all the elements with a virtual truss. This adaptive shaping and virtual truss function with a number of closed loop adaptive systems to compensate for errors and disturbances, and deliver quality optical instrument performance.

Space telescopes have been evolving in this direction, but none have yet made the final leap, as does this concept. The evolution is illustrated in Figure 1-1. The 2.5 m Hubble Space Telescope uses a large precision truss and thick glass primary, and while it has attained phenomenal performance it weighs 12,000 Kg, which means its areal density is about 2,500 Kg per square meter of aperture.

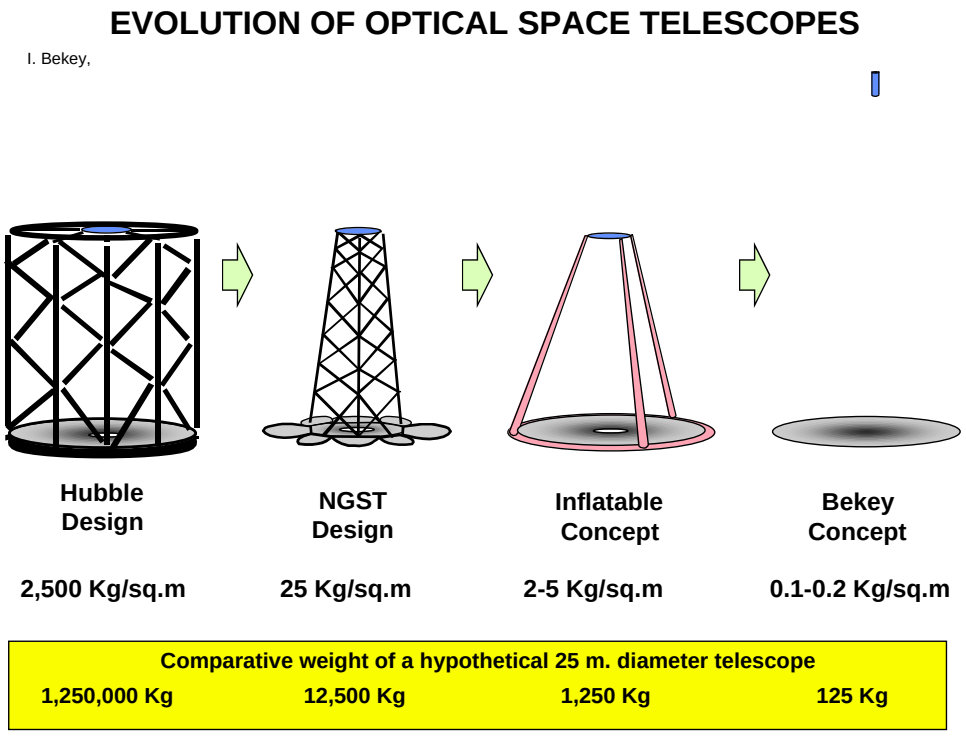

Figure 1-1

The new 8 m NASA Next Generation Space Telescope (NGST) will use lighter weight composite deployable mirror segments and a light-weight composite truss, and its areal density will be two orders of magnitude less: 25 Kg per square meter of aperture. A number of

inflatable membrane mirror concepts with inflatable controlled trusses have been studied, but none are defined to the point of demonstrating even conceptual feasibility, but if they could be made to work their areal density would probably be at most an order of magnitude less, or about 2-5 Kg per square meter of aperture.

While the weight of the truss has been decreasing, none of these designs have yet thought it through all the way: there is no need for any truss in space. Telescope trusses are a carryover of earth-bound thinking. Since g forces do not have to be resisted in space there is no need to have a truss to hold the elements at precise separations, and precision stationkeeping can be used just as well instead, forming a virtual truss. In addition, the large primary membrane mirror can also substitute information for mass if its shape is not precision predetermined on the ground but rather commanded by software in space. Both the stationkeeping and the shape adjustment can then be made responsive to outside disturbances, and closed loop correction control introduced. Thus the telescope's separated parts and flimsy membrane can be maintained in a virtual structure indistinguishable from that of a heavy fixed precision truss and solid mirror.

Sizing calculations done in this study will show that this new concept can achieve 0.1-0.2 Kg per square meter of aperture, which is 4 orders of magnitude lighter than the Hubble Space telescope, 2 orders of magnitude lighter than the NASA NGST design, and at least one order of magnitude lighter than inflatable concepts would be if they could be made feasible.

The impact of this weight reduction is also dramatically illustrated in Figure 1-1, which shows the comparative weights of hypothetical 25 m. diameter filled aperture telescopes if they were to be built using the technologies of Hubble, NGST, inflatable, and the present concepts. The weight of a 25 m telescope would be reduced from 1,250,000 Kg to 125 Kg.

1.1 General

The concept is described in principle, though not to scale, in Figure 1-2. The telescope consists of an unsupported and unstretched (not inflatable) adaptive piezoelectric film membrane, whose figure and surface accuracy are continuously corrected by a scanning electron beam. The signals for the beam current density are generated in response to a figure sensor which detects both gross and fine scale characteristics of the surface. These surface characteristics are turned into beam commands by a computer.

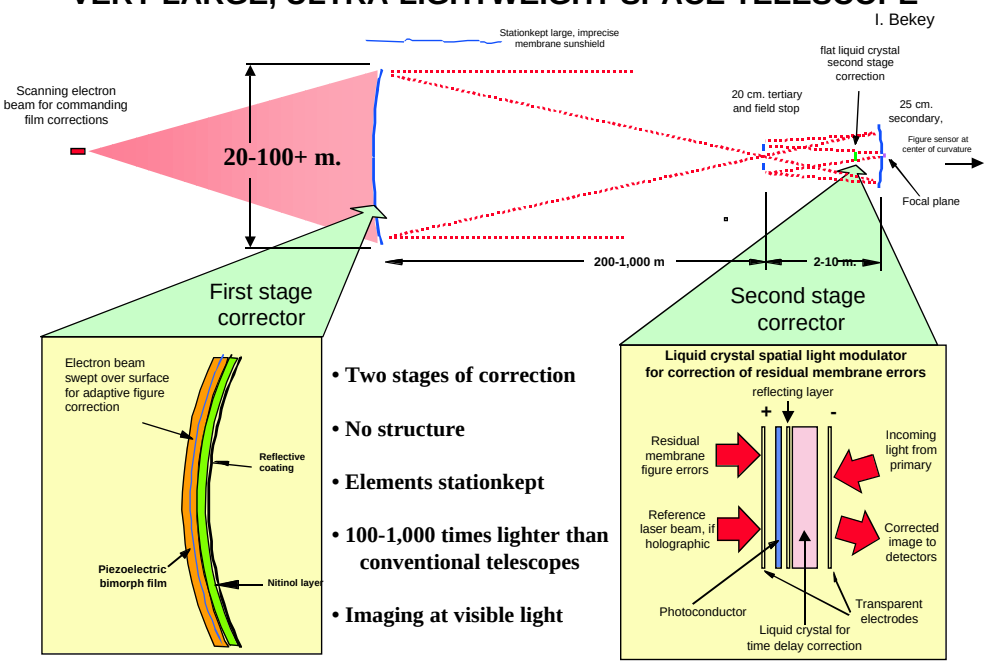

Figure 1-2

The remaining errors in the primary are corrected by a second stage of correction, which is a liquid crystal located in front of the focal array. The liquid crystal is driven by a voltage obtained from a fine figure sensor, which generates a 2-dimensional spatial distribution of the residual errors of the membrane surface after the adaptive loop has done all it can. This voltage causes a distribution of the index of refraction across the liquid crystal, which in turn affects the speed of light though it, in accordance with the residual errors. The aberrated light from the primary is thus corrected as it transits this liquid crystal, resulting in a phase-corrected image. The net effect of the two stages of correction is to generate a diffraction limited image starting from an initially flat and wrinkly membrane.

The focal plane is located in a focal assembly, which is stationkept at the focal point of the primary mirror. A large focal length is used, 10 times the aperture diameter, making for a telescope of f/10. This large f number, together with aspheric design of secondary and tertiary mirrors, results in vanishingly small spherical aberrations, astigmatism, and coma, and makes for a relatively flat primary which is easier to shape by the piezoelectric forces than if the f number were smaller.

The use of f/10 for telescope is a first estimate. If subsequent analyses indicate the control of aberrations in the design would benefit from a larger f number, there is essentially no penalty for

increasing the focal length to any desired number, for example f/100 or even f/1,000. All that is involved is a larger stationkeeping distance, which is no problem to a telescope in solar orbit.

Thus the nominal telescope has a 25 meter aperture and an f/10 design. A scale layout of the telescope appears in Figure 1-3. The focal assembly contains at least an aspheric secondary and is stationkept at 250 m from the primary aperture on axis. The figure sensor is stationkept at the center of curvature at 500 m. on axis. Were it desired to have a telescope design with larger f number, say f/100, the focal assembly would be stationkept 2500 m away and the figure sensor 5000 m away, on the axis of the primary.

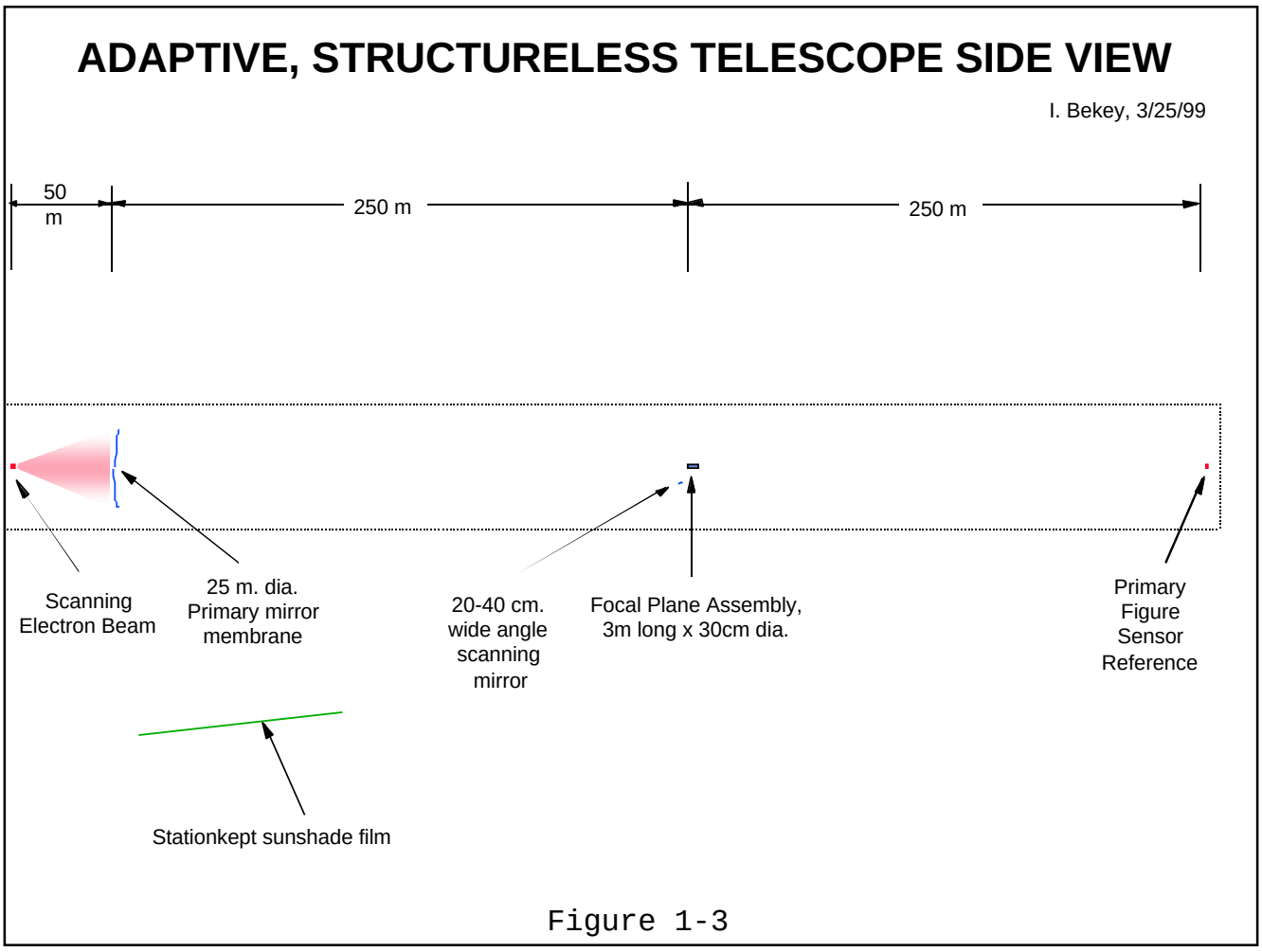

Figure 1-3

There are two additional features that make this concept unique: First, the primary membrane is perpetually shaded from sunlight by a stationkept film sunshade to prevent thermal distortions and dynamics, moving radially around the primary to maintain shielding as the telescope orbits. Second, there exist a pair of very small mirrors attached to and in the vicinity of the focal assembly that al-

low the field of view of the telescope to be rapidly and frequently changed by many degrees without moving either the membrane, the e-beam generator, the focal assembly, or the figure sensor. This avoids both large propellant expenditures and introducing dynamic disturbances into the system.

It is envisioned that the entire telescope assembly would be emplaced in deep space for operation as a celestial instrument, being located in solar orbit at 1 AU or further away from the sun if required. Or it could be located at a Lagrangian point of the Earth-Moon system. The telescope could also be located in geostationary orbit (GEO) for Earth viewing, be it for remote sensing or other National Security applications.

The entire telescope will be extremely lightweight, the result of substituting information for structure. The weight breakdown of the entire telescope system in space is shown in Figure 1-4, which is detailed in the subsystems section 4. It is seen that a 25 meter diameter telescope will weigh less than 150 Kg., a phenomenal achievement which will revolutionize both space astronomy and remote sensing of the earth.

WEIGHT ESTIMATE OF A 25 M. DIAMETER FILLED APERTURE TELESCOPE

•E-beam generator	5 Kg.
•Membrane assembly	25 Kg.
•Steering mirror assembly	5 Kg.
•Focal array assembly	28 Kg.
•Figure sensor assembly	5 Kg.
•Sunshade/power projector	8 Kg.
•Computation/communications	32 Kg
•Packaging	25 Kg.

Total launch weight	**123 Kg.**
Resultant areal density	**0.25 Kg.sq.m.**

Figure 1-4

In operation the telescope assemblies would be rotated and translated until they form the axial configuration of Figure 1.3 pointing to the desired target region. Actually the best plan would be for the primary membrane to rotate only, avoiding translational stresses and propellant, with all other elements translating as well as rotating. Once in stable configurations and all dynamic perturbations damped down, observations could begin. Viewing objects within several degrees of the telescope axis would then be accomplished by moving only the small fast steering mirrors, without rotating or translating any other telescope components.

The basic concept can be assembled into a dilute array consisting of many primaries and a combining assembly, illustrated in Figure 1-5. The number, size, and spacing of the primaries can be chosen such that a snapshot imaging capability exists, or a much sparser array can be formed functioning as an interferometer, trading resolution

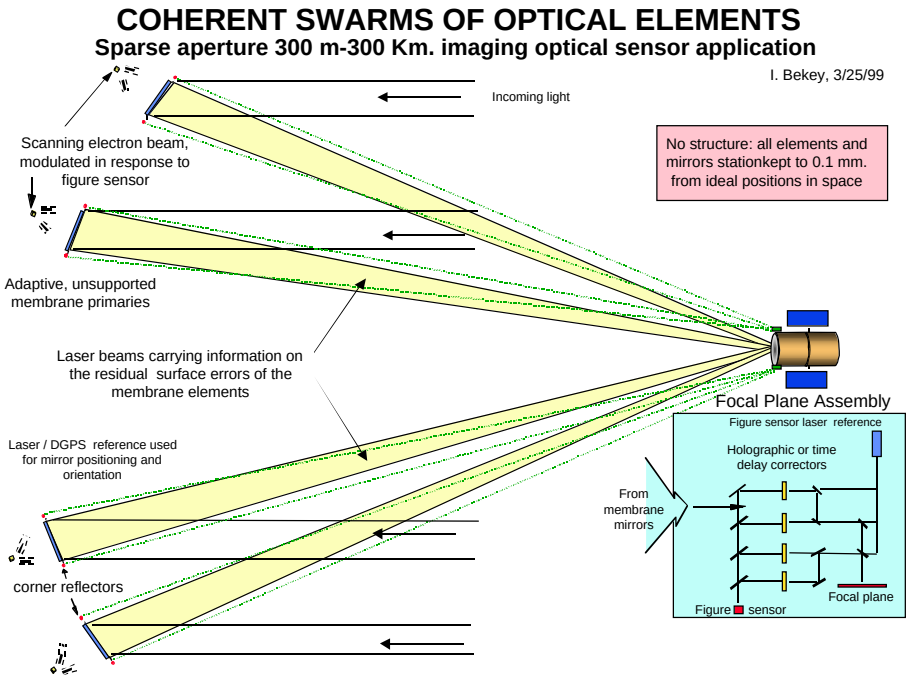

Figure 1-5

for rapid image formation. In either case, the primaries would be identical in principle to those in the single primary telescope, each with its own e-beam figure corrector, but the combining assembly would have a more complex inner path resulting from the use of one liquid crystal corrector per primary aperture, resulting in their subsequent in-phase light addition.

1.2 Adaptive membrane primary

A lightweight primary membrane mirror is the heart of a lightweight telescope, and the biggest stumbling block at the same time. There is extensive research ongoing in several laboratories to employ an inflatable reflective membrane, supported by gas pressure against a clear front membrane. The desire to stretch the membrane by gas pressure is driven by the low weight and possible ready deployability of such designs, the ability to make apertures larger than the diameter of the launch vehicle, and the ability to remove surface wrinkles and by the stretching action. Of these the last is the most significant, since surface irregularities constitute the irreducible minimum affecting image quality.

While these approaches are a reasonable extension of current telescope practice but using lighter materials throughout, they are deliberately avoided in this concept for three reasons:

- Inflation always results a figure which is neither a sphere nor a parabola ("the infamous W curve shows that the difference between a parabola and an inflated membrane always has a W shape), and which is very difficult to compensate with another optical surface

- It requires an inflatable torus or other compression member at the membrane periphery in order to impart the desired stretching forces, which will add weight to the aperture and which could be sensitive to puncture by micrometeorites

- Stretching and shaping the membrane by gas pressure requires a second membrane to contain the inflation forces. This second transparent membrane is unavoidably in the light path, which makes to transits through it. The resultant scattering cannot be corrected, and will create a haze or fog in the image which will seriously limit the telescope's attainable sensitivity.

As a result of the above difficulties inflation was rejected, and the primary membrane for the concept was conceived to be a fully adaptive but unsupported and unstretched film membrane. This membrane is constructed from a piezoelectric bimorph film, which is curved at will not by pressure or tension but by applying a charge distribution to it via a scanning electron beam. Since there are essentially no differential forces over tens of meters in deep space, the electron beam current can be so adjusted that any desired curvature is attained without any net tension forces arising in the membrane, and without requiring any transmissive films to be in the light path. The concept is illustrated in Figure 1-6.

ADAPTIVE MEMBRANE CORRECTION

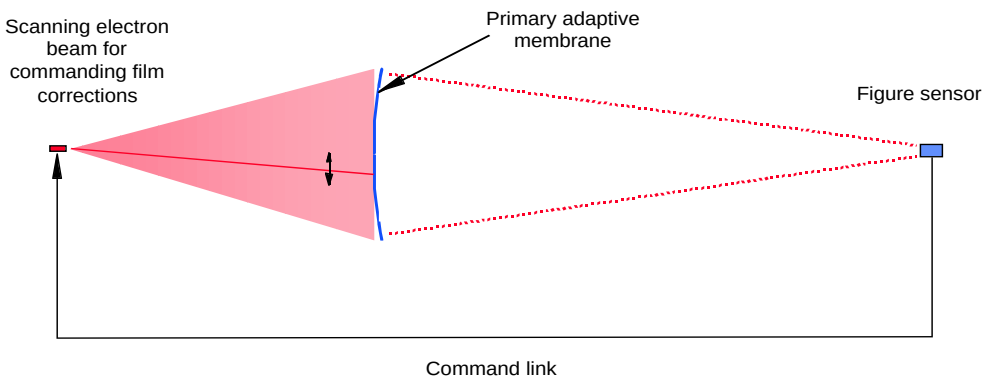

Figure 1-6

The use of this technique results in a membrane whose gross as well as fine scale curvatures are continuously adjusted in response to either disturbances or commanded to change shape. This will have the further beneficial effects of being much lighter than any stretched or inflated membrane design, as tension forces do not have to be resisted. This allowing the use of extremely thin films and the avoidance of a large diameter torus.

The difference between a plane and a parabolic shape is about 0.1 m. at the membrane center for a mirror with focal length 10 times the diameter. Thus a 25 m aperture would have a radius of curvature of 500 m. and a focal distance of 250 m. Such a “nearly flat” membrane will be much easier to construct and adaptively shape that would be one for an f/1 design, which would then require about 25 m. of dishing.

The unsupported film has a second major advantage over a stretched film surface. While in principle the adaptive membrane will have sufficient “artificial stiffness” induced by the piezoelectric bimorph layers to be moved as a unit and to maintain any desired shape in space, the absence of tension to attain that stiffness makes for very weak wave propagation along its surface. This will avoid the dynamic disturbances of the typical “drum-head” modes of membrane dynamics.

There is one major disadvantage of using an unstretched film, which is that while large wrinkles and gross curvature errors are readily removed by the piezoelectric action under electron beam irradiation, smaller scale wrinkles with spatial extent smaller than the electron

beam diameter cannot be removed as they generally are by stretching. Thus, while larger errors are indeed removed by the electron beam-induced changes in the piezoelectric film, the technique is limited in the dimensions of the fine scale errors that can be removed simply by limits in the ability to sharply focus the electron beam.

Further, the resolution limits of the liquid crystal second stage corrector will set a lower limit on the ability to remove the effects of extremely fine scale surface irregularities, thus placing greater demands on the fine-scale uniformity of the film surface. While materials with very small fine scale surface irregularities exist, much remains to be determined as to their production and handling, particularly in very thin films. In addition, the piezoelectric film may not have the simultaneously the best correction ability and the smoothest surface, forcing the addition of other layers of different materials. This is discussed further in Section 4.2.

It is envisioned that the primary membrane will have a third major layer consisting of a very thin Nitinol film. This is illustrated in the crossection shown in Figure 1-7. This film, which is a shape-memory alloy, will allow the membrane to be folded like a blanket for launch, and will automatically deploy the film to its original flat shape when sun-heated in space. The presence of any

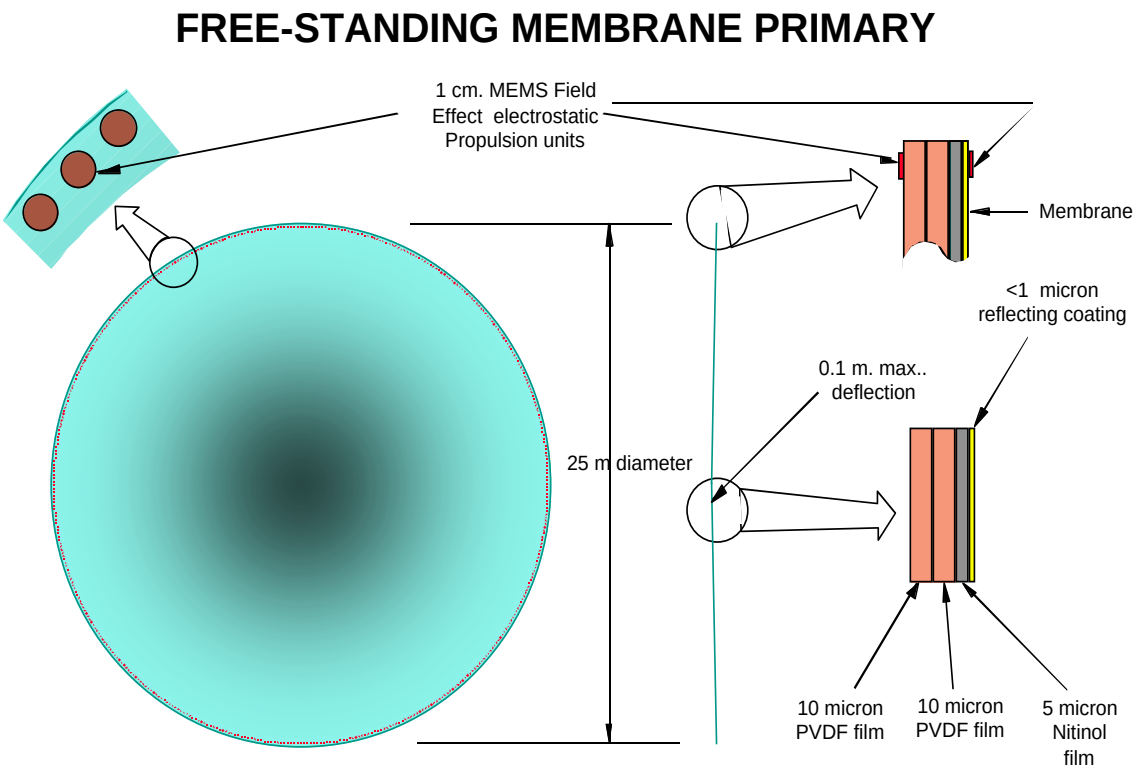

Figure 1-7

creases or ridges along the membrane resulting from these folds will be mostly removed by the adaptive piezoelectric control, and their residual errors will be corrected by the liquid crystal stage. This technique will make it possible to fold the primary membrane into a very small and compact package, which can then be launched on a small booster. This is illustrated in Figure 1-8.

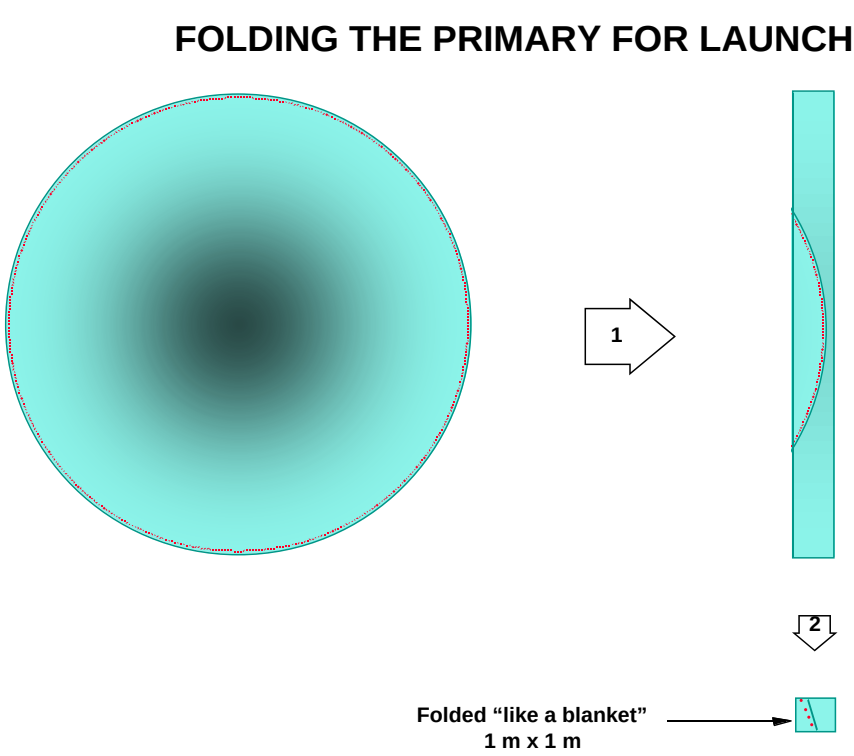

Figure 1-8

The primary membrane is envisioned to have a large number of solid state MEMS propulsion units attached at its periphery to allow rotational and translational control. These units would use field Effect Electrostatic Propulsion thusters (FEEP) and integral propellants to attain the high specific impulse but very low thrust required. The presence of the “artificial stiffness” in the membrane allows the thrusters to move the otherwise limp membrane as a unit.

These propulsion units are powered by electricity, which must be supplied to them by means other than solar cells, as the membrane will be permanently shadowed by the sunshade. The solution is to convert solar energy into microwaves at the sunshade, and transmit the small power required by the membrane thrusters by microwaves, to be received and rectified at each MEMS unit. This can be done with good efficiency and light weight, and is further discussed in Section 4.8.

1.3 Liquid crystal corrector

The liquid crystal corrector which is the second stage correction device produces a 2-dimensional pattern of index of refraction changes, which are proportional to equivalent time delays, in response to signals from the Figure sensor. This corrector is illustrated in Figure 1-9. It is similar in principle to correctors operating in the laboratory at the Air Force Research Laboratories in Albuquerque, however is designed with both different principles and new materials. The current correctors have a range of correction limited to a few wavelengths, and are designed for high frequency response, being aimed at correcting atmospheric fluctuations.

The concept adopted for the space telescope requires a much greater correction capability so as to be able to correct the errors left over in the primary membrane after shaping, as well as stationkeeping errors. However, the devices do not need high frequency response as the disturbances are expected to be very slowly

LIQUID CRYSTAL SECOND STAGE CORRECTOR (typical)

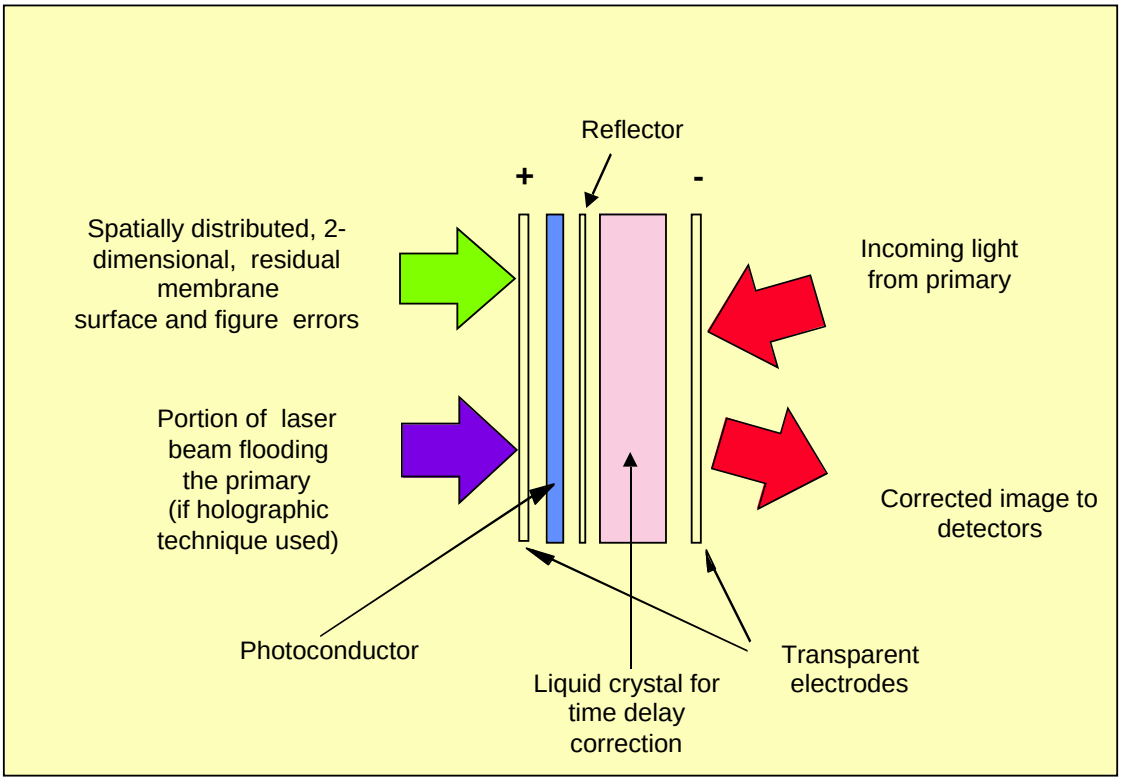

Figure 1-9

varying with time compared to any atmospheric phenomena. Thus the liquid crystal contemplated has a range exceeding many hundreds of waves of correction while having very low scattering and yet will have sufficiently agile frequency response to correct for the expected disturbances.

The liquid crystal could be spatially driven or electrically driven by pixels. Furthermore there are a number of ways of generating the error signals to drive it, ranging from holographic to direct amplitude error imposition. In the holographic technique, a laser beam with spherical beam front is formed and illuminates the entire primary. A portion of this beam is transmitted to the focal assembly where it is combined with the light from the primary. This combination in effect creates a hologram of the remaining errors in the primary after the electron beam correction has done all that it can. This hologram is impressed on a photocathode or otherwise caused to form a 2 dimensional spatial error distribution across the liquid crystal. This potential distribution in turn creates a like distribution of changes in the index of refraction of the liquid crystal.

When the light from the primary aperture is passed through the crystal, the changes in its index of refraction result in proportional changes in the speed of propagation of light through it. Thus the surface errors in the primary, which have the effect of variable time delays, are canceled out by the corresponding but oppositely phased time delays in transiting the liquid crystal. All this happens in parallel across all areas of the liquid crystal, in effect “reading” the hologram. The result is a corrected wavefront that in principle can result in diffraction-limited performance.

The second technique is similar but senses the surface errors directly without creating a hologram, and creates the 2-dimensional voltage distribution across the liquid crystal directly. It uses a new heterodyne laser interferometer which is now operating on the bench at the USAF Research Laboratories, which can produce an illuminating coherent wavefront on the primary with variable wavelength. This has the advantage that by sweeping the two heterodyning lasers a synthetic wavelength can be created which is long for sensing of coarse scale errors, short for sensing the very fine surface errors, or in between wavelengths, and yet maintain high sensitivity for all wavelengths. This second type of figure sensor has the potential to become the only figure sensor in the telescope, while the use of the heterodyne system may require a separate coarse figure sensor.

Liquid crystal second stage correctors are further discussed in Section 4.3.

1.4 Focal assembly

The focal assembly is relatively conventional, in that it can use conventional construction mirrors since they are so small as to make their weight inconsequential. The assembly, which is illustrated in **Figure 1-10** for the nominal f/10 telescope, could consist of individually stationkept mirrors, using the same FEEP MEMS propulsive units as employed for the membrane, or a composite tube could be used with those propulsive units on its periphery. In the latter case if further design shows that the bending cannot be readily controlled sufficiently, a second sunshade can be stationkept "up-sun" from it to place it into a stable, permanently shadowed configuration.

In the event that further analysis in Phase II indicates a considerably larger f number would be desirable, a quaternary mirror would be added to the focal assembly, and the secondary mirror separated from it and stationkept independently on the axis in front of the focal assembly. This will allow the focal assembly to remain a relatively short and compact cylindrical package, while the addition

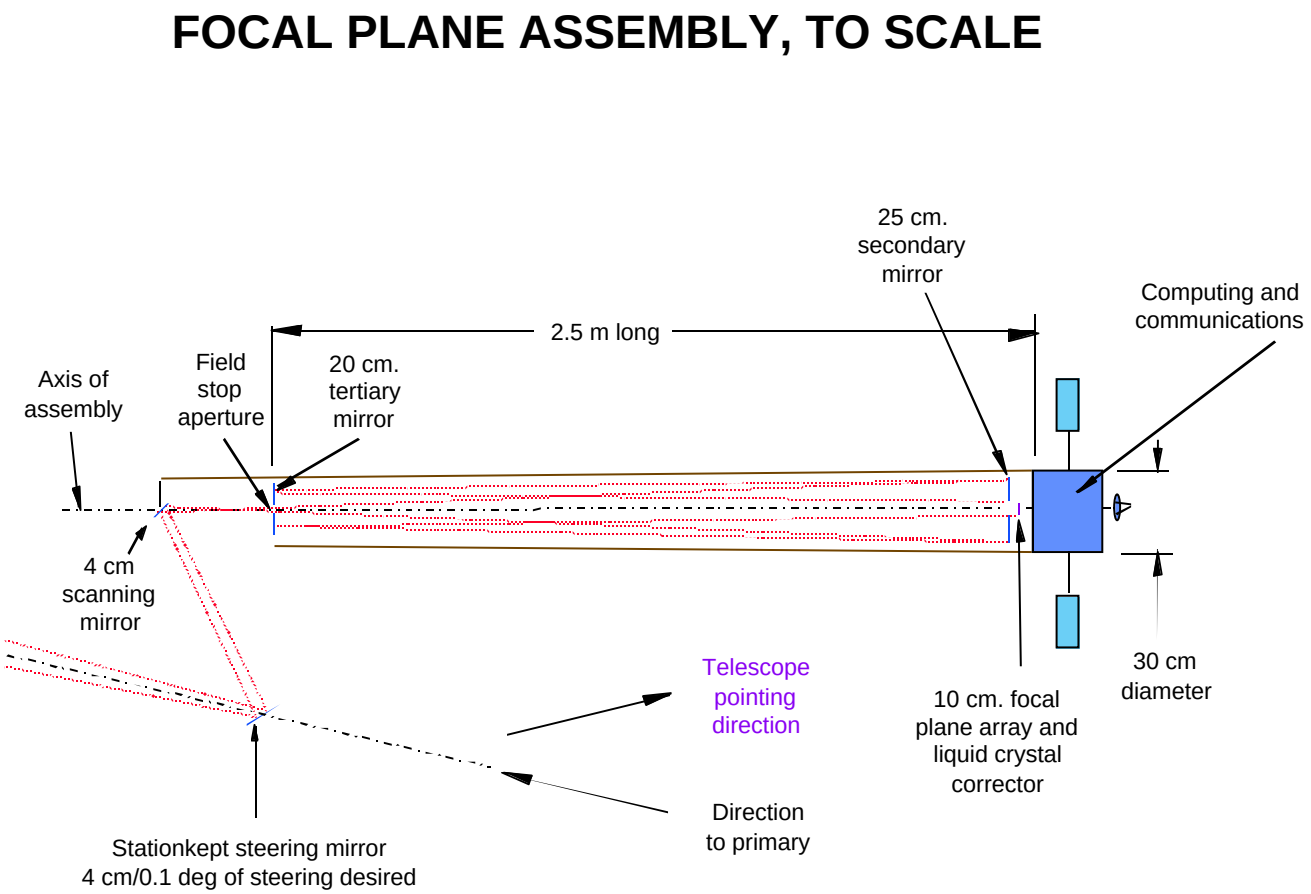

Figure 1-10

of one more stationkept element to an ensemble that already has 5 axial and perhaps three off-axis elements is a small penalty to pay for that convenience.

The focal plane is expected to be a conventional array, which could be a CCD device. The state of the art will allow the 10 cm focal plane to be populated with an array of 10,000 x 10,000 detectors, each 10 microns in size. This will allow a good field of view, while also permitting use of focal plane processing both for image formation and for tracking to accomplish cross-axis stationkeeping.

One of the fast steering mirrors is envisioned to be attached to the focal assembly, as it does not need to translate, only rotate. If hard mounted, a dynamic counterbalance should be used to ensure that steering disturbances are not created which cause jitter or loss of track in the telescope.

The focal assembly is discussed in more detail in Section 4.3.

1.5 Fast steering mirrors

It is highly undesirable to translate or rotate any of the elements of the telescope to repoint the field of view, because any such motion will produce disturbances that will affect the jitter or location of the image, or both. Thus the telescope will be pointed to the center of the desired area in the celestial sphere, all disturbances allowed to damp out and settle down, and then imaging will proceed. However, the field of view can be rapidly and easily moved several degrees total without moving any major element of the telescope. This is done using the fast steering mirrors.

These two small fast steering mirrors are a unique invention, conceived by Glenn Zeiders of Sirius Associates. These fast steering mirrors were shown on the focal assembly illustration of Figure 1-10, and their action is illustrated in Figure 1-11. One mirror (the steering mirror) is stationkept in the close vicinity of the entrance end of the assembly. It directs light from the primary toward the second or scanning mirror, which is mounted on the assembly axis. By translating the steering mirror further away from the assembly and properly rotating both mirrors, it is possible to receive light far from the Primary telescope axis yet continue to direct that light exactly into the assembly axis without moving either the primary or the focal assembly.

This results in an ability to steer the field of view of the telescope by rotating only a 4 cm mirror and rotating and translating the other mirror, and leave the large, heavy, and sensitive primary,

assembly, and ancillary devices on its axis completely unperturbed. The translating mirror must have a diameter of 43 cm per degree of pointing desired. No additional aberrations and image errors are introduced by this steering technique since the primary is a sphere, and the performance is independent of which portion of the sphere is used.

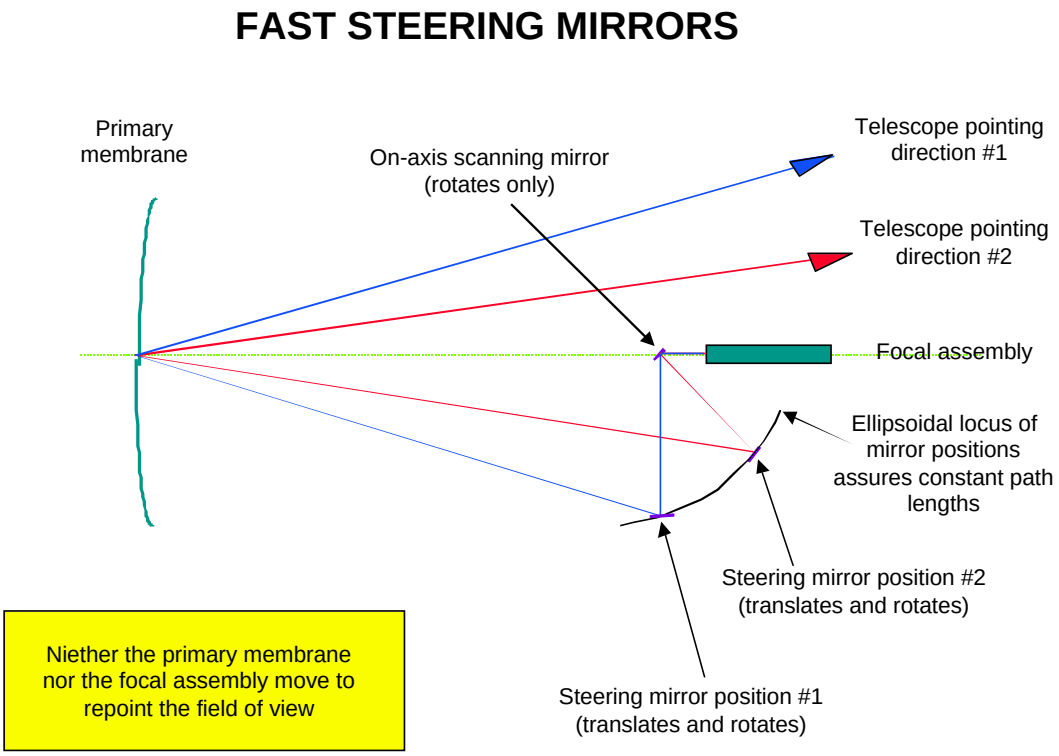

Figure 1-11

This fast steering technique requires that the primary aperture be either increased somewhat to accept the off-axis rays, or that some vignetting be accepted in its performance. Since the primary is a sphere, no additional errors are expected if it is made a little larger than needed for off-axis pointing of the field of view. . These fast steering mirrors are discussed in detail in Section 4.5.

1.6 Electron beam assembly

The electron beam assembly generates a scanning electron beam which is focused on the piezoelectric membrane material. It is illustrated in Figure 1-12. The beam deposits a charge wherever it hits, and the presence of a thin conductive coating (a “back plate”) conducts the electrons back to the source. The means of this conductance could be a very fine and compliant wire from the coating, or a separate non-scanning electron beam could furnish this path. The

electrons flow only during charging of the piezoelectric bimorph, which is capacitor. The piezoelectric film thus stores the charge, and bends locally in response to it.

PRIMARY MEMBRANE SHAPING AND CORRECTION

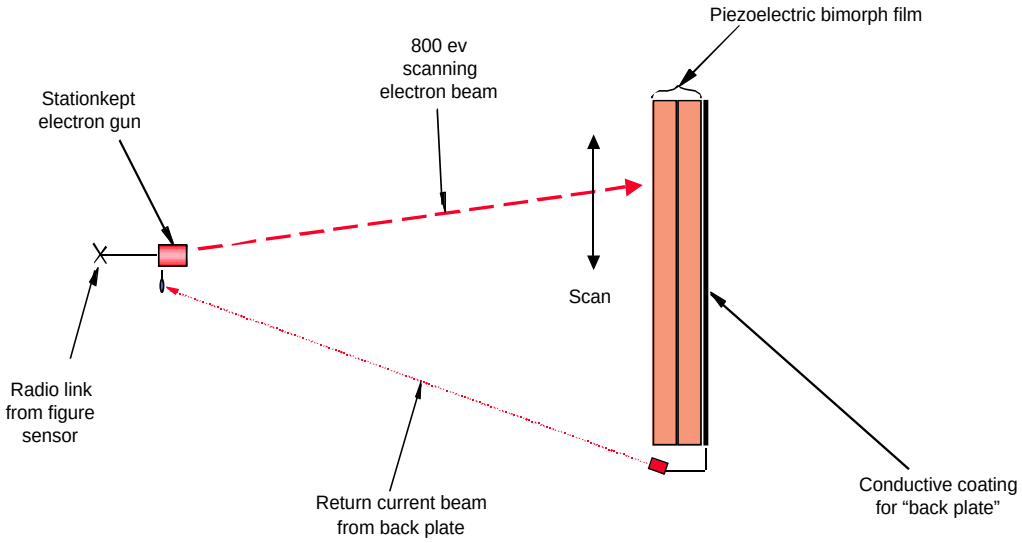

Figure 1-12

The charge deposited in any particular point on the film will eventually diffuse laterally, as well as leak through the film due to non-infinite impedance across it. At some point the charge will have to be replenished to maintain constant local curvature. In laboratory experiments, this time constant was observed to be many minutes, with 5-10 minutes being typical. Thus the electron beam source has to be sized so as to provide for recharging the surface periodically in response to dynamically changing errors, but mot less frequently than several minutes.

Nonetheless it is vital to appreciate that in principle, the curvature of the primary will hold even when the electron beam it turned off, so that the average beam current is far smaller than if it were required to maintain a steady state current. This is because the entire membrane acts like a giant capacitor. The electron beam source will have its own power supply from a solar array, and will be stationkept via master control from the Formation Flying computer. Should further analysis indicate that power must not be lost during eclipse, the Sunshade assembly could also beam the required power to the electron beam assembly.

Precise orientation and direction of the electron beam will be obtained not only by the metrology system, but it will be aided by the figure sensor, as the impingement point of the beam on the membrane will be clearly deterministic, allowing for closed loop fine tracking control. The electron beam assembly is discussed in more detail in Section 4.6.

1.7. Figure sensor

The figure sensor is located at the center of curvature of the primary membrane mirror so that its metrology beamed will reflect from the membrane surface without requiring any holographic or special reflector patches, as would be the case were it collocated with the focal assembly. It is illustrated in Figure 1-13. The figure sensor assembly has two principal functions: it senses the gross and fine scale figure of the primary mirror membrane for controlling the electron beam that corrects these errors, and it furnishes an external laser reference that causes a holographic fine scale error formation or a heterodyne error formation, whichever technique of correction is used in the liquid crystal.

FIGURE SENSOR ASSEMBLY

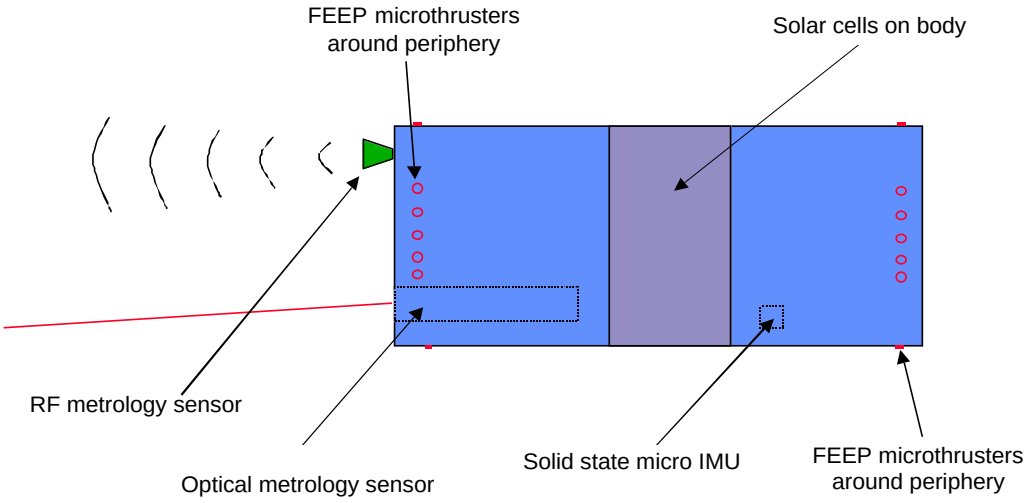

Figure 1-13

The assembly is also stationkept, responsive to the same master metrology and control system as controls the entire system. The assembly would also be translated and rotated via FEEP MEMS propulsion units mounted on its periphery. This assembly is further discussed in Section 4.7.

1.8 Sunshade/power projector

The primary membrane (and perhaps the focal assembly and the electron beam generator) will be shielded from direct sunlight by a stationkept sunshade, illustrated in Figure 1-14. In order to ensure full shading the sunshade will be somewhat larger than the primary even when coaxial. Electric propulsion on this sunshade will resist solar pressure for the life of the missions via FEEP propulsion units mounted on its surface. In addition, these thrusters will provide the propulsion required for stationkeeping the sunshade, and moving it so as to always shade the primary membrane.

The surface accuracy of this film is immaterial as it is not part of the telescope optical system, and it is therefore easy to make and deploy. It will be made as thin as practical consistent with keeping its rough shape, and might consist of only a Nitinol layer with reflecting coating. It will have to have solar cells to generate the power required by the FEEP propulsion units, but as the shade will always be oriented to the sun, these can be simple amorphous silicon plated on the shade surface.

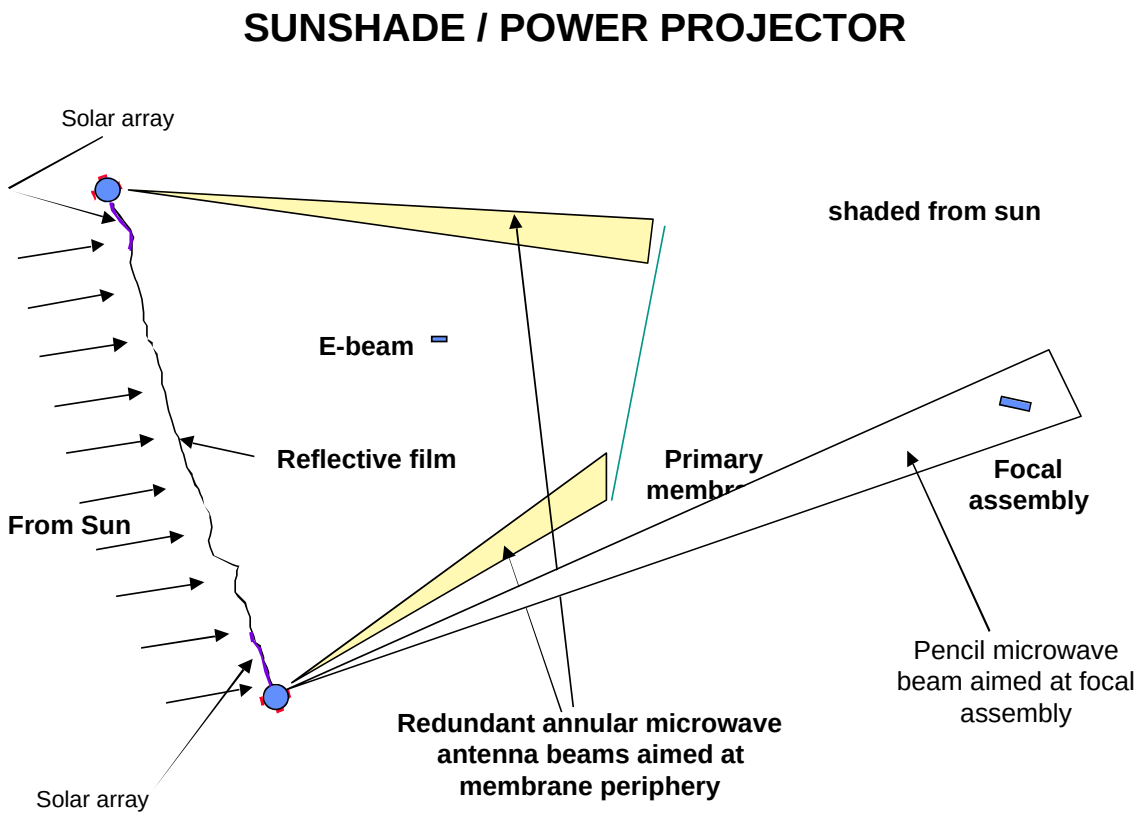

Figure 1-14

The sunshade will play a second and critical role, that is converting solar energy to microwaves that it will beam toward the primary, which will be rectified and used there for powering its FEEP propulsion units. For that purpose distributed solid state microwave transmitters would be placed on the sunshade that together create an antenna pattern that just covers the FEEP units on the primary membrane. Since the distance between the two membranes is anticipated to be small, 25-50 meters, and the aperture available for power transmission will be greater than 25 meters, it will be easy to form the beam patter required for efficient power transfer. It is therefor estimated that a DC-DC overall efficiency of the power transmission system of 75% can be attained, and that the power transmission systems will be modestly sized. This system is further described in Section 4.8.

1.9 Formation flying metrology

A dedicated metrology system will be used to determine relative distances and orientations in the ensemble. This system will consist of both microwave and optical active and passive components. It will be designed to obtain range, range rate, and angular information using corner reflectors in a number of locations on each major element of the telescope with respect to each other, as illustrated in Figure 1-15. These data are planned to be obtained by sources and reflectors contained within the envelope of the elements. However, if there is insufficiently accurate information obtained this way, obtaining more angular diversity may require the stationing of one or two such sources in a plane normal to the telescope axis. These would be small and lightweight references, whose presence could be controlled readily as that of the other elements.

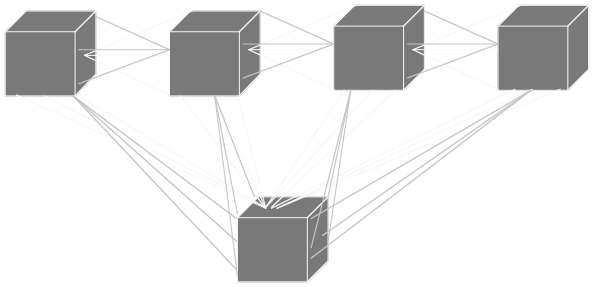

Figure 1-15

The requirements on these components are similar to those for the NASA Deep Space 3 and Separated Interferometer Missions. While those missions will not stationkeep to the accuracies envisioned for

this telescope, relying instead on mechanically adjustable optical path length adjustments in each interferometer path, the measurement accuracies are comparable. It is therefore reasonable that the metrology system is considered to be feasible in the time frame. Much more detailed tratment of this coplex topic and system descriptions and operation considerations are found in Section 4.9.

1.10 Information processing/communications

There will be a centralized information processing system that will perform a number of functions, including:

- Image fine tracking
- Formation flying control of all the elements
- Primary membrane shaping and control
- Liquid crystal secondary correction control
- Positioning and attitude of the entire telescope ensemble for coarse pointing of the telescope
- Positioning of the fast scanning mirrors for field of view control
- Control of the sunshade for primary membrane shielding
- Image processing
- Image formatting and data transmission to the ground
- Reception and translation of ground commands from a sequence of telescope functions to a sequence of synchronized element commands

In addition, for the case where there will be more than one primary aperture, the above functions will be performed as the necessary sequence of actions for the telescope ensemble to function as one coherent whole. In addition, there will be specialized image processing and metrology functions for coherent image combination from the multiple sources, be they deconvolution for image formation, pairwise interferometric measurements for the case of multiple widely separated interferometers, or both. These are further described in Section 4.10.

2. ARCHITECTURE/OVERALL DESIGN

This section discusses the architectural options for a telescope of this kind, and the reasons used to select the chosen architecture and major features of the telescope design. It is crucial to result in a practical system that can be built, and whose performance will be as desired. It will also bear heavily on whether the system is feasible or not, which is, after all, the principal objective of the Phase I study: to determine feasibility

2.1 Architecture

The basic architecture of the telescope has a number of major options. These are discussed with reference to Figure 2-1. In each case the telescope consists of a stationkept primary and one or more stationkept other elements, and no truss structure.

The most basic architecture is to focus the light from the primary directly onto the focal plane. Assuming that all accuracies can be met, this has the advantage of no other optical elements being required, but the great disadvantage that stray light rejection does not exist, and the detectors may well be swamped with incident light from other sources such as the earth, sun, or even bright or extended targets. It is not useful in this application.

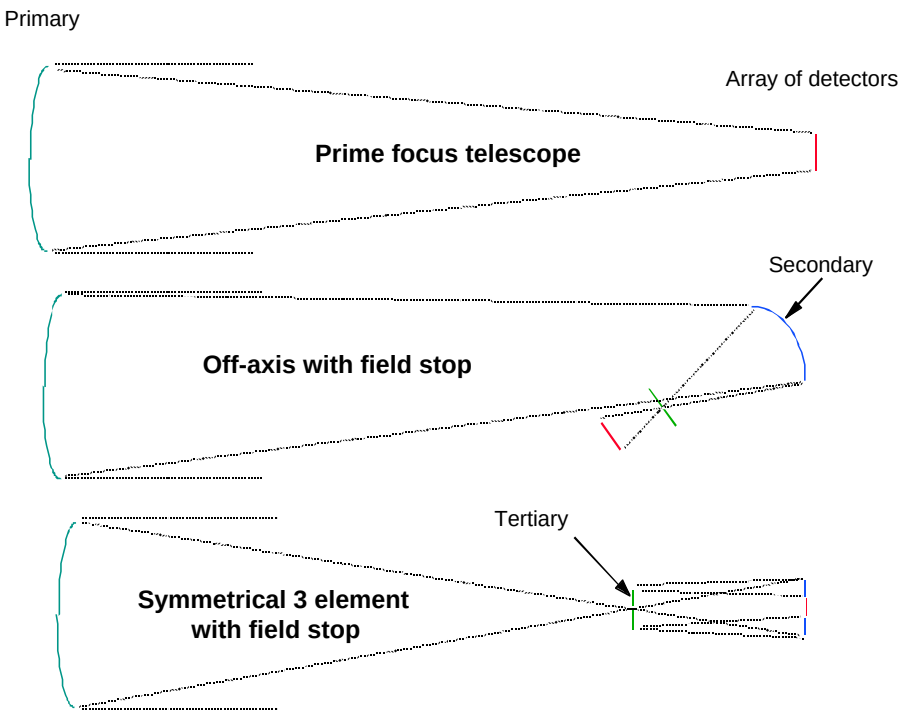

Figure 2-1

A second configuration uses a small aperture at the focus point of the primary to limit the off-axis light that is accepted by the rest of the telescope. This requires a secondary mirror, and can be used as either on-axis or off-axis configuration. The on-axis configuration has some blockage by the focal plane, and so the off-axis configuration may be preferable if that blockage becomes objectionable.

This configuration is amenable to placing the secondary, the field stop, and the focal plane in a single assembly, rather than having to be independently stationkeep. While this architecture has the advantage of stray light rejection it has the disadvantages of difficulty in scanning a wide angle; and the location of the focal plane is bad, being far in front of the focal assembly for a long focal length system. More fundamentally, the use of only 2 elements—a primary and a secondary—allow correction of the primary's spherical aberration but not of coma or astigmatism.

Most of the disadvantage of these architectures disappear when a tertiary element is added. The presence of the tertiary with negative power enables the shortening of the optical path so that it can all be folded inside of a reasonable assembly. It also allows correcting for coma or astigmatism in the system, in addition to spherical aberration. The length/diameter ratio of this assembly can be made essentially equal to the f number of the primary. Furthermore, the field stop aperture can be in the center of the tertiary, while the focal plane can be located in a hole in the secondary. Should wide field of view scanning be needed (as it probably will be) then the small steering mirrors discussed above can be employed at the front of the assembly of mirrors, near the tertiary. Thus its narrow field of view will not be a disadvantage at all.

<u>It is important to note that reimaging is not required or used</u>. This is a widely misunderstood subject. Reimaging is required when the field of view is large. However, a reimaging system requires a secondary about half the diameter of the primary and a tertiary proportionately large—a very painful proposition when discussion 25-100 m primary systems. However, the long focal length narrow field of view system is made practical by means of the fast steering mirrors that steer the narrow field over large angles, eliminating the need for reimaging. This makes the secondary and tertiary mirrors very much smaller and lighter.

Therefore, based on the above considerations, a three element system with additional steering mirrors was chosen. While the details of the design are discussed in Section 4.4 and 4.5, the following gives a feel for the numbers involved.

The focal assembly could be structural and made from a cylindrical thin tube, inflatable, or other lightweight structure; or the mirrors could themselves be stationkept (with the secondary holding the focal array) eliminating all structure. Indeed, for the nominal f/10 design it is not clear which would be preferred. For an f/100 system the mirrors would be stationkept individually in order to avoid a very long tube

The net result is that the telescope focal assembly can be modestly sized: the secondary mirror is only 25 cm diameter, and the tertiary 20 cm. The focal plane is an array 10 cm across. Thus the entire assembly can be a tube 30 cm. diameter and 2.5 m. long, and will be extremely low weight.

The fast steering mirrors need only be small, and thus they can be lightweight and yet made rigid for fast movements without being very heavy. The scanning mirror on the focal assembly axis need only be 4 cm diameter and the steering mirror that does both translating and rotating only 43 cm. diameter (for steering the field of view by 2 degrees). This will allow leaving the large, heavy, and sensitive primary, focal assembly, and ancillary devices on its axis completely unperturbed.

This fast steering technique requires that the primary aperture be either increased somewhat to accept the off-axis rays, or that some vignetting be accepted in its performance. Since the primary is very low weight, a little additional weight is probably of little practical consequence.

2.2 Overall design

In the overall design it is fundamental that the basic feature of space be addressed: the absence of g forces. So elementary a consideration has been totally absent in all space telescope designs to date. All ground and space telescopes incorporate precision trusses to hold the primary aperture relative to the focal plane and/or other apertures. But why is this? Trusses are needed on the Earth to resist g forces. These trusses have been carried into space for telescope designs.

Ground telescope primary apertures are usually highly concave, with small f numbers being desirable. These highly dished and therefore expensive apertures are desirable because they minimize the weight and difficulty of the truss, which, together with the primary mirror are the most difficult, heavy, and expensive elements in a space telescope.

However if take advantage of the unique characteristics of space, we can eliminate the truss, as the secular forces that must be resisted are near zero, particular in higher orbits and deep space, substituting it with weak thrusters operated in a stationkeeping mode. Particularly in deep space or solar orbit, therefore we can use a large focal length telescope as readily as a short focal length one, and the performance generally will be independent of the primary’s

focal length for a celestial object telescope. This means that the primary can be made only very slightly concave with no real penalty.

The real advantages of a long focal length telescope are that the spherical aberrations, astigmatism, and coma of the primary can be readily made to be vanishingly small. It then becomes easier to make the primary out of a membrane, and it no longer matters whether it is a parabola or sphere. This, in itself will simplify the system, as we shall see below.

The aberrations which are generated are estimated as follows:

The following are useful expressions for the RMS path length shifts in terms of the diameter, f-number, and total off-axis angle y = 2q:

Spherical Aberration: $DS_{rms}/D = \sqrt{4/5}/f^3/512 = 0.00175/f^3$

Coma: $DS_{rms}/D = \sqrt{2}y/f^2/128 = 0.0110y/f^2$

Astigmatism: $DS_{rms}/D = \sqrt{6}y^2/f/384 = 0.00638y^2/f$

Recall that the general rule of thumb is that the total RMS error for an optical system not exceed l/14, so each of the above should be less than that. For operation at l = 0.5m this means a surface accuracy of 3.8×10^{-8} m. For a 25 m aperture, the spherical aberrations would be tolerable if the f number were 100 or greater, if the surface were a parabola, or if an aspheric corrector is used as a secondary element. We will Envoke the last method, so that the spherical aberrations will be inconsequential, even at f/10.

The coma aberrations require an estimate of the total field of view. Assuming a 10 cm. focal array and an f/25 design, the field of view is 0.4 milliradians. Thus the coma required accuracy requires an f number greater than 11, which is essentially satisfied. Similarly the astigmatism requires an f number greater than 0.03, readily met by any practical design. Therefore we conclude that any focal length greater than about 10 times the diameter of the primary will suffice, with a spherical primary and an aspheric secondary element. Thus we end up with a large focal length/diameter ratio (the f/number).

Because of this, the primary will be very slightly curved, as illustrated in Figure 2-2. From this figure the deflection in the center of a 25 meter spherical primary with f/10 is calculated at only 7.8 cm. out of 25 meters. In fact, the deflection of a parabola of the same f number is only 15.6 cm. out of 25 meters. Thus the difference between a parabola and a sphere is 7.8 cm.

This means that a membrane primary can be constructed flat, and then shaped in space with a strain of only 1.2 cm per meter of radial distance. This is a bend of about 1.2 mm per cm of film, or 10%. It is a very slight bending indeed, and well suited to piezoelectric actuation.

Now then we calculate the main focus and error correction required in the primary and the liquid crystal. The 25 m primary will have a spot size of $d = 2\lambda/D$. Since we are operating in the visible spectrum, the spot size at the focal plane is 10 microns. Since state

CURVATURE OF THE MEMBRANE PRIMARY
for a 25 m. f/10 design

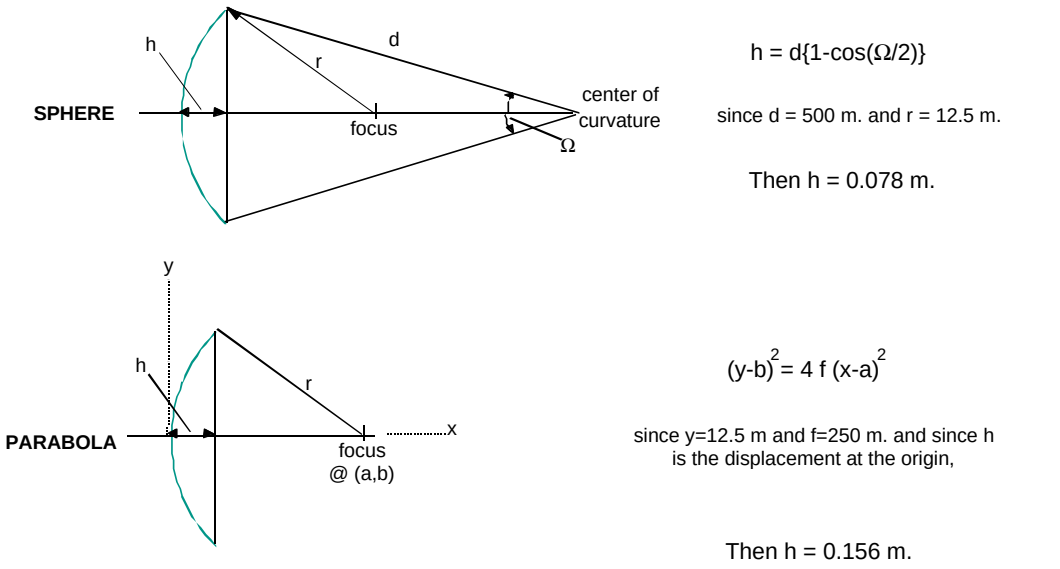

Thus a spherical 25 m. membrane is flat within 8 cm.
and
The depth difference between a sphere and a parabola is a maximum of 8 cm.

Figure 2-2

of the art focal planes will support 10,000 x 10,000 detectors, the focal array will be 10 cm across, and will have 100 million detectors.

The focus position must be held to $f = 2\lambda(f/d)^2$ which is 100 microns. So the piston tolerance will be 100 microns. The tip/tilt errors must be held to an accuracy where the spot size is held to rest on one detector. Since this is 10 microns out of a distance of 250

meters from the primary, this means an angle stability of 4×10^{-8} radians. This does not have to be the absolute tolerance of the line of sight, however, as the image can be processed in the focal plane, and closed loop tracking instituted to keep the image of a star on a detector. Thus the accuracy must only be to keep the spot on the focal array, or 10,000 times less stringent, or 0.4 milliradians which is doable.

The most critical aspect of the system, its ability to correct errors of the primary aperture, needs to be determined. Start with the liquid crystal correction plate, located immediately in front of the detectors. The best resolution being discussed for liquid crystals in 10 years is about 100 line pairs per millimeter. This is equivalent to a resolution of 10 microns, which matches that of the detector sizes in the focal array.

Since the magnification of the system is 250 (25m primary divided by a 10 cm. focal array), then the smallest areas resolvable by the liquid crystal on the primary surface are 2.5 mm across. This means that larger spatial scale errors can be corrected by the crystal, but that the membrane smoothness must be such that smaller spatial scale errors are smaller than those tolerable for a good quality image. This places a requirement on the surface finish of the membrane material, since it is not planned to stretch the membrane to remove surface irregularities.

It should be mentioned that it may be possible to plate or otherwise deposit a very thin coating on the membrane in order to reduce the size of the very small scale irregularities in lieu of stretching. If all fails, the membrane could be stretched, either within or beyond its yield point, in order to smooth these surface errors. This would involve more weight for some sort of toroidal structure. If gas pressure were used to stretch the membrane against the restraint of a transparent membrane, then the scatter from the transparent front membrane would be severely limiting, resulting in a haze of light that would limit viewing dim objects in the near vicinity of brighter ones.

This haze is the antithesis of the “dark field” desired by astronomers, and is the main effect of a transparent membrane, not the signal attenuation or its discrete scatter. It is for this reason that the surface irregularities of the Hubble Space Telescope are held to rms values of less than 10 manometers. A possible way out is to stretch a metallic membrane past its yield point, thus rigidizing it, and then discarding the transparent inflation membrane. Such an approach has been successfully demonstrated by Neville Marzwell of JPL, in the last 2 years for 1 meter class stainless steel mem-

branes, but it is not known whether the technique can be extended to very large apertures such as 25 meters or greater, or what the weight scaling factor would be.

Returning to the correction system performance. If we assume that the electron beam technique can reduce the initial errors of a piezoelectric membrane by a factor of 100 (a not unreasonable expectation given the performance of many existing closed loop systems with similar parameters), then the initial errors in the membrane before e-beam correction can be as large as 100 times 2.5 mm, or 25 cm. These and the following numbers are illustrated in Figure 2-3.

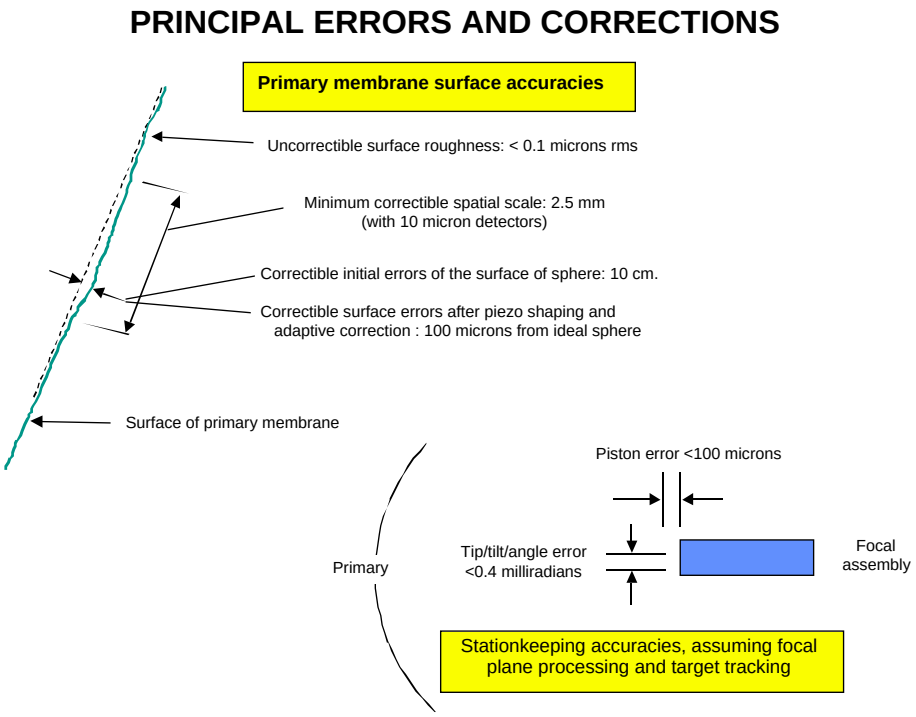

Figure 2-3

The allowable presence of 25 cm initial errors in a 25 m. diameter membrane means that the membrane can be flat before it is shaped by the electron beam, since it was shown above that the deviation between a parabola or a sphere from flatness never exceeded 12.5 cm. This can be achieved without any stretching, unless such is required by the remaining fine scale surface errors.

Although in principle it is possible to line the front of the primary membrane with liquid crystal material, so that the light rays exiting the primary are fully corrected, the weight of such a layer will dominate the weight of the telescope due to its 25 m. size, particularly because it is likely to be thick to attain the large

correction capability envisioned. It is therefore better to place the liquid crystal corrector in front of the focal array, where its size need only match that of the focal array, or 10 cm.

At this point, therefore we have sized the principal features of the telescope.

2.3 Design Reference Missions

Three typical missions for such a telescope and arrays of telescopes were assembled, to act as references for performance calculations and characteristics determination. These are shown in Figure 2-4. These design reference missions were chosen to stress the concept and demonstrate challenging missions not possible or disadvantageous to implement in other ways, while at the same time span a reasonable range of missions which would likely be of interest to NASA in the long term future.

Three classes of missions were settled on: Earth observation missions, general astronomy missions, and implementation of imaging of planets around other stars. A number of missions were described in a general way within each of the above categories. These were reviewed individually, and combined into three specific Design Reference Missions (DRMs) which encompass most of the objectives of all classes.

DESIGN REFERENCE MISSION SUMMARY

	DRM-1	DRM-2	DRM-3
Principal mission	General Astronomy	Earth science	Kuiper/Oort imaging
Secondary missions	Imaging planets as part of Origins; Earth observation	Weather/climate Astronomy Earth observation	Extrasolar Planet Multipixel Imaging; Earth observation
Location	GEO or solar orbit	GEO or solar orbit	GEO or solar orbit
Collector diameter	25 meters	4 meters	25 meters
Total diameter	25 meters	60 meters	200m-200 Km.
Fill factor	100%	15%	5% or less
Wavelengths	vis and near IR	vis and near IR	vis and near IR
Spectral width	broadband	multispectral	broadband
Sunlight exposure	shielded	shielded	shielded
Target capability			
FOW steering	4π steradians	4π steradians	4π steradians
Rapid scanning angle	10 deg	none	none
Targets imaged (5 yrs)	10,000	10,000	10,000
Average reorientation	10 deg	10 deg	10 deg
Reorientation time	1 hour	1 hour	1 hour

Figure 2-4

- DRM-1

This instrument implements a filled aperture telescope 25 meters in diameter. It encompasses both a general astronomy instrument such as Hubble and NGST, as well as the largest single collector currently called for by the Origins program to image earth-sized planets around nearby stars. It operates in the visible light region and near-IR to about 2-3 microns wavelength, avoiding longer wavelengths to avoid active cooling. It is a direct imaging and spectroscopy instrument, not an interferometer, though it could be used in arrays to form interferometers. It will demonstrate the practicality of implementing a filled aperture telescope with adaptive thin film membrane optics, liquid crystal or equivalent second stage correction, and an absence of a truss structure. It could be located in GEO, solar orbit or one of the Earth-Moon Lagrangian points.

- DRM-2

This instrument implements a dilute imager sparse array 60 meters overall diameter, with 24 individual apertures of 4 meters diameter each. It is intended to continuously image the Earth from GEO at high resolutions for earth science and for fine scale weather and climate data, as well as for national security applications. In addition it would be an astronomical telescope for general purpose astronomy where very high resolution was principally needed, such as to resolve individuals in star and galaxy clusters at extreme ranges. Its chief benefit would be its ability to dwell for long times on specific areas for change detection, both diurnal and longer term, while obtaining data at a very fine resolution; to scan large Earth areas at the same high resolution; as well as function at very low photon levels with extremely high resolution for astronomical applications. For weather and climate applications it would greatly increase the data points sampled on the global grid, and allow much more accurate forecasting globally.

This instrument would represent a 15% filled dilute imager with snapshot capability, which does not require any movement to fill the u-v plane and obtain quality images. It is not an interferometer. Though it was not evaluated for such use, it could be operated in an interferometric mode, either within the array or between widely separated apertures, for the Origins Program.

- DRM-3

  This instrument implements a dilute imager sparse array of 200-1,000 meters overall diameter, with 124 individual apertures of 20-25 meters diameter each. It would be aimed at high resolution astronomical imaging of Kuiper belt and Oort cloud objects and planetoids, as well as other extremely fine resolution and extremely sensitive astronomy. It would have the ability to do snapshot imaging without involving spacecraft movements to fill the u,v plane, yet obtain quality images. It could also do astrometry and general astronomy. Though it was not evaluated for such use, it could also be operated in an interferometric mode. For such use the elements would be much more widely separated, up to hundreds of Km. and interferometry used either by pairs within the array or even between widely separated identical arrays.

  This instrument would represent on one extreme an extremely dilute imager, only 5% filled. Although such instruments could also be used for earth science, their resolution is much greater than useful. It could, however, be used for national security applications. Its best NASA application would be the implementation of the so-called Terrestrial Planet Imager, the end desired point on the Origins program, to image Earth-sized planets around other stars with multi-pixel resolution.

The above missions are typical of NASA space and earth science future desired aaplications of large space telescopes.

3. EXPECTED PERFORMANCE AND UTILITY

3.1 Performance

The performance of the telescope and telescope arrays, operated in the three design reference missions is readily calculated, given their overall construction as per Chapter 2.

In each case, the telescopes are operated in the visible light region, about 0.5 microns wavelength. It is recognized that for astronomical use there is increasing preference for long-wave infrared observations, partially to penetrate interstellar dust and partially because of the increasing apparent red-shift with distance. Such observations require cooling of the optical elements below temperatures that can be readily attained by passive means, and much lower temperature of the detectors. These requirements result in power, weight, and complexity.

While there are no inherent reasons why membrane telescopes could not be designed to operate in the LWIR, the added complexity was rejected for this first proof-of-principle Phase I study. Thus, while the telescope designs in this study can operate at near-infra-red wavelength, perhaps to 2-3 microns without additional cooling other than obtained by passive means, it is recognized that more detailed and/or follow-on studies should address LWIR concept de-signs. These are, however, beyond the means of the intended Phase II, and are really a separate study.

The 25 m. filled aperture telescope will have a total field of view given by its focal length and detector array size. For 250 m. and 10 cm. respectively, this results in a 0.4 milliradian field of view. Likewise its resolution is given by the detector size in 250 m., or 40 nanoradians. These numbers are shown in Figure 3-1.

By any measure, any of the three telescope configurations will have impressive performance.

OVERALL PERFORMANCE

	DRM-1 One 25 m. aperture	DRM-2 4 m. apertures, 60 m. diameter	DRM-3	
			25 m. apertures, 200 m. diameter	25 m. apertures, 200 Km. dia.
Field of view	4×10^{-4} radians	1.6×10^{-4} radians	10 arc sec.	1×10^{-2} arc sec.
Resolution	4×10^{-8} radians	1.6×10^{-8} radians	1×10^{-3} arc sec.	1×10^{-7} arc sec.
Sensitivity (compared to NGST)	100 x	61 x	12,640 x	12,640 x
Sensitivity (compared to Hubble)	10 x	6 x	1,230 x	1,230 x

Figure 3-1

Additionally, the telescope performance if used to image the ground from GEO will be phenomenal, with ground resolution of less than 1 m. continuously from GEO. even with array diameter limited to 60 m. It should be mentioned that for ground or atmospheric imaging much smaller primary apertures suffice, with 4 m. diameter chosen for the reference design, as the signal is ample compared to celestial observations. Spreadsheets from a precision imaging sensor design and performance algorithm were created that completely define the performance of the 25 m telescope when viewing both celestial sphere objects and terrestrial objects.

The performance of the telescope may also be described in terms of its weight and areal density. This is because most telescopes of the same primary aperture will have similar resolution if well designed, due to the fundamental diffraction limit which they all approach. Thus one measure of telescope performance is indeed how lightweight a telescope is for its aperture diameter.

The estimated weight of the concept is shown as a function of its aperture in Figure 3-2. It is seen that the all-up weight in GEO orbit of the telescope is about 150 Kg for a 25 m. aperture, and about 800 Kg for a 100 m aperture.

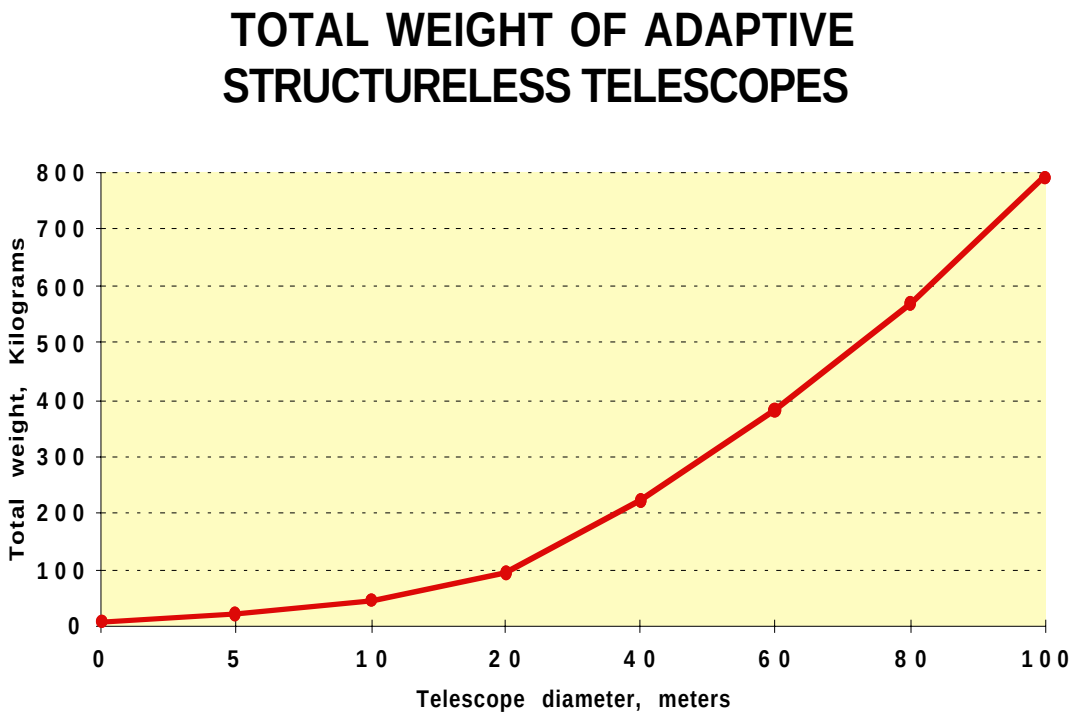

Figure 3-2

In addition, the areal density of a telescope is a means to assess its relative performance readily. Figure 3-3 shows that the areal density of the all-up telescope is 0.2 Kg/square m. at a diameter of 25 m., but drops to less than 0.1 Kg/square m. for a diameter of 100 m. Even at 0.2 Kg/sq.m., this is four orders of magnitude less than that of the Hubble Space Telescope and two orders of magnitude lighter than NGST, verifying that the new concept is truly revolutionary.

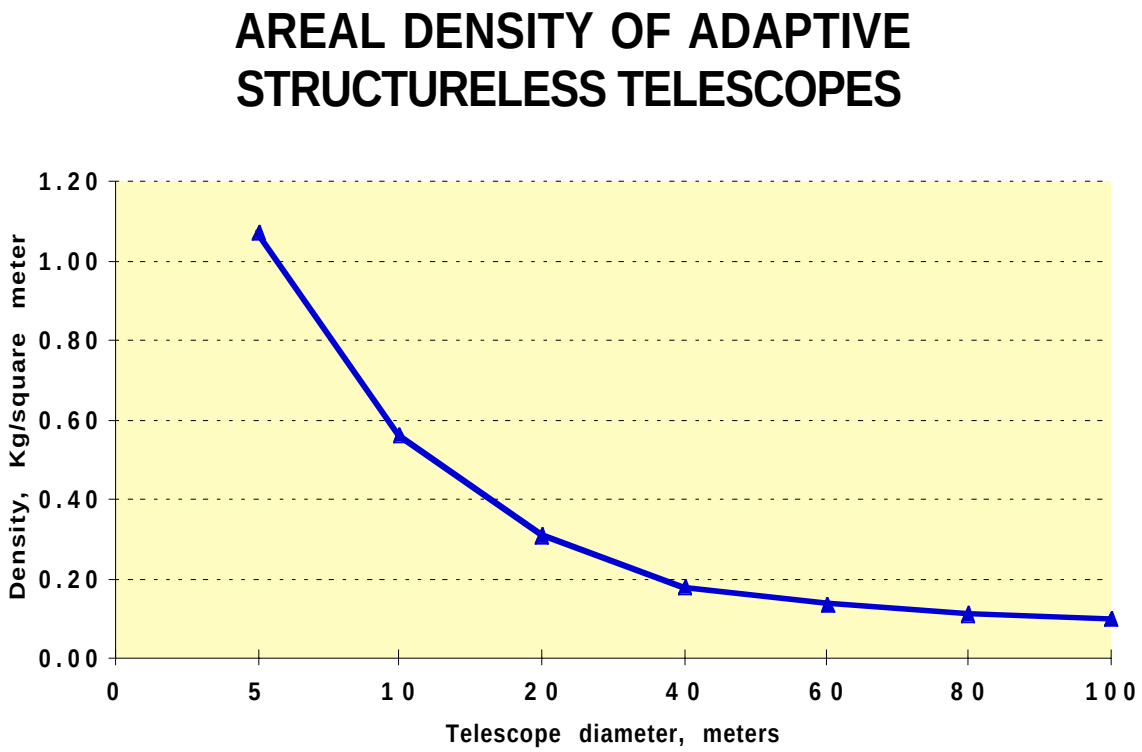

Figure 3-3

3.2 Utility

Astronomers have always pursued larger and larger apertures, and more lately, separation of large apertures, in their quest for resolving power. The separation buys great resolving power, but large apertures must be used as the photons collected from dimmer and dimmer objects require larger and larger apertures to record data, even with very long integration times.

3.2.1 General astronomy

A 25 meter telescope with filled aperture would be able to see 100 times fainter celestial objects than Hubble at the same distance, or the same stellar magnitude objects 10 times further. For practical purposes this means that it would certainly be able to detect objects at Hubble's limiting sensitivity (30th magnitude objects) out to the edge of the universe, and the beginning of time.

Another way of stating that is that it would be able to detect stars that are 8 stellar magnitudes fainter than those barely detectable by Hubble. It would, of course, image extended objects such as globular clusters, nebulae, gas clouds, remnants of novae, and other celestial objects. It would certainly be able to find and image many gravitational lens effects, and by better calibration of cepheid variables obtain a more accurate yardstick for the size of the universe and everything in it. A 100 meter telescope would do the same, but of course a factor of 4 further or a factor of 16 dimmer (6.4 stellar magnitudes, for a total of 14.4 stellar magnitudes).

The general astronomy observations which this telescope could facilitate include obtaining a better understanding of:

- Formation and evolution of galaxies
- Formation of supernovae rates
- Verification of the Cepheid Variables as yardsticks
- Structure of cluster galaxies
- Brown dwarf stars and extrasolar planets
- Detection of circumstellar accretion disks
- Observations of Kuiper Belt and Oort cloud objects

3.2.2 Imaging planets around other stars

This telescope would be the means to implement the NASA Origins Program's Terrestrial Planet Imager, which aims to obtain 10-100 pixels images of Earth sized planets orbiting nearby stars. The Origins program has defined its needs as 25 telescope clusters, each composed of two 25 m telescopes and two 12 m telescopes operated as star-nulling interferometers within the cluster, with the 25 clusters operated as a giant interferometer ring several hundred kilometers across.

The 25 m. filled aperture telescope defined in this study is the first design concept that will meet these NASA requirements, and allow the terrestrial planet imager to be built.

There are other conceptual means for making 25 m diameter telescopes, but all of them are at least an order of magnitude heavier, and including launch costs will be about 2 orders of magnitude costlier. In addition, they are all brute force concepts which strive for mechanical precision that boggles the mind, and are unlikely to be practical, let alone affordable.

3.2.3 Earth observations from GEO

In addition the instrument can make earth observation for phenomena ranging from atmospheric, pollution, weather, and climate observations to a host of the kind of surface and ocean observations that EOS will make. The difference is that rather than making separate observations in short passes, it can dwell over an area as long as desired, obtaining exquisitely detailed information with both spectral and spatial resolution only possible from low altitudes today. The fact that the concept lends itself to GEO deployment means that far fewer spacecraft will be needed than in any LEO constellation, and their operation is far simpler due to their continuous staring design.

The downward looking telescopes can be fitted with a 2 m fast scanning mirror, which will allow steering the field of view over essentially the entire visible earth from GEO without repointing the ensemble. This kind of instrument thus could be initially an adjunct to the LEO satellites of the Earth Observing System, supplying log term climate and resources change information by continuous direct observation. Eventually three such spacecraft in GEO would supplant the EOS system, aided by one LEO satellite for polar coverage.

Whatever the eventual constellation design, it is clear that the ability to continuously monitor areas in high spectral and spatial resolution will be extremely useful for earth observation goals of NASA.

3.3 Cost

Space systems have always had a cost roughly proportional to their weight. This is mostly because in the past and current systems the weight is proportional to the number of man-hours required to design, develop, manufacture, and test the spacecraft. This is because everything has to be designed and manufactured to high precision as it is generally not possible to make adjustments in space (the Hubble repair is an exception, since other spacecraft are not designed to be serviced. Furthermore the design of Hubble for ser-

vicing was hugely expensive). The actual cost of the raw materials going into a typical spacecraft is minuscule. Nonetheless the weight of a spacecraft was usually correlated with its performance, and also with its cost.

When we replace structures with information, and use MEMS-scale integrated units throughout, the information processing equipment is extremely lightweight compared to its powerful functions, breaking the historical correlation. The materials costs will still be minuscule, but since precision will no longer be necessary , at least not to the degree it is required in current systems, the systems engineering man hours for these new systems will be greatly reduced. This is a chief result of having the several adaptive closed loops of the conceptual design, so that the desired precision is achieved by software after the device is in space.

While it is not yet clear that making adaptive extremely lightweight telescopes like the present concept will reduce their cost proportionately to their weight, it may approach that. This is because mechanical complexity and mass are replaced by intelligent use of the space medium, which substitutes information-intensive functions. Given the plummeting cost of ever more complex and capable information processing devices, the weight-cost relationship of all previous spacecraft may actually be a reasonable model still, but operating in an entirely different regime.

Of course, there is no data to support that contention. However, it is also clear that cost analysts haven’t the faintest idea of how to go about estimating the cost of these new classes of adaptive gossamer spacecraft, as their tools are historical. No history—no cost prediction. Nonetheless, since weight-based costing has proven so successful in the past, cost analysts will first try to extrapolate that technique to the new spacecraft.

Let us do that. Let us assume that the same relationships still hold for very large but very lightweight spacecraft. If that were the case, using today’s cost estimating weight based techniques, a complex first build scientific spacecraft will cost About $0.3 million dollars per kilogram. Even using that relationship unquestioned, a 150 Kg 25 m diameter telescope would only cost $ 45 million. With the launch being on a Pegasus class launch vehicle, the entire cost of a 25 m telescope would be about $60 Million.

Compare that with a 25 m telescope built using the NGST techniques of deployable solid optics and a composite truss, which weighs about 25 Kg/sq.m aperture, which is 2 orders of magnitude more that the present concept. The NGST-type telescope would weigh 12,500 Kg, and

cost about $4 Billion. Its launch would cost another 0.5 billion on a Titan Class vehicle with special upper stage, for a total cost estimate of 4.5 Billion. It is clear that telescopes as large as 25 m are unaffordable unless constructed in entirely new paradigms.

In addition, let us estimate the cost to develop and launch the 100 telescopes required for the Terrestrial Planet Imager. 100 telescopes of the NGST class would cost 100 times 4.5 billion, or 450 billion. In contrast, 100 telescopes of the current concept would cost 100 times 60 million, or 6 billion. If we assume these costs to be spread over 10 years, then we have $45 Billion per year for the NGST type telescopes versus $600 million per year for the new concept.

The difference is not only nearly two orders of magnitude, it is the difference between being ridiculously unaffordable versus being no more expensive than other major NASA programs. In fact, developing a new concept Terrestrial Planet Imager of 100 25 meter diameter telescopes would cost no more that about 1/3 the annual cost of the International Space Station. Thus the new concept is absolutely required for cost reasons alone if the Terrestrial Planet Imager is to ever be more than a paper dream. This crude cost comparison is illustrated in Figure 3-4.

VERY PRELIMINARY COST ASSESSMENT

(Using current cost estimating relationships)

	New Concept	NGST technology
25 m. general purpose astronomical telescope (launched, and in solar orbit)		
•Weight	150 Kg.	12,500 Kg.
•Cost	$ 60 Million	$ 4.5 Billion
Terresterial Planet Imager (100 25 m. telescopes, launched and in solar orbit)		
•Weight	15,000 Kg.	1.25 Million Kg.
•Cost	$ 6 Billion	$ 450 Billion
•Annual cost, decade program	$ 600 Million	$ 45 Billion

Figure 3-4

4. SUBSYSTEMS/TELESCOPE ELEMENTS

This chapter details the design considerations for the various sub-systems and elements of the telescope concept.

4.1 General

The feasibility assessment of the new concept can only be performed after all its subsystem elements are defined to a first level. This chapter therefore contains those designs and design considerations that were generated during the Phase I analysis.

It must be recognized that the very limited funds of Phase I only permitted a “conceptual” level of design to be performed, rather than the more detailed design usually expected for a systems design study. Nonetheless all elements and subsystems were investigated to the point where some numbers were obtained for their characteristics and performance.

In addition, greater resources were expended to better define the key elements of the system, those being the adaptive membrane, sun-shade/power projector, focal assembly, and liquid crystal corrector. It is recognized that much more detailed design analyses must be done on all the elements before most system engineers would feel comfortable with the numbers. That is exactly as it should be, for if this concept is found feasible and useful, NASA’s resources then could be applied to carrying out well funded Phase A studies to fully define the system.

In addition, many of the necessary technologies require a degree of advancement, some more than others. These technologies will be identified in Chapter 7 for pursual into a Phase II activity. Once Phase II defines the technology developments necessary and develops a roadmap/development plan for them, the concept can be recommended to NASA as a candidate inclusion into the main line space science activities of the agency. These could include funding of space and/or ground demonstrations, and other programmatic options.

The major elements of the telescope concept are the adaptive membrane; the liquid crystal corrector; the focal assembly; the fast steering mirrors; the electron beam assembly; the figure sensor; the sunshade/power projector; the formation flying metrology; and the information processing, command, and communications system. These will be discussed individually in sections bearing the same titles.

4.2 Adaptive membrane primary mirror

The primary mirror is the heart of the telescope, and at the same time its biggest stumbling block. There is extensive research ongoing in several laboratories to employ an inflatable reflective membrane, supported and shaped by gas pressure against a clear front membrane. The current aims of stretching the membrane by gas pressure are driven by the low weight and possible ready deployability of such designs, the ability to make apertures larger than the diameter of the launch vehicle, and the ability to remove most surface wrinkles and irregularities by the stretching action. Of these the last is the most significant, since surface irregularities constitute the irreducible minimum for image quality.

The most work is being done by the USAF Research Laboratories in Albuquerque. There Dan Marker and Richard Carreras have been pursuing a DOD funded effort to develop inflated, stretched membranes for telescope primary mirrors. These efforts have been supported by those of Sergio Restaino and Mark Grunheisen, who have pursued combining them with a liquid crystal corrector to take out the remaining surface errors. These efforts are aimed both at ground telescopes and at space deployable telescopes. They have published extensively on this subject. See the bibliography in the appendix.

Their basic approach is to use a liquid crystal spatial light modulator, described more deeply in Section 4.3, to correct the inaccuracies in the membrane primary. Their approach must try to reduce membrane errors to a few to tens of wavelengths from the ideal, because that is the correction range of their liquid crystal corrector. There is a benchtop simulator in operation which demonstrates both the stretched membrane and the liquid crystal corrector, though not yet together.

The aim of most of these efforts for the membrane is to more closely approximate a parabola, rather than the dreaded “W” curve, which is a term describing the fundamental shape of the errors between all stretched membranes and a parabola. By using separate vacuum rings to set the initial curvature and then to apply tension with minimal curvature changes, they have shown that such errors can be reduced somewhat, however it is not clear how such techniques would be applied in space, where pressure must be used for actuation.

While these techniques may ultimately work, they have great disadvantages in being applied in space. This is because the stretching requires high tensile strength in the membrane, and the required large forces require heavy rings and toroidal supports against which to apply the tension, which partially negate the weight benefits of

the membrane. Additionally, there must exist a clear membrane to contain the pressure. This is a fundamental sticking point, inasmuch as the reflective membrane must either be rigidized and the clear membrane cut away, or the effects of scattering from the clear membrane must be accepted. This scattering will significantly limit the utility of the telescope. In addition, a clear concept of how the membranes are to be folded, and yet deployed without surface mars from creases. has yet to emerge.

Thus the approaches being pursued by AFRL and others, while admirable, are likely to be difficult, heavy to implement, or both, and result in a requirement for liquid crystal correction range greatly in excess of what they have available. Fundamentally, these approaches still follow the mindset of earth-based techniques and experience, and will not result in practical devices for space use. This is why these techniques are deliberately avoided in this study.

A number of other inflatable telescope concepts were also investigatigated by L'Garde Inc. under USAF contract, and also by Robert Freeland of JPL. Forecasts from these sources indicate that some combination of passive techniques using pre-dimensioned materials can undoubtedly be made to work for very large (perhaps up to 100 m) antennas at frequencies up to 30 GHz, yielding space antennas weighing 5-10 Kg/sq.m. However, except for encouraging words, there is little confidence and not much innovation in extending these techniques to large optical wavelength telescopes, which are at least 4 orders of magnitude more difficult to address.

4.2.1 A new and fundamentally better approach

It is fundamental that most investigators are trying to extend earth-based techniques using some form of truss and stretching structure, necessary in 1 g, but these are the wrong techniques for use in zero-g space. As a result of the above the present concept was conceived to use an unsupported membrane whose shape is remotely adjustable, and to stationkeep all the other elements so as to avoid the need for any truss whatsoever.

The primary membrane for this concept is thus conceived to be a very thin piezoelectric bimorph film, which is curved at will not by pressure or tension but by applying a charge distribution across its entire surface via a scanning electron beam. Since there are essentially no differential forces over tens of meters in deep space, the electron beam current can be so adjusted that any desired curvature is attained without any net tension forces being required in the membrane, and without requiring any transmissive films to be in the light path.

The electron beam charge distribution can then be varied in accordance to a downstream figure sensor, which detects the gross as well as the fine scale actual surface shape of the membrane and compares it to a reference figure. Having thus created a closed loop, the system will remove irregularities from the surface and modify its gross curvature shape to meet any desired primary mirror figure. It will then hold that shape against disturbances. Furthermore, this shaping will be responsive to software commands, so that a parabola shape can be created whose focal length can be varied at will by software. The principle of closed loop figure control is illustrated in Figure 4.2-1. Its implementation is illustrated in Figure 4.2-2.

In addition to forming and maintaining a given parabolic shape, this principle can have a number of unique applications such as zooming telescopes, as well as easing the requirements for precision relative stationkeeping of the telescope elements. This membrane concept will have the further beneficial effects of being much lighter than any stretched membrane, as tension forces do not have to be resisted thus allowing use of extremely thin films, and because no large diameter torus is required.

ADAPTIVE MEMBRANE CORRECTION

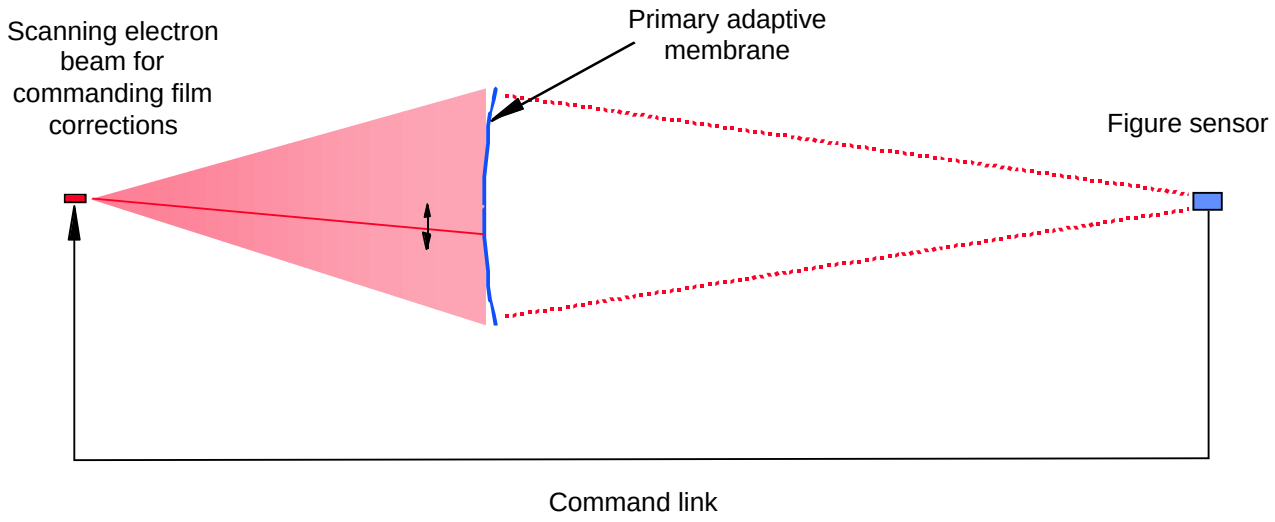

Figure 4.2.-1

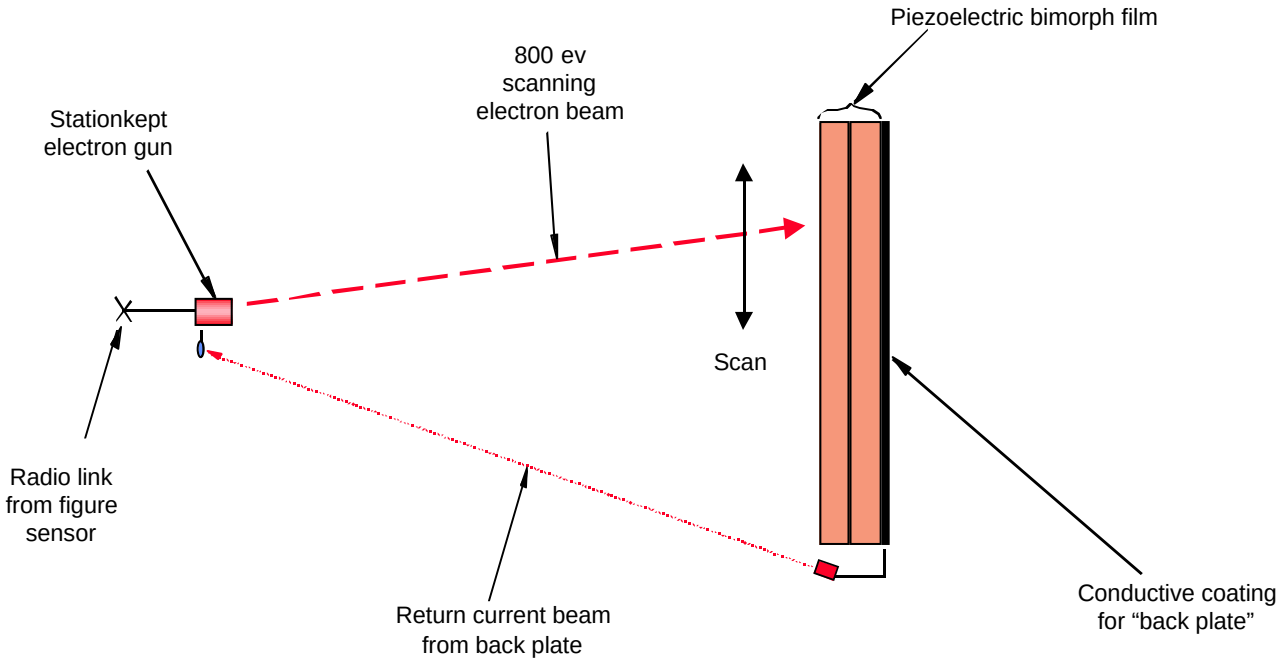

Figure 4.2-2

While it will be shown in this chapter that this approach has enormous potential, it is not without difficulties and risks, which are also discussed, leading to a required technology program which is recommended in Chapter 7.

4.2.2 Materials

The choice of materials for the adaptive membrane depends on a number of aspects, the most crucial of which is its surface characteristics. This is because, when all is said and done, the membrane must act as a good quality optical reflecting surface, which generally means that the surface irregularities must not exceed about 1/14th of the dimensions of light, rms. This means about 30 nanometers rms for visible light.

Although the closed loop adaptive control system will greatly diminish the amplitude of irregularities, it will be unable to do so for spatial scale errors smaller than its ability to sense and/or control. Since the electron beam is unlikely to be able to be focused to a spot smaller than a millimeter or so

at the offset range likely to be needed—tens of meters, errors in the surface smaller will not be correctable. These will then produce unwanted effects in the optical performance, including defocusing, light smear, and image intensity loss. These effects are so severe that current telescopes generally grind them out to well below tens of nanometers so that the system errors will not exceed that. In fact, in order to attain an extremely dark field, Hubble's primary mirror polishes down to 1 nanometer surface irregularities.

There is a paucity of data on the surface roughness of plastic films at the micron level. Some measurements of thin films have been found, and are shown in Figure 4.2-3. These clearly show that the scale of surface errors found in Mylar films of various thicknesses was 0.03-0.045 wavelengths, which is equivalent to about 0.02 microns or 20 nanometers. In itself this is not bad at all, though structure is apparent that is caused by the manufacturing process (such as roller roughness).

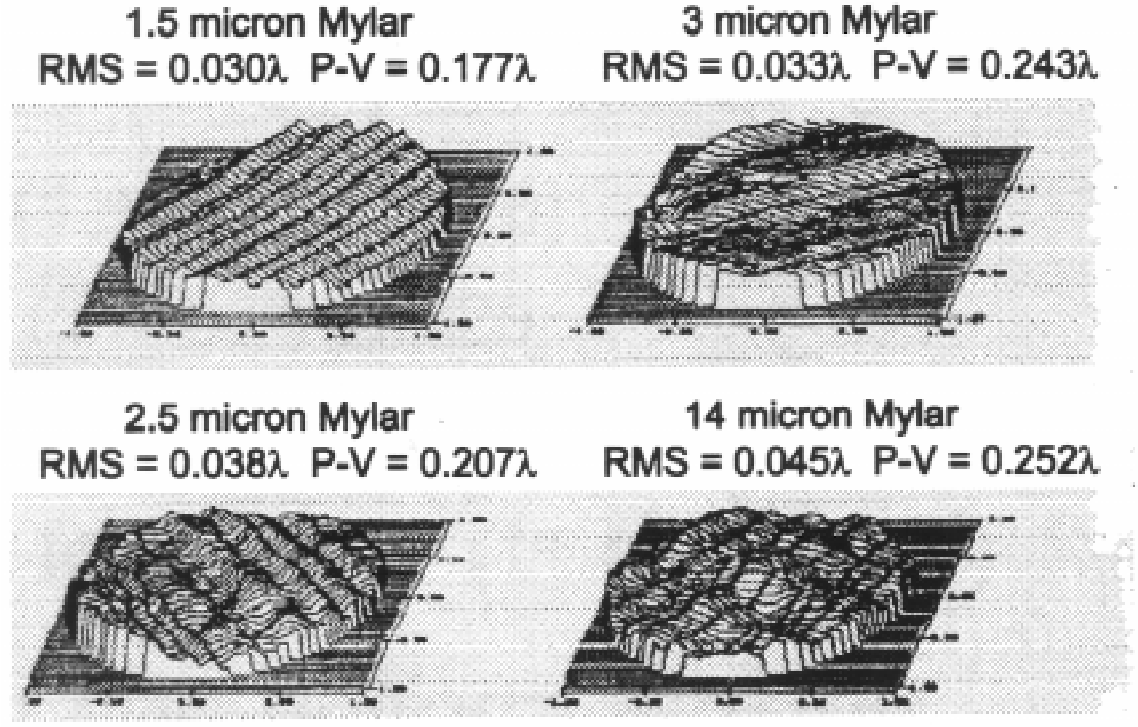

Figure 4.2-3

While the magnitude of the roughness is tolerable, the structure in the surface will result in patterns on the focal plane Furier transform amounting to correlated scatter. Though not calculated its effects are not good. Thus this data is inter-

preted as fairly benign, inasmuch as particular attention to manufacturing processes could probably result in substantially smaller surface roughness, removal of the patterns, or both.

Discussions were held with Neville Marzwell, JPL, who led their activities in large unconventional mirrors. In a number of tests he determined that a number of different plastic films had surface roughness of 3-5 microns peak-to valley, which is equivalent to about
0.5-0,8 microns of rms roughness. He determined that if these films were stretched, their subsequent roughness was reduced to 0.01-0.1 microns rms error, though the measurements were not comprehensive.

In all materials examined the roughness after stretching returned to an intermediate value unless the material was stretched beyond its yield point. However in that case there are severe problems of thermal creep, and even worse, the material roughness becomes much greater upon thermal cycling, which is difficult (though not impossible) to eliminate in spacecraft.

A number of companies are actively producing precision films for the optics industry, among them being Dupont, Celanese, and Newport Research. Cellulite and Teflar are good candidates. The best are aimed at holographic films, and achieve remarkable smoothness in the surface and stability in the film. They are only produced in small sizes, but the companies could readily be induced to produce them in large sizes and quantities with appropriate contracts, and the likely cost will be low compared to typical space hardware.

The plastic materials investigated had their surface roughness considerably reduced by vapor deposition of a thin layer of aluminum, which is needed for high reflectivity anyway, if applied after the stretching process. This aluminum should not be electrodeposited, as that will tend to exaggerate the peaks and underfill the valleys, making the roughness worse. None of the above rules out plastic film, particularly if stretched, covered with aluminum or other “filler” material, allowed to destretch, and avoid all thermal cycling.

Marzwell investigated a different approach: namely stretching a thin stainless steel membrane by air pressure against a membrane that is later discarded. The metal is tensioned well beyond it yield point, and develops both a smooth surface and a rigid “set” which maintains its shape after depressurization.

The surface roughness is materially smaller than any plastic film he tested. Experimentation with other metals for the membrane are needed, as well as larger sizes than the 1 meter sample he tried in the laboratory.

Nonetheless it is clear that a rigidized metal membrane can probably be built with fine scale surface roughness. However it has the disadvantage that a compression ring is needed at its periphery to sustain the stretching forces, which could be heavy. It also cannot be adjusted after manufacture, and thus its figure must be precise on the ground in 1 g, with a different figure than it will have in space, compensating for the 0 g environment. This is very difficult. Worse, a 25 m memebrane would require a 25 m diameter launch vehicle. It could be stretched in space, but then the toroidal support will be heavier. The biggest shortcoming, however, is that it is unlikely that 25-100 meter mirrors can be made either in space or on the ground whose shape is precise enough for an optical telescope without some form of active control for adjustments.

Thus in these stretched metallic films the surface roughness problem solution has been traded for weight and lack of closed loop adaptation to disturbances and manufacturing as well as deployment imprecisions.

Discussions were also held with Dr. Patrick Mather, Air Force Research Laboratories in Wright Field. He is making small plastic film samples by the spin cast method, promising smaller surface roughness due to the absence of roller processing. These can be made in uniform or non-uniform thicknesses, but no designs for large scale mirrors have yet been considered, and no one knows whether that technique is capable of mirrors tens of meters across.

Even then , there would be stretching required, and there would not be any closed loop shape control in either the gross or fine spatial scales. However Dr. Mather is pursuing a number of other approaches that may make the manufacture of the required films in large sizes practically attainable.

Another very promising line of research is being pursued by the Directed Energy division of the Air Force Research Laboratories in Albuquerque. Their interest in membrane optics for high energy laser systems places even more stringent demands on the membrane that the telescope application, having to not only have an optically smooth surface but also to have extremely high reflectivity.

The latter requirement stems from the need to keep the heat input to the membrane at a minimum as it is exposed to megawatt laser beams. However, their surface requirements are the sane as for a telescope, as they also must have near-diffraction limited performance and low scatter losses. There are reportedly some very promising film material with such characteristics, being manufactured by SRS Technologies for AFRL.

In view of the above the possibility of manufacturing thin plastic films with the required surface roughness is very real, especially as the membrane thermal cycling can be essentially eliminated because it will be shielded at all times from the sun. Therefore the unsupported and unstretched but fully adaptive membrane is still the preferred solution even though much material research is needed before the right surface film is identified.

It is recognized that either an inflatable membrane or a rigidized metallic film could be used as a backup in case insurmountable difficulties arise in further investigations, even though neither would then have the adaptive feature that is such a powerful concept. <u>However, we state again that such showstopping problems have not been found to date.</u>

<u>4.2 3 Adaptive Control</u>

The implementation of a primary that is adaptive over its entire surface is completely new. The concept is founded on differential expansion of a piezoelectric bimorph film under electrical potential. This concept was investigated at very small scale by Dr. John Main, now at the University of Kentucky.

Though simple membrane tests were performed by John Main in the last few years which clearly showed that bimorph films could be bent by an electron beam, they were only crude deflection tests, only thick films were measured, no optical performance was measured, and little in the way of models was generated. While a sound basis for the basic principle was demonstrated, the work falls far short of what is required for this telescope concept.

The piezoelectric investigated by Dr. Main was polyvinylidene fluoride (PVDF) film, which is flexible, stable commercial product. It is available from commercial vendors in thicknesses down to 9 microns, but can be made much thinner, with films as thin as 200 Angstroms having demonstrated the effect.

There are a number of other materials that also exhibit the same effect, including PVC, nylon, and polynorbornene, however none found to date have as high a moment per unit voltage input.

If the entire primary membrane is made from a bimorph, that is two thin PVDF films bonded together, each of which is polarized in an orthogonal direction, the membrane will be caused to bend when a voltage is applied across it. This is because one layer shrinks while other expands. The principle is illustrated Figure 4.2-4.

The curvature produced by the local bending will be of radius r:

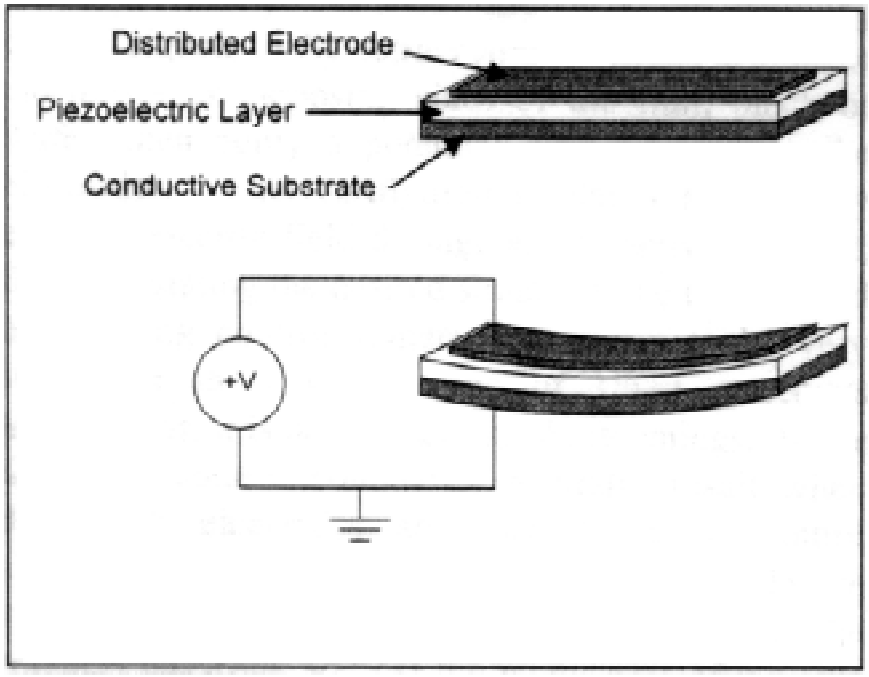

Figure 4.2-4 (From John Main paper)

$$r = k\frac{At}{Q}$$

Where A is the area to which a charge is applied, t is the material thickness, and Q is the charge deposited. This is illustrated in Figure 4.2-5. This means that for large curvature effect (small r) and a constant area, the thinner the section the less charge will be required for a given curvature attained. Thus the thin films contemplated in this telescope should be easy to drive from a charge point of view.

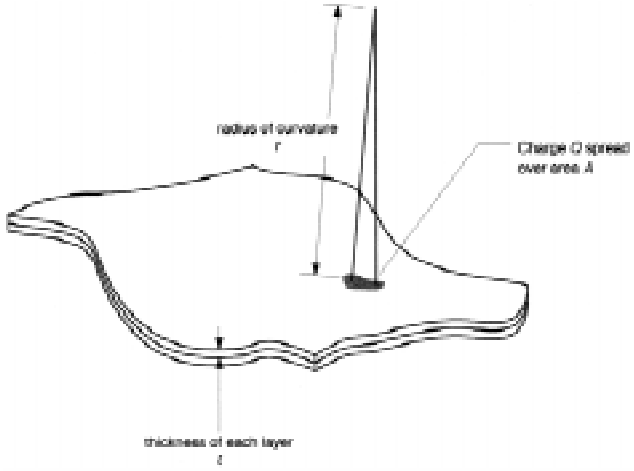

Figure 4.2-5 (From John Main paper)

The charge could be applied via electrodes plated on one electrode in a pixel pattern, with large numbers of X-Y leads to select the pixel where bending was desired. A better way was tested by Main, and reported in the literature, in which he aims an electron gun at the surface, depositing charge at the impingement point. This is illustrated in Figure 4.2-6. An electron gun is swept across the surface. It deposits charge on an area as small as the crossection of the e-beam. Since

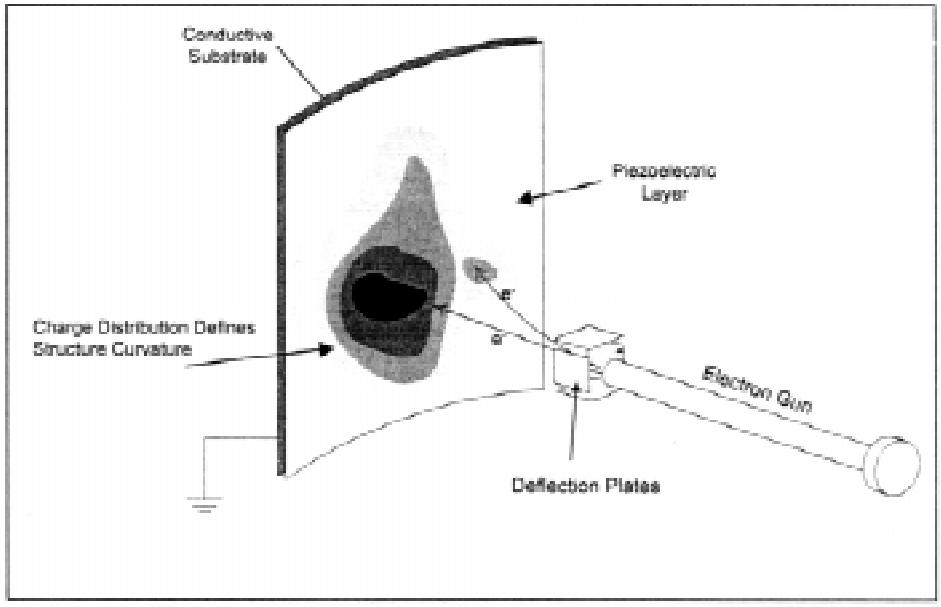

Figure 4.2-6

the PVDF is a good insulator, the charge will not bleed off immediately, but can take many minutes to do so. Thus the electron beam can be turned off after charging an area, and its

curvature will not change until it has to be replenished. This will limit the current and power required.

Experiments have shown that secondary electrons are created when a surface is illuminated by the beam. Those electrons tend to subtract from the deposited charge if the beam electron energy is below about 800 eV, and add to it if above. This is illustrated in Figure 4.2-7.

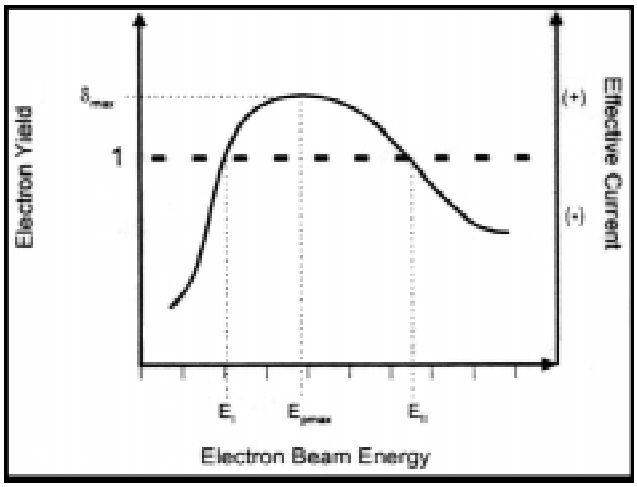

Fig 2.2-7 (From John Main)

As a result it is possible to obtain bi-directional bending of a piezoelectric bimorph by changing the energy of the electrons. This is illustrated in Figure 4.2-8 in which the electron beam generator is connected to an electrode plated on the

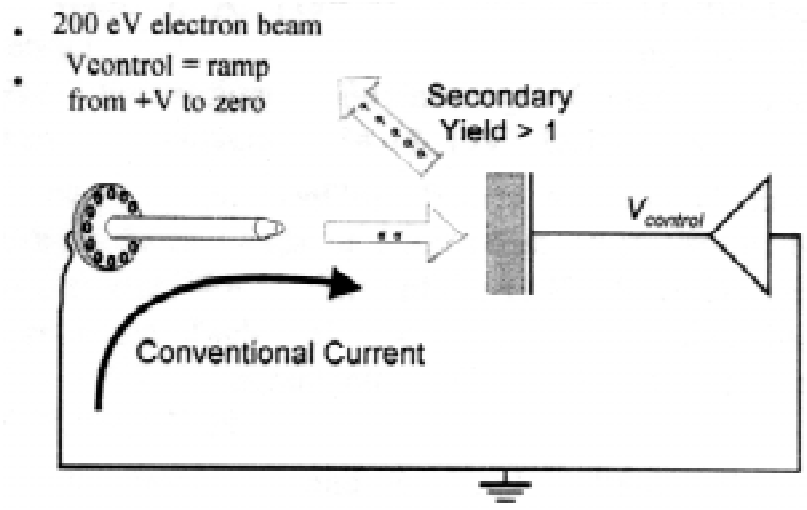

Figure 4.2-8 (from John Main)

back face of the film, controlling the current as well as the voltage between it and the back electrode of the bimorph.

While reverse curvatures may or may not be necessary in the steady state of the adaptive mirror, depending on the magnitude of the ripples compared to the gross desired curvature they may be needed in initial shaping. The ability to reverse the current will certainly be needed for removing charge to reduce bending in any area.

The measurements produced to date, though fairly crude due to instrumentation limits, demonstrate that bi-directional control is possible. The data, a portion of which is illustrated in Figure 4.2-9, also indicate that the effect is approximately linear over wide ranges, but the data quality is insufficient to verify that. Nonetheless sufficient data exists that a first conceptual design for an adaptive primary membrane mirror could be carried out.

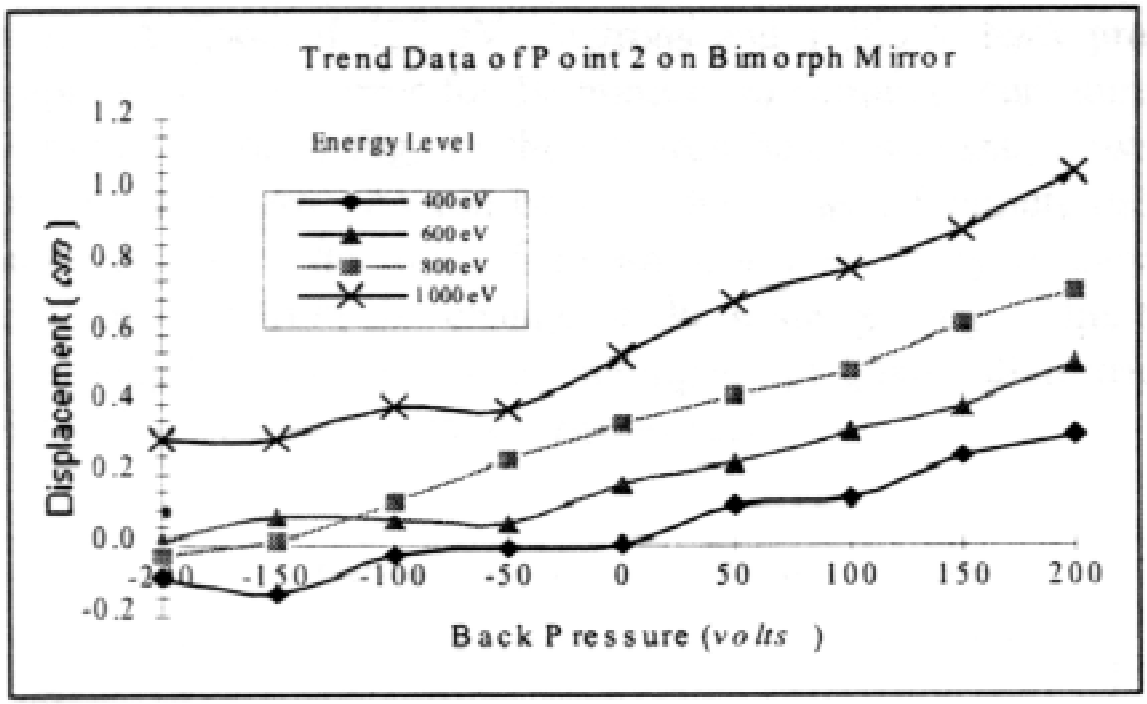

Figure 4.2-9 (from John Main paper)

The weight of the primary will be dominated by the weight of the PVDF film. The weight is given by

$$W = At\rho$$

Where A is the area, t the thickness, and ρ the density of the material. For a 25 m diameter aperture, the area is 490 square meters, the density of PVDF is 1800 Kg/cubic meter, and so the weight will be 0.9 Kg per micron of total film thickness. Since 9 micron films are available, it should be possible to construct a bimorph with two 9 micron PVDF layers, a 2 micron bond layer, and a shape memory alloy layer discussed later, to make a 25 micron thin sandwich weighing under 25 Kg. This would be the total weight of a 25 m diameter primary membrane.

To that must be added the weight of the electron beam generator and its power supply, and whatever propulsion devices will be necessary for membrane translation and attitude control. These will all be discussed later.

4.2.4 Artificial stiffness

The very thin films being considered in order to keep the weight low and allow sharp bending without permanent creases will result in a very “limp” film, with little inherent stiffness. However, upon application of the electron beam current, the membrane wiggles are straightened out under the commands of the figure sensor. Furthermore, if a force attempted to move a portion of the membrane without applying forces elsewhere as well, this would be resisted by the piezoelectric forces commanded by the figure sensor. This action is indistinguishable from the resisting forces caused by the natural stiffness, or resistance to forces, possessed by stiff solid materials.

As a result, the membrane will have a degree of “artificial stiffness” even if completely compliant before energizing. What’s more, this stiffness exists to a degree even after the electron beam is turned off, until the charges dissipate, but the restoring forces would be weaker due the missing closed loop.

Nonetheless, under normal use the adaptive membrane will act as though it has been “rigidized”. This will allow propulsive control and attitude reorientations by thrusters attached to the membrane, to be discussed next. The extent of such rigidization requires determination, and is proposed as a task for Phase II.

4.2.5 Membrane propulsive control

It is, of course, necessary to stabilize the entire membrane in space after is shaped correctly. The telescope must be pointed,

and its principal axis will be the axis of the primary membrane. Therefore propulsive units must be attached to it for control.

A major architectural construct made in a ground rule that the membrane would be rotated to a desired direction, but would neither translate nor stationkeep with the other telescope elements. It is assumed that the membrane is in solar orbit, with few disturbances. Once rotated to point in the proper direction, all the other elements would translate and rotate to place themselves on the membrane's axis, and perform the fine propulsive maneuvers to stationkeep there. Thus all elements would be slaved to follow the primary. Thus during a measurement interval, be it minutes or days, the membrane propulsion would be essentially quiescent for minimum disturbances to the membrane. Then the membrane would be rotated again to a new direction, and the process repeated. There would be a period allowed for the membrane dynamics, if any, to settle down prior to measurements beginning.

Because the membrane will posses the artificial stiffness discussed above, it will be possible to move it as a unit, albeit very slowly with minuscule thrust levels. The design concept adopted for this is to bond a large number of very tiny MEMS devices containing the thrusters around the membrane periphery. Thus the thrust will be very distributed, avoiding the stress concentrations that would be difficult for the membrane to resist without great thickness increases, with their concomittant weight.

This leads to the conceptual design illustrated before and repeated here as Figure 4.2-10. The propulsive units are envisioned to be MEMS versions of the Field Effect Electrostatic Propulsion thrusters that were conceived in Europe and are now in test. These thrusters have exhibited specific impulses of 1000-5000 using a variety of propellants, Indium for the lower and Cesium/Xenon for the large values. These thrusters would be ideal as they are proportional, avoiding the "minimum impulse bit" dynamic inputs. These thrusters have already been tested for over 640 hours in space.

Work has been going on at various laboratories, most notably at The Aerospace Corporation, to microminiaturize these thrusters into wholly solid state chip-like packages that would be both compact and lightweight, and inexpensive to produce in quantity. These FEEPs are ideally suited for such microminiaturization since they depend on large field strengths for their

FREE-STANDING MEMBRANE PRIMARY

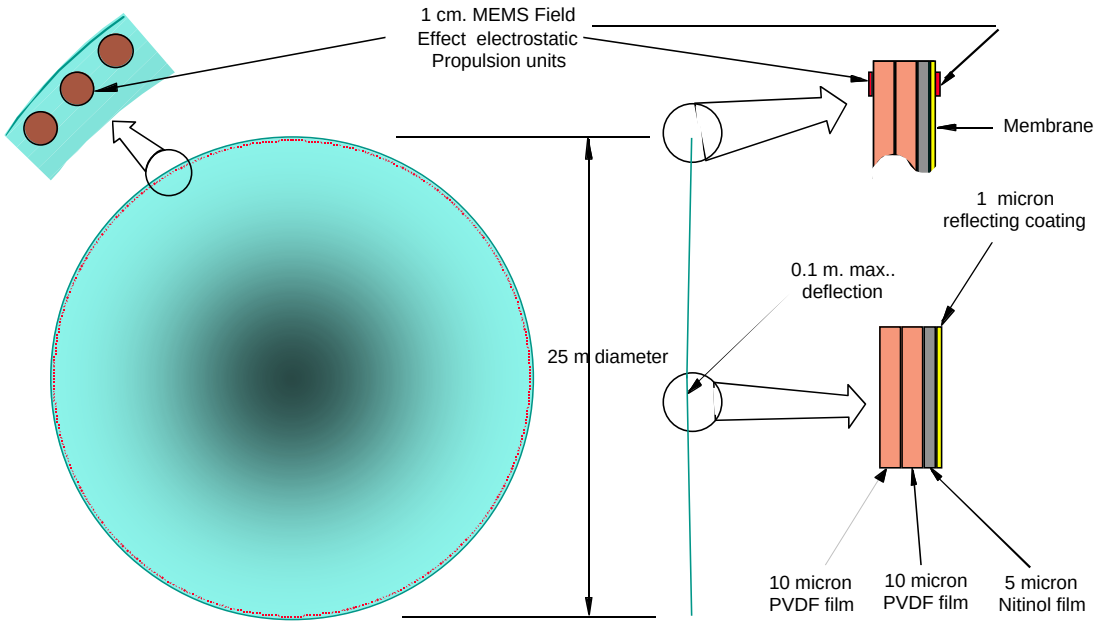

Figure 4.2-10

effect, which can be generated via sharp microscopic needlepoints even at fairly low voltages. The propellant can then feed through the hollow tips and be ionized and accelerated. The FEEP concept is illustrated in Figure 4.2-11.

FEEPs today are still too cumbersome and heavy to be useful on a thin membrane, being constructed from standard piece-part

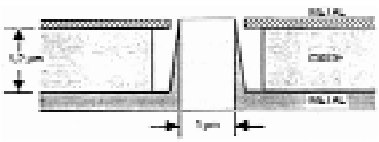

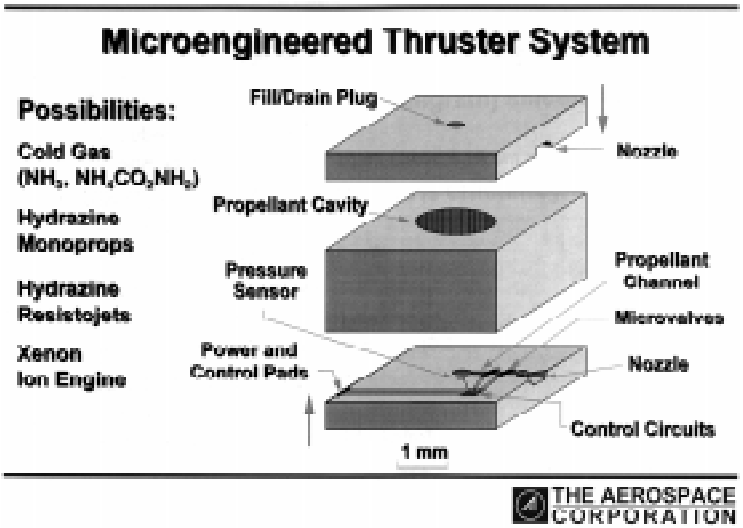

Figure 4.2-11

assembly techniques. however MEMS solid state designs have been performed at Aerospace and will be impressively small and efficient. Figure 4.2-12 describes their predicted characteristics within the next 10 years.

Characteristics of Field Effect Electrostatic Propulsion (FEEP)

AREA	1999 (Conventional)	2010 (MEMS)
Thrust each	25 micro N	10 micro N
Volume each	250 cu. cm.	0.2 cu. cm.
Weight each	4 Kg	0.00046 Kg
Power each	5 W	0.1 W
Specific impulse	1000-5000	1000-5000
Specific weight	**52,000 Kg/N**	**77 Kg/N**
Specific power needs	**200,000 W/N**	**10,000 W/N**
Specific volume	**10 cu. m./N**	**0.03 cu. m./N**

Note: the 2010 numbers are for Isp=1000

Figure 4.2-12

The calculation of required size and number of propulsive units for membrane control, and the weight of propellant required, follows setting of the measurement parameters desired. We assume that the telescope will have requirements as set forth in the Design Reference Missions of Figure 2-4. It will view 12 celestial sphere areas, each area being 10 degrees wide, per day for 5 years, requiring 20,000 major reorientations during its life. This allows one hour for the measurements and one hour for reorientation to the new direction. Once pointed in the new direction, the fast steering mirrors will be used to view many targets within the 10 degree viewing area, without reorientation of any major elements of the telescope.

The reorientation of the membrane will be done by accelerating torque for 5 degrees, followed by decelerating torque for 5 degrees. The membrane is treated as a solid lamina for this purpose, with moment of inertia about a line normal to its axis

and passing through its center. Given a membrane with mass of 24 Kg and radius of 12.5 m., its moment of inertia is 1875 s^4. The angular acceleration to attain 5 degrees of motion in 1/2 hour is $\alpha = \left(5/57.3\right)\left(2/1800^{2}\right) = 5.3x10^{-8}\ r/s$. The torque required to achieve this angular acceleration is $I\alpha = 1875x5.3x10^{-8} = 1x10^{-4}$ Newton meters. Since the radius id 12.5 meters, the force at the edge of the membrane (where the thrusters are located) must be $F = 1x10^{-4}/12.5 = 8z10^{-6}$ Newtons. This is indeed a very small force. Since we get about the same force from a single MEMS FEEP unit, we will throttle it back and use 100 such units over half the periphery of the membrane in order to distribute the force. Then the weight of all the thrusters will be 200 times that of a single unit. But the weight of a MEMS FEEP unit is small: it will be 1 cmx1cmx2 mm deep, at most. Thus its volume will be 0.2 cubic centimeters, and since they are silicon, which weighs2300Kg per cubic meter, the thrusters will weigh $W = 200x\left(0.2/10^{6}\right)x2300 = 9.2x10^{-2}$ Kg, or about 1/10 of a Kg. This is indeed small.

The propellant that the thrusters require is given by the total impulse in the 5 years of operation divided by the specific impulse. Thus $M = Ft/\left(I_{sp}xg\right) = \left(8x10^{-6}x1.6x10^{8}\right)/(1000x10) = 0.128$ Kg. The propellant required for the reorientations is so minuscule that it can be stored within the FEEP MEMS units themselves.

The FEEPS will require power to operate. This power will be $P = 6x10^{-6}\ N/6x10^{-5}\ N/W = 0.1$ Watts of power. Since two opposing thruster groups are required for balanced torque, the total power will be 0.2 watts when reorienting, which is about 50% of the time. Thus the average power will be 0.1 watts.

It is planned to permanently shade the membrane from sunlight in order to eliminate any differential heating effects, thermal transients, and sources of dynamic disturbance. Because of this, the power cannot be supplied to the thrusters via solar cells, and will be instead produces by solar cells on the sunshade, and beamed to the thrusters via a microwave or millimeter wave link. This is described in section 4.8.

It is therefore seen that the presence of some 200 MEMS FEEP thrusters around the membrane periphery will only increase its weight by less than 1 Kg. Since silicon is about the same density as PVDF, there will not be a great discontinuity in mass

and moment of inertia at the membrane periphery when the thrusters are attached. Due to their low thrust, they should be able to move the membrane as a solid unit, neatly solving the propulsion problem for very limp large thin films.

4.2.6 Packaging and deployment

One of the advantages of using a very thin membrane is the potential ability to fold it for launch into a very compact package, and have it deploy automatically by internal stored energy. This must be done in such a way as to attain the desired deployment shape while avoiding incurring any permanent creases, whose interference with the membrane's optical performance could be extremely damaging to its performance.

It is envisioned that the primary aperture film will have a third major layer, consisting of a very thin Nitinol film. This film, which is a shape-memory alloy, will allow the membrane to be folded like a blanket for launch, and will automatically deploy the film to its original flat shape when sun-heated in space. A number of shape memory alloys exist in addition to Nitinol that could be well suited for this application.

Nitinol has a restoring force almost two orders of magnitude greater than that of PVDF films, and so a very thin layer will probably have to be used so as not to overpower the piezoelectric effects. This should be no problem, as micron thick layers are routinely utilized Prof. Greg Carman, UCLA, who takes a film of Nitinol, crumples it in his hand, and after heating the film returns to its original flat shape with no creases visible to the naked eye. It is for this reason that the membrane incorporates a 5 micron layer of Nitinol. The actual thickness will be determined in Phase II.

In application, the alloy would be so composed as to have a transition temperature near to that expected in the operating environment in space. The membrane would be manufactured at room temperature, then cooled to a temperature lower than its transition temperature and maintained there until it reached its space destination. There it would be exposed to the sun and heated to just above its transition temperature, which would cause it to deploy to its original flat shape. The electron beam action on the PVDF layer would then shape it to the desired figure. Thus it appears as though folding the membrane into a small package can be accomplished in a manner similar to that illustrated in Figure 4.2-13.

FOLDING THE PRIMARY FOR LAUNCH

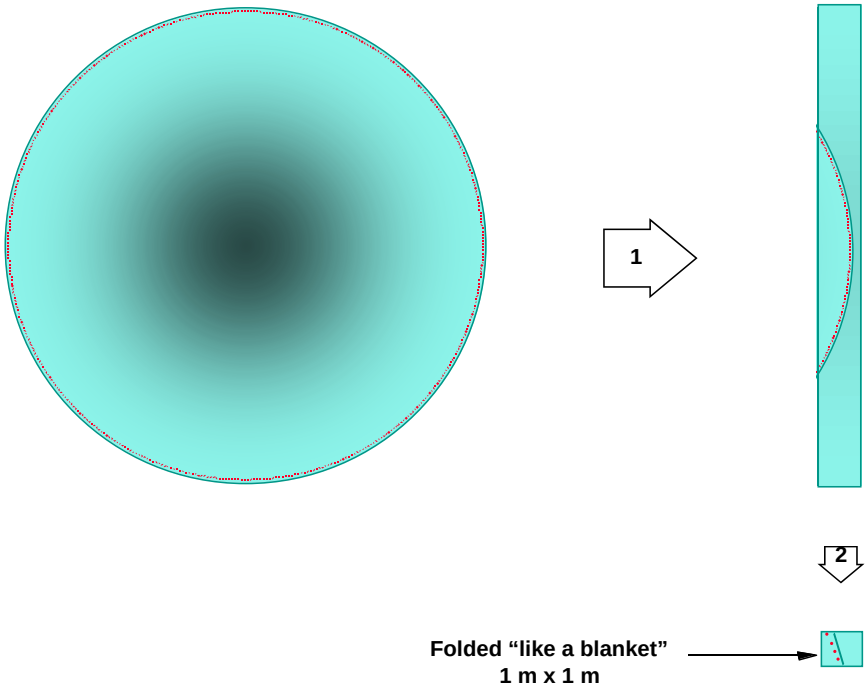

Fig 4.2-13

While attractive in concept, this method of folding is sure to produce a number of creases after unfolding. These creases will be reduced in size by the closed loop action of the adaptive membrane, for the system cannot tell intentional from unintentional surface imperfections, nor would we want it to. In addition the remaining errors of the membrane will be further reduced by the liquid crystal, within its correction capability. Thus, if the creases that may be formed are reduced to no larger than about 0.1 mm, which is the nominal liquid crystal correction range, and if their spatial scale is a few millimeters across, which is probably the smallest scale of errors that will be correctible, their effects will be completely corrected out. If the liquid crystal is able to have 1000 waves of correction in the visible light region, then surface errors up to 0.5 mm can be completely compensated out.

Unfortunately there are no calculations of the size of these likely creases, nor therefore whether they might be completely removed by the closed adaptive telescope loops. However it seems unlikely that they can be comletely removed or compensated. The actual size of the creases has to be determined experimentally for the particular films and deployment techniques being considered. This is planned for Phase II.

Thus, we have to be prepared for the possibility that such folding creases will prove to not be completely correctable, and if so this could be show-stopper for this telescope concept. **To guard against this possibility we have conceived a number of proprietary techniques that have the promise to mostly eliminate this problem. These are presented in the proprietary annex to this report.**

4.2.7 Dynamics

Dynamic perturbations must be prevented, as their magnitude could readily swamp the adaptive capabilities of the telescope. The classical approach is to make the surface thicker and stiffer, raising the natural frequency above that considered harmful in the system functioning. We will have no such luxury here because the membrane is intentionally very thin.

However, nature comes to our rescue. The unsupported film has a major advantage over a stretched film surface or over a solid surface. While it will have sufficient “artificial stiffness” induced by the piezoelectric bimorph layers to be moved as a unit and to maintain any desired shape in space, the absence of tension to attain that stiffness makes for very weak wave propagation along the surface. This will avoid the dynamic disturbances of the typical “drum-head” vibration modes of stretched membranes.

The remaining dynamic disturbances will probably propagate only weakly along the membrane, as it will not support shear forces, and so if they propagate at all will damp out rapidly. Thus this membrane will attain what most space structures cannot, which is to have high damping of disturbances. The numbers associated with this effect require complex simulation, which is proposed for Phase II.

4.2.8 Adaptive membrane weight

The weight of the adaptive, self-deploying membrane is indeed very low. The membrane weight is proportional to the square of the diameter and inversely proportional to its thickness. A 25 micron thick 25 m diameter membrane discussed above weighs 25 Kg. It weighs under 400 Kg. for a 100 m. telescope.

4.2.9 Conclusions

This section has discussed the major features of the adaptive membrane. Though there are number of important details that require analysis, if not experimentation, it appears that a fully adaptive, unsupported membrane in space is not only possible, but practical to make, launch, deploy, and operate in space. Confirmation of the technologies for these features is planned in Phase II.

4.3 Liquid crystal corrector

Liquid crystals have optical properties which make them uniquely suited to act as second stage correctors in this optical system concept, removing errors left over after the adaptive membrane has done as much as it can. The principal effect of these devices is to produce a 2-dimensional pattern of index of refraction changes, which are proportional to equivalent time delays, in response to signals from the Figure sensor. These time delays change the effective path length corresponding to the inverse pattern of errors on the primary, thus removing their effect. In principle a system can be diffraction limited after such corrections. The principle of these liquid crystal correctors is illustrated in Figure 4.3-1.

LIQUID CRYSTAL SECOND STAGE CORRECTOR
(typical)

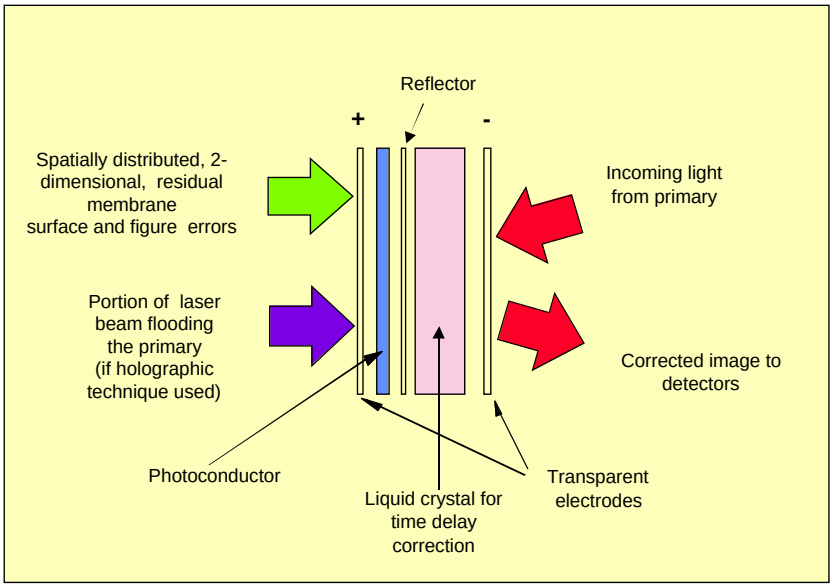

Figure 4.3-1

Liquid crystals are found in many common applications everywhere, ranging from watches and clocks to computer display screens. As a result of intense research promoted by the lucrative potential of these commercial applications, they are now thin, can be made large, have good resolution, and can display in colors. The commercial attraction of large format flat panel displays continues to improve on all their characteristics.

They are also used as nonlinear optics devices in laboratories, and have found application in adaptive optical systems of all sorts, for DOD, civil, and commercial purposes. Liquid crystal light correctors similar in principle to the use contemplated are operating in the laboratory at the Air Force Research Laboratories in Albuquerque. This application of liquid crystal has been extensively advocated and published by Dan Marker and Mark Grunheisen of AFRL.

The USAF experiments have demonstrated both optical and electrically addressed liquid crystals as spatial light modulators. A benchtop experimental unit was able to remove “a few” waves of equivalent path delay error, and according to Mark Grunheisen and Sergio Restaino, the technique appear to hold promise for 10-20 waves of delay.

There are two experimental setups, the largest of which uses a holographic technique which illuminates the membrane primary with a paraboloidal beam, develops a hologram of the errors in the membrane by combining a portion of this light with the reference laser, and impresses (“writes” the hologram on a photocathode in contact with the liquid crystal. The 2 dimensional distribution of light is thus transformed into a 2 dimensional distribution of electric potential, which drives the liquid crystal. The main light bundle from the primary is then passed through the liquid crystal, undergoing a phase or time delay proportional to the impressed voltage. This time delay is subtracted from the delays caused by the irregularities of the primary membrane (“read”) the hologram, and the resulting light is corrected. This application is illustrated in Figure 4.3-2.

The USAF AFRL setup works well in the lab, but has a number of drawbacks which make its application to the present concept highly doubtful. This is because the liquid crystal is being used in a mode where it probably cannot generate more than at most 10-20 waves of delay without causing large attenuation, scattering losses, and great loss of frequency response. Thus a search was made for more promising techniques, which are described below.

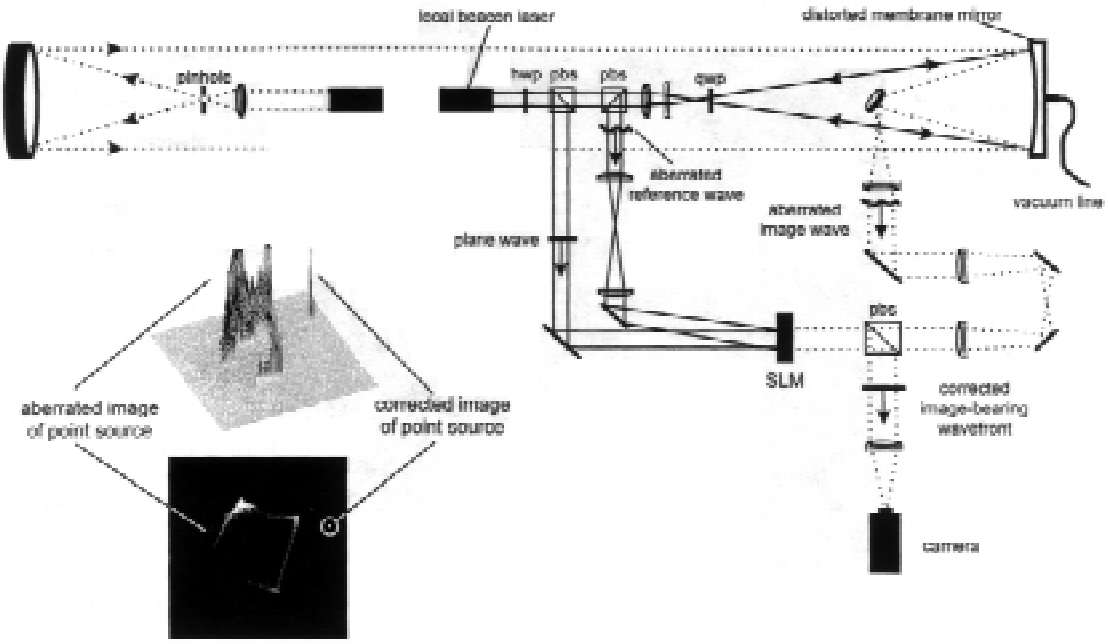

Figure 4.3-2

The concept adopted for the space telescope requires a much greater correction capability so as to be able to correct the errors left over in the primary membrane after shaping, as we are aiming for extremely large membrane primaries which will likely have residual errors far in excess of 20 waves. In addition we will have a formation flying system, the stationkeeping of whose elements becomes increasingly difficult as the precision is increased. Thus the optimization we seek requires a liquid crystal that has 1-2 orders of magnitude greater delay capability than the one used by AFRL. However, the devices do not need high frequency response as the disturbances are expected to be very slowly varying with time compared to any atmospheric phenomena.

Thus the liquid crystal contemplated must have a range exceeding many hundreds to one thousand waves of correction, while having very low scattering and sufficiently agile frequency response to correct for the expected disturbances.

4.3.1 Approaches to attaining large correction capability

Semiconductors and photorefractive crystals are known to exhibit effects suitable for optical light modulation. However, neither semiconductors nor photorefractive crystals are able to match the light modulating properties of liquid crystals, which uniquely combine several physical properties essential in electro-optical applications [See references 1-3]. These are a very large modulation capability of the refractive index (30%),

and small control voltage (V ~ 1 V), and very broadband capability.

Liquid crystals also offer technological advantages such as straightforward material engineering, integration with micro- and nano-electronics, capability to make large area optical elements; and inexpensive manufacturing. As a result of the foregoing, liquid crystals prove to be the material of choice for the design of adaptive optics elements for correction of large phase distortions [4,5].

4.3.2. Fundamental problems in using liquid crystals for very large correction

Due to the electrically induced modulation of the orientation of liquid crystal, the phase of a light beam of wavelength l can be varied for as much as $dL/l = L(n_e - n_o)/l$ wavelengths, where L is the thickness of the liquid crystal layer, and $n_e - n_o$ is the optical anisotropy of the liquid crystal. Thus, while in principle arbitrarily large corrections should be possible by making the liquid crystal thicker, the discussion below shows that there are fundamental and technological problems that limit the thickness of the liquid crystal layer to $L \leq 1$ mm. These are the scattering losses, attenuation, phase distortions, phase resolution, response time, and technological difficulties.

4.3.2.1 Scattering losses

Fundamentally, the scattering of light transiting the crystal makes thick cells opaque due to extremely large light scattering cross section of liquid crystals. This cross section itself increases with the thickness of the liquid crystal [6,7]:

$$s^{(e)} \approx 0.5 s_0 \sin^2(2a) \ln(L/l) \qquad (1)$$

where

$$\sigma_0 = \pi\varepsilon^2 k_b T \big/ \lambda^2 K \eta_0 \eta_e \qquad (2)$$

In Eqs. (1) and (2) we have standard notations: k = 4x10^{-14} erg/K is the Boltzmann's constant; T is the absolute temperature; $e = n_e^2 - n_o^2 \sim 0.5$ is the anisotropy of the dielectric constant of the nematic liquid crystal at the light frequency; $K \sim 10^{-6}$ erg/cm is the elastic constant of the liquid crystal, and a is the angle made by the propagation

direction of the incident light with the orientation of the optical axis of the liquid crystal. Typically $s \sim 10$ cm^{-1}.

Thus, if we assume the practical limit for the thickness of the liquid crystal-cell to be 1 mm, then the maximal

$$\sigma_o = \frac{\pi \varepsilon_a^{\,2} k_B T}{\lambda^2 K n_o n_e} \qquad (2)$$

phase modulation can be determined to be $dL/l = L(n_e - n_o)/l = 600$ for visible wavelength $l = 0.5$ mm, and for highly anisotropic liquid crystal with $n_e - n_o = 0.3$. In doing that, however, the attenuation of the beam is increased so as to be $I_{out}/I_{in} \sim 7 \times 10^{-3}$, or three orders of magnitude. This is not a useful result.

4.3.2.2 Phase distortions

Fluctuations of the director of a liquid crystal affect also phase of the light beam propagating through the cell. The following expression can be used for evaluating the phase fluctuations [8]:

$$\left\langle \delta\Phi^2 \right\rangle = \left(\frac{2\pi\varepsilon_a}{\lambda n_e} \right)^2 \sin^2\alpha \left\langle H^2 \right\rangle$$

where a is the angle of refraction of the beam into the planarly oriented liquid crystal. The parameter $\langle H^2 \rangle$ is equal to

$$\left\langle H^2 \right\rangle = \frac{8 k_B T}{\pi^4 K S} L^3$$

in case the area of the beam S is larger than the cell thickness L, and

$$\left\langle H^2 \right\rangle = \frac{4 k_B T}{\pi^3 K} L \ln \frac{1}{\tan\alpha} \qquad (3)$$

for narrow beams and for relatively small angle of incidence $a \ll 1$.
Since we are principally interested in narrow beams, we can represent the fluctuations of phase through the scat-

tering cross-section using Eq. (2):

$$\left\langle \delta\Phi^2 \right\rangle \approx \sigma_0 L \sin^2\alpha \ln\frac{1}{\tan\alpha} \quad (4)$$

Evaluations of Eq. (6) and the above indicated parameter values show that thick samples of strongly anisotropic liquid crystals can affect the phase of the beam as much as 1.6 radians (a quarter of a wavelength), which would be unacceptable. (5)

4.3.2.3 Spatial resolution and response time

Both the spatial resolution of liquid crystals and their response time are determined by the thickness of the liquid crystal cell. The spatial resolution is limited by the thickness of the cell. The response time *t* can be evaluated by the expression (6)

where *g* is the orientational viscosity of the liquid crystal.

Thus, increasing the cell thickness by one order of magnitude yields an increase in its response time of two orders of magnitude. This is a serious effect, though may not be catastrophic for space applications where the disturbance frequencies are very low.

4.3.2.4 Technological problems

Technically, many procedures well developed by the liquid crystal industry are not applicable to thick cells. In

$$\tau = \frac{\gamma L^2}{\pi^2 K} \quad (7)$$

particular the main method of orienting thin layers of liquid crystals, which is based on micro-pearl sputtering on the cell substrates, would be unacceptable for thick cells. Moreover, the homogeneity of thicker layers of liquid crystals tends to decay due to formation of domains.

These are serious problems. However there are several approaches with which we may be able to avoid these effects to a great extent. these are discussed below.

4.3.3. Multipass liquid crystal devices

Multilayer liquid crystal systems have been discussed in the literature as one means of obtaining large phase modulation while maintaining short relaxation times, and thus time response [9-11]. In such systems, each layer of liquid crystal can be made thin so as to maintain the fine spatial resolution and fast response time of the layers taken independently. Consider now the possibility of stacking together several layers of such liquid crystals for correction of large phase distortions, as illustrated in Figure 4.3-3. With a number of N layers, the maximally achievable phase shift can be extended N times to

$$DL = NL(n_e - n_o)/l \qquad (8)$$

wavelengths. By doing that the scattering losses of the whole system will increase from

$$I_{out}(1) = I_{in} \exp(-s(L)L) \qquad (9)$$

for one layer to

$$I_{out}(N) = I_{in} \exp(-Ns(L)L) \qquad (10)$$

for N layers.

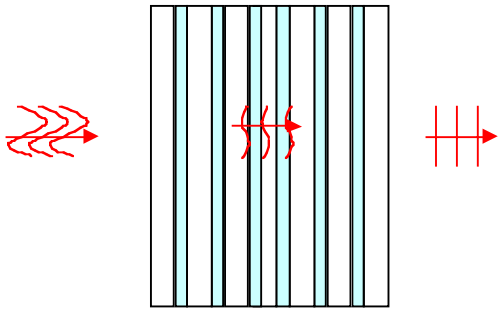

Figure 4.3-3

The optical anisotropy of the liquid crystal $n_a = n_e - n_o$ is the key control parameter that allows to keep the effective cross section of light scattering NsL small. Therefore, since $s \sim n_a^2$ while $DL \sim n_a$, the scattering cross section can be effectively reduced while only slightly affecting the phase modulating capability of the liquid crystal.

Some numerical evaluations were made to get a feel for these capabilities. One result shows that phase corrections of the order of $DL = 240\lambda$ using $L = 100$ mm thick liquid crystal layers with optical anisotropy $n = n_e - n_o = 0.3$ can be achieved with $N = DL/Ln_a = 240\lambda/Ln_a = 4$ layers (for the wavelength $\lambda = 0.5$ mm). For this large delay, however, the scattering losses, were determined to be

$$I_l/I_{in} = 1 - I_{out}(N)/I_{in} = 1 - \exp(-NsL)$$

are found to be 86% with the aid of Eqs. (1) and (2). These results, as well as others to be discussed will be shown later.

If we use a liquid crystal with 3 times smaller optical anisotropy, $n = n_e - n_o = 0.1$, we will require 3 times greater number of layers for the same effect. In this case the scattering losses will be reduced to 47%. These are still rather high losses, and smaller optical anisotropy may be required to reduce them to acceptable values.

The situation is more favorable with longer wavelengths since the scattering losses are reduced inversely proportional to λ^2. One can get a phase correction over 500 mm for a radiation of 10 mm wavelength (correction over 50 wavelengths) with only 1% scattering losses and 12 passes through the liquid crystal layer. Thus it is seen that increasing the number of liquid crystal layers will produce larger correction with lower scattering losses, however it will complicate the electronics that control the phase modulating properties of the system. The number of layers can be substantially reduced with the aid of optical schemes that allow for three and more passes of the light through the same layers. Accordingly the phase modulation with the aid of a 2 layer/3passes system shown in Figure 4.3-4 yields the same phase modulation as the 6 layer/1 pass system.

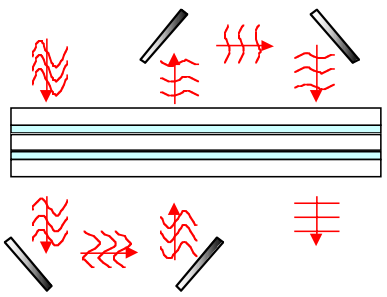

Figure 4.3-4

(11)

4.3.4 Direct laser control of phase modulation

Conventional way of controlling the phase modulating properties of multiple cells with the aid of electric fields may give rise to additional problems such as stronger beam attenuation due to additional absorption and reflection in the electrode layers. Direct laser addressing can help in overcoming this problem. Laser-induced reorientation of liquid crystal has been discovered in 1979-80 by I.C. Khoo, N.V. Tabiryan, and their colleagues [12,13]. Since then, numerous groups in many laboratories in the world have been involved in intense research in the area, which is nowadays in the stage of development into the first commercial products. An SBIR Phase 2 project is presently underway at BEAM Corp. with the goal of developing the new, nonlinear optical, technology of laser beam measurements suggested by the Principal Investigator of the project N.V. Tabiryan.

In the process of direct laser addressing, the influence on the orientation of liquid crystal takes place throughout the volume of the liquid crystal unlike the conventional case where the electric field is applied to the Liquid crystal through its boundaries. This opens up perspectives for effectively enhancing the resolution of the system, decreasing the response time, and simplifying the construction of the phase modulating cells.

Thus, as discussed in a number of papers, the spatial scale of the director reorientation of a nematic liquid crystal induced by a laser beam of the waist radius w is $L \sim (Lw)^{1/2}$ where L is the thickness of the Liquid crystal-cell [12-14]. Since the waist radius of focused laser beams can be rather small compared to the thickness of the Liquid crystal layer, the spatial resolution of the Liquid crystal can be enhanced by a factor $(L/w)^{1/2}$ due to direct laser addressing. Figure 4.3-5 illustrates the mechanism of laser-induced reorientation of liquid crystals.

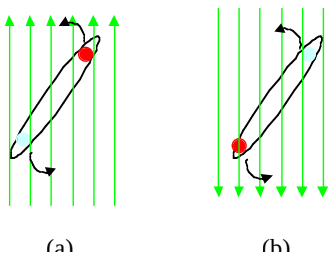

Figure 4.3-5

4.3.5 Thermally induced phase modulation with externally suppressed fluctuations

Among the unique benefits that direct laser addressing promises for the design of adaptive optics elements with extraordinarily large phase correction capability is the possibility of large changes in the refractive index of the liquid crystal material without any reorientation of the molecules, due to the spatially localized heating that influences the refractive index of the liquid crystal (thermal indexing). This process uses the following principles.

In nematic liquid crystals are characterized by extremely strong coefficient of thermal indexing:

$$\partial \eta_e \big/ \partial T \approx -10^{-2}\, K^{-1}$$

Since the process does not require reorientation, very thick layers of liquid crystals can be used and the orientational state of the liquid crystal is supported externally. In addition, the external influences can considerably suppress the fluctuations and enhance the transparency of the very thick layers of the Liquid crystal. An more advantage of thermal indexing is the response time of thermal effects which is in the range of microseconds.

A feasible liquid crystal-cell with stabilization of orientation and suppression of fluctuations is illustrated in Figure 4.3-6. Polymer Network Liquid Crystals (PN) have been under intense study recent years, and several procedures of “growing” oriented networks that support the orientation of liquid crystals has been developed, see, e.g. [15,16]. However, the electro-optical properties of PN liquid crystals are not suitable for adaptive optics for two reasons.

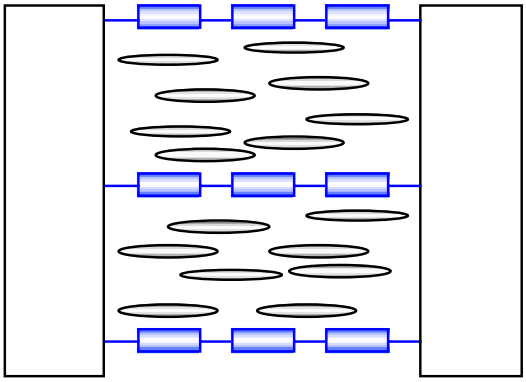

Figure 4.3-6

The first is that the threshold voltage for reorientation in PN liquid crystals is 1-2 orders of magnitude larger than the threshold voltage of a pure nematic liquid crystal cell, and the second is that the presence of the network prevents the reorientations from being homogenous across the crystal. As a result, application of an electric field to the system leads to the formation of strongly scattering domains.

As a result of the above, thermal indexing in PN liquid crystals with the aid of a control laser beam, unlike the case of electro-optical applications of PN liquid crystals, can yield very large phase modulation with no deterioration of the transparency state as will be recommended as the technique with the greatest promise for these applications. The above several cases are shown combined in the table of Figure 4.3-7.

PHASE MODULATION OF MUTILAYER CELLS

Wavelength, μm	0.5	0.5	0.5	1	10
Cell thickness L, μm	100	100	500	500	500
Na =Ne - No	0.3	0.1	0.02	0.05	0.1
Number of layers, N	4	12	12	12	12
Phase Shift, Lna/w	240	240	240	300	60
Scattering ∂ (1/cm)	48.3	5.3	0.28	0.39	0.01
Equivalent cell	61	7.8	0.38	0.55	0.02
Losses, %	86	47	15	21	0.6
Equivalent cell	91	61	20	28	1
Response time, s	0.5	0.5	13	13	13
Equivalent cell	8	73	1830	1830	1830

Figure 4.3-7

4.3.6. liquid crystal phase modulators for use in the Infrared.

The optical anisotropy of liquid crystal does not diminish with longer wavelengths of radiation. The transparency of liquid crystal is also sufficiently high in the IR, though there are some deep nulls in their absorption spectra. Nevertheless it is clear that it is possible to use liquid crystals for infrared telescopes. The applicable numbers are also shown in the table of Figure 4.3-7, resenting several results of IR operation of liquid crystals. An important advantage that liquid crystals have for use in the IR region is that their cross-section for light scattering decreases as l^2. Some nonlinear optical phenomena due to the recording of thermal dynamic gratings in liquid crystal under the action of IR light beams has been reported by Khoo [17].

4.3.7 Bistability, optical storage, dynamic-to-permanent conversion

There are different mechanisms of optical bistability and memory effect that can be realized in liquid crystal-systems. Particularly, it has been shown that an externally applied voltage induces bistability for direct orientational interaction of light beams with liquid crystals [18,19]. Recently, several liquid crystal-systems have been reported where the orientational pattern can be stored, or can be made dynamic depending on the conditions in the recording light beams [20,21]. Further study and development of these opportunities, planned for Phase II, should result in refreshable phase correcting devices where the energy is consumed only in the process of refreshing the state of the system.

4.3.8 Experiments performed in this NIAC Phase I

Several experiments have been carried out under this Phase I grant in order to verify the feasibility of realizing very large phase modulation using liquid crystals, since that is a key requirement for the adaptive mirror stationkept telescope concept.

4.3.8.1. Electrically addressed single cells

Very thick layers of homogeneously oriented liquid crystal cells have been developed for the for experiments in nonlinear optical research and applications. Specifically, we tested planarly oriented nematic liquid crystal cells of 300 microns thickness. The liquid crystal was sand-

wiched between glass plates that contained transparent electrodes, allowing application of an electric field onto the liquid crystal. The amplitude of the electric field varied up to 7 V at 1 KHz. The optical axis of the liquid crystal made to lie at 45° angle with respect to the axes of the polarizer and the analyzer. A photodetector registered the intensity of the laser beam transmitted through the system, illustrated in Figure 4.3-8. The output registered signal is proportional to

$$I_{out} \sim I_{in} \cos[2p(n_e - n_o)L/l]$$

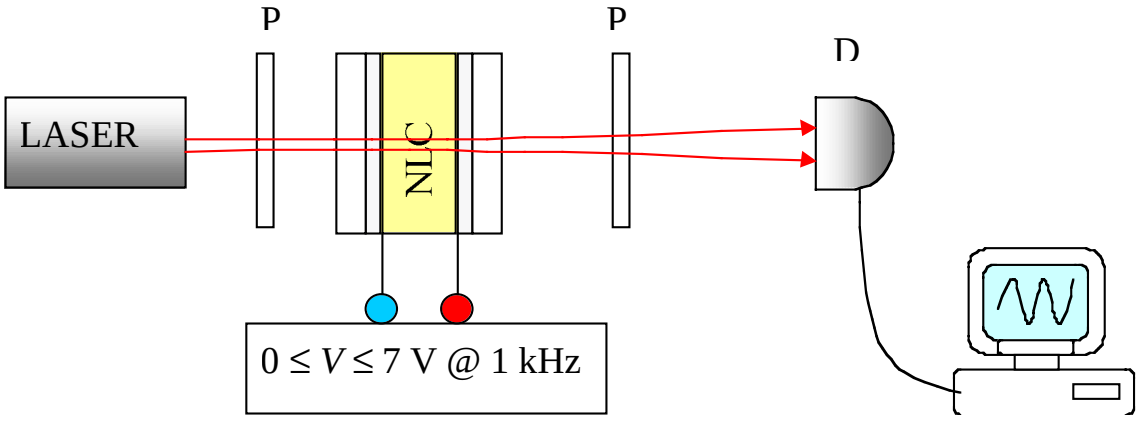

Figure 4.3-8

(12)

Since the refractive index n_e for the beam of extraordinary polarization varies with reorientation of the liquid crystal under the action of the electric field, the output signal oscillates, and the number of peaks is the actual count of the phase modulation in the delay of the wavelengths of the radiation (l = 0.628 mm). Figure 4.3-9 shows that in this single layer we could achieve an extraordinarily large phase modulating capability of about 100 wavelengths. Even then the transmission of the liquid crystal was about 75%, and no significant deterioration of the image quality transmitted through the layer was observed. This is a hopeful beginning, but by no means the end of the capability of this type of liquid crystal.

4.3.8.2. All-optically addressed multiple layer cells

A liquid crystal cell containing three layers of a liquid crystal wafers was made in order to test the feasibility

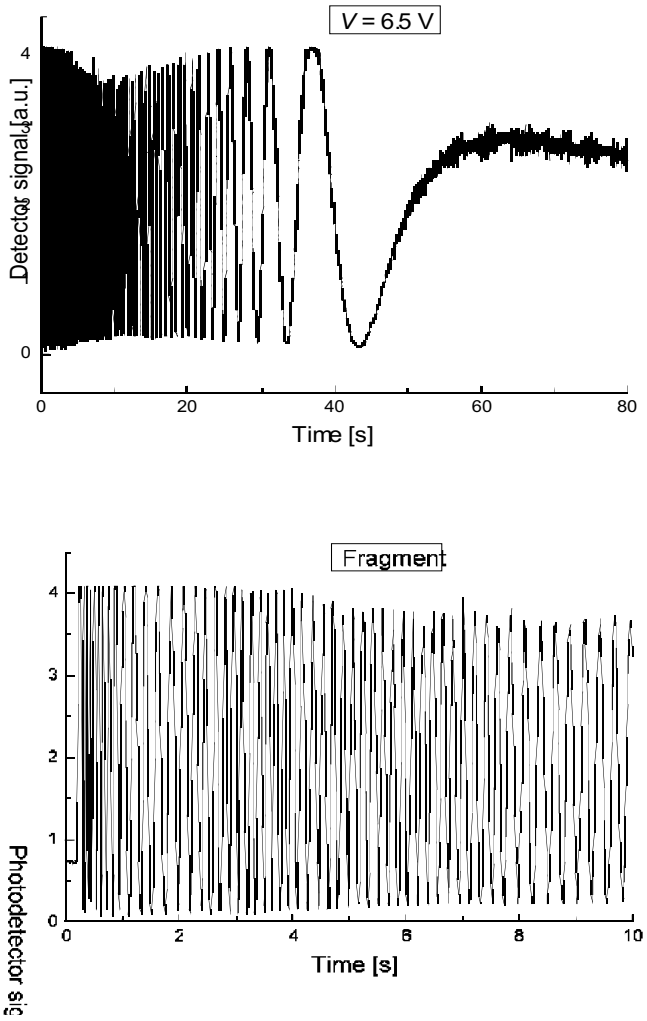

Figure 4.3-9

of all-optical addressing of multilayer cells. Each individual layer of the liquid crystal was 100 microns thick. The layers were separated with 300 microns thick glass plates. The reorientation of the liquid crystals was induced with the aid of a He-Ne laser focused onto the liquid crystal within a spot of about 40 microns radius. The magnitude of the laser induced phase shift was determined by counting the number of fringes that appeared in the far field due to the self-diffraction of the Gaussian laser beam [12,13].

This test setup is illustrated in Figure 4.3-10. The multiple layer cell was made in a way that allowed testing of one, two or all three of the layers in the same cell. The number of annular fringes was 10 when the laser was fo-

cused on the part of the cell with a single layer of liquid crystal. We indeed observed that the number of the rings doubled to 20 when the laser was focused into the 2-layer part of the of the cell. When the laser beam was focused onto the 3-layer part of the cell, the number of fringes again increased greatly, but was hard to count due to high density of the fringes in the central part of the picture and the low contrast at the edges of the system of rings.

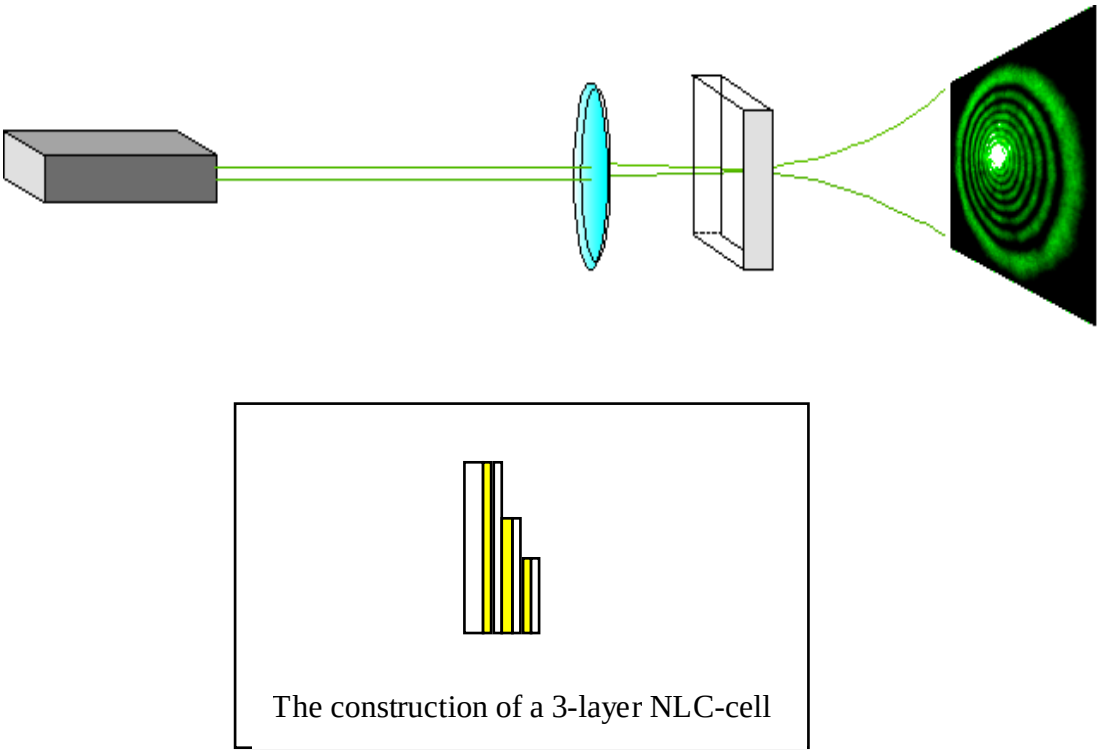

Figure 4.3-10

This is the result of a quick but inexpensive test setup, and there is no question that the number of fringes, and therefore the delay, was proportional to the number of layers transited by the beam. As fundamental was the observation that the response time was the same in all three situations and it was observed to be in the order of 1 second.

4.3.8.3. Phase modulation due to thermal indexing

As discussed above reorientation of the liquid crystal molecules, with their long time constants, can be avoided

while still obtaining substantial index of refraction changes by utilizing the thermal indexing effect. We constructed special liquid crystal cells where traces of a dye (0.1% by weight) produced some absorption with only minor effect on the transparency of the system.

Focusing the beam of He-Ne laser on such cells gave rise to a phase shift that can be observed simply by the change in the appearance of the ring pattern in the output beam. Up to 8 wavelengths of phase shift were observed in a 36 micron thick cell. The characteristic response time of the system was observed to be a few milliseconds. Time and funds prevented these tests from being extended to thicker cells in a multipass configuration, but the tests that were performed are extremely promising, and will be extended to much greater delay capabilities in Phase II.

4.3.9. Conclusions

Liquid crystals are materials with unique combination of electro-optical properties that makes them the main, and apparently the only, candidate for use in adaptive optical systems for correction of very large phase distortions with no mechanically moving parts. We have defined the large phase modulation capabilities of liquid crystals for use in such applications, and identified the main problems imposed by fundamental and technological limitations. We have identified several techniques that have great promise to overcome these problems.

In addition to analyses, we have performed laboratory experiments that demonstrated up to 100 wavelengths of phase correction capability with only 6.5 volts applied to the liquid crystal. Other experiments and analytical work pointed to the extraordinary potential of direct laser addressing of a liquid crystal with thermal indexing, as opposed to molecular rotation, as the most promising of new techniques. Unfortunately the resources in Phase I were insufficient to support quantitative experimental data on this technique.

We conclude therefore that there is evidence, both analytic and experimental, that direct laser addressing of special liquid crystal materials has the potential of realizing adaptive optics elements capable of very large phase corrections — of the order of 1,000 wavelengths — yet with response times of only a few milliseconds. As fundamental, these liquid crystals would also have low scatter and high transmissivity., as well as be capable of very fine resolution of 10-100 microns.

The potential of different liquid crystal-materials, systems, and methods for correction of large optical phase distortions without mechanical or moving parts requires considerable further investigation. These investigations, both analytical and experimental, will be proposed to be carried out in Phase II of the NIAC effort.

4.4 focal assembly

The focal assembly contains all the elements required to accept light from the primary membrane and produce an image on the focal array. The focal assembly contains the small entrance aperture which limits stray light from the telescope, a secondary mirror which corrects the spherical aberration of the primary membrane, a tertiary mirror which corrects any left over astigmatism or coma (though very little is expected due to the long focal length of the primary), the liquid crystal second stage of correction, the focal plane detector array, and the computation/command/communications unit.

The focal assembly is of relatively conventional but lightweight construction and can use conventional solid mirrors since they are so small as to make their weight inconsequential. The assembly was illustrated in Chapter 1 and is reproduced here as Figure 4.4-1.

4.4.1 General description

It could consist of individually stationkept mirrors using the same FEEP MEMS propulsive units as employed for the membrane, or a composite tube could be used with FEEP propulsive units on its periphery. In order to simplify the design and construction it was decided to make the entire assembly one piece, using a lightweight composite tube as the structure, This reduced the number of elements that have to be stationkept, and thus system complexity, in an area where stationkeeping is probably of marginal value

One potential drawback of using a structure is that of potential deformations and transients due to solar illumination attitude changes and eclipses. Should that turn out to be problematical for alignment accuracy or tolerances, then a second sunshade can be stationkept “up-sun” from the focal assembly in order to place it into a permanently shadowed, and thus more stable, configuration.

FOCAL PLANE ASSEMBLY, TO SCALE

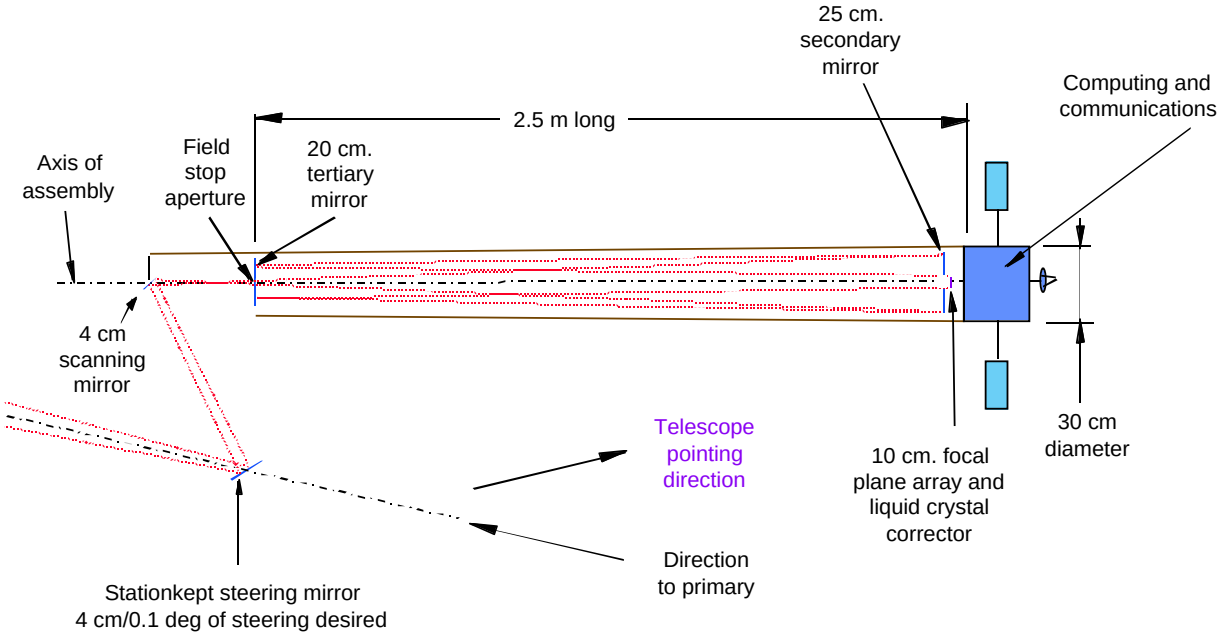

Figure 4.4-1

The focal plane is expected to be a conventional detector array, which could be a CCD device. The state of the art will allow the 10 cm focal plane to be populated with an array of about 10,000 x 10,000 detectors, each 10 microns in size. This will allow a good field of view while also permitting use of focal plane processing, both for image formation and for tracking to accomplish cross-axis stationkeeping.

The shape of the focal assembly is dictated by the f number of the primary, the desired focal distance between the tertiary and the focal plane which sets the image size, and the secondary-tertiary distance. The latter governs, and thus the assembly will have the same proportions as the overall telescope—10/1 ratio of l/d. As was mentioned in section 1, there is great freedom in choosing the sizes of the secondary and tertiary mirrors, as the telescope does not do reimaging. Thus the sizes of the mirrors are set only by their relative distance from the focus point of the primary and the desired final internal focal length.

If the secondary is to have a hole through which the 10 cm focal array and liquid crystal fit and are viewed, then it must

have a diameter of about 25 cm. to avoid to many aberrations. Thus the distance between the tertiary, with its entrance aperture, and the secondary must have the same proportions as the primary diameter/focal length, or 10/1. That sets the structural tube length at 2.5 m. Since it has to hold a 25 cm primary, which will be the largest mirror, the tube diameter can be 30 cm.

The tertiary mirror must have a resolution spot size no larger than the detector size. Since we chose 10 micron detectors, the tertiary can be any size greater than 10 cm. A 20 cm size was chosen both to ensure no overlap in spot to adjacent detectors, as well as to provide a more rigid structural tube.

The liquid crystal cell is placed immediately in front of the focal plane detector array, as it is expected that it would be the same size. The details of the internal optics to route the light through the liquid crystal are beyond the resources for Phase I and will be defined in Phase II. However, based on similarities with the experimental setup for the holographic liquid crystal corrector plate operating at the AFRL Albuquerque labs, this is a straightforward optics layout with no new technology.

One of the fast steering mirrors is envisioned to be attached to the focal assembly, as it does not need to translate, only rotate. It will be hard mounted through a 2 degree of freedom gimbal, as described in Section 4.5. It will be dynamically counterbalanced to ensure that steering disturbances are not created which cause jitter or loss of track in the telescope.

The communications/command/computation master unit is attached to the rear end of the tube. It can use solar arrays for power, or also receive microwave power from the sunshade/power propulsion element. It is envisioned that this unit would use all solid state advanced technology so that weight would be kept at a minimum in keeping with the philosophy of the other elements of the telescope.

4.4.2 Weight and power derivation

The weight of this focal assembly will be estimated after the propulsion and propellant weights are determined.

The attitude reorientations of the focal assembly are calculated assuming an initial value of 50 Kg for the entire assembly, including the command/comm equipment.

The structure is thus 2.5 m long, 30 cm dia., weighs 50 Kg. We calculate the moment of inertia of the long axis about the cg:

$I = m/12\left[6r^2 + l^2\right] = 50/12\left[6\times 0.15^2 + 2.5^2\right] = 26.6$ Then:

Angular acceleration $\alpha = (\theta/57.3)\times\left(2/1800^2\right) = 5.3\times10^{-8}$ r/s/s

Torque required for 2 thrusters $T = I\alpha = 26.6\times5.3\times10^{-8} = 1.3\times10^{-6}$ Nm

Force at each tube end= $F = \left(2\times1.3\times10^{-6}\right)/2.5 = 1\times10^{-6}$ N

Weight of thrusters= $W = 2\times\left(1\times10^{-6}N\right)\times77Kg/N = 1.5\times10^{-4}$ Kg

Total impulse required= $I = \left(2\times10^{-6}N\right)\times1.6\times10^{8}\sec = 320$ Ns

Propellant mass needed= $P = 320/1000\times10 = 3.2\times10^{-2}$ Kg.

Thruster power required $W = 2\times\left(1\times10^{-6}N\right)/6\times10^{-5}N/W = 3.3\times10^{-2}$ watts.

This is a minuscule amount of weight and propellants. We now calculate the translational maneuver requirements, again per the design reference mission requirements which maneuver the telescope 10 degrees every time. Since the focal assembly is 250 m from the primary, it will have to translate $L = \sin(10)\times250 = 44$ m. For conservatism call it 50 m. This will be done by accelerating 25 m and then decelerating 50 m.

Acceleration required $a = 2\times25/1800^2 = 1.5\times10^{-5}$ m/s/s

Force required $F = ma = 50\times1.5\times10^{-5} = 7.5\times10^{-4}$ N

Thruster weight $W = \left(7.5\times10^{-4}N\right)\times77Kg/N = 5.8\times10^{-2}$ Kg.

Thrusters will have a 50% duty cycle (1hr on-1 hr off).

Total impulse required $I = Nt = \left(7.5\times10^{-4}N\right)\times\left(1.6\times10^{8}s\right)/2 = 6\times10^{4}$ Ns

Propellant mass required $P = 6\times10^{4}/1000\times10 = 6$ Kg.

Thruster power required $W = 7.5\times10^{-4}N/6\times10^{-5}N/W = 12.5$ watts.

Thus the maneuvers of the focal assembly will require less than 7 Kg of added weight for the thrusters and their propellant for 5 years. They require that 12.5 watts of power be delivered to the thrusters. To this must be added the power required by the computer and the communications equipment. No design was undertaken due to the complexity of the functions assigned to the image processing and formation flying, but they are estimated to require 50 watts total. Thus 60 watts of power are required at the focal assembly. . If this is supplied via solar array, it would weigh about 2 Kg including conditioner, all solid state, in 10 years.

Thus the total focal assembly weight will be under 60 Kg. at the beginning of life. However, let us check the estimated weight of the components. Conservative estimates for the secondary and tertiary mirrors are 1 Kg each. The focal plane and liquid crystal are under 1 Kg. each. The weight of the tubular structure, if made of a double wall 1 mm thick composite, would be 14 Kg. The added weight of the 4 cm scanning mirror and its 2 degree of freedom gimbal is under 3 Kg. Thus a 60 Kg budget allows 60-14-2-1-1-3-7=32 Kg for the command, control, computation, and communications equipment. This is a reasonable estimate for 10 years into the future for all solid state/integrated silicon MEMS construction.

4.5 Fast steering mirrors

The very large ultralight telescope presents a variety of difficult design and operational problems, notable among which is the desire to repoint the system without moving the flimsy primary membrane or complex focal assembly, so as to minimize disturbance creation and large settling times.

If the system contains a focal assembly containing secondary and tertiary optics, and a small entrance pupil, then the focus of the primary will always be located near or just inside that pupil. That being the case, auxiliary steering and scanning mirrors can be introduced that allow steering the field of view of the telescope over a very much greater angle than that subtended by the focal array. This arrangement of mirrors is illustrated in Figure 4.5-1.

Fundamental to the concept is the requirement that the focal assembly subsystem act as a rigid body (i.e., that it remain internally aligned) so that its optics can be externally represented from an alignment standpoint by its optical axis and a point upon it (e.g., the auxiliary focus.) A spherical primary with a given radius is essentially defined by its center of curvature alone; its surface center plays only a secondary role from an alignment standpoint, but a “primary axis” is defined by the desired overall pointing direction and the center of curvature. The two subsystems are transversely aligned when the center of curvature of the primary lies upon the optical axis of the focal assembly, and axial alignment is reached thereafter when the two reference points are properly spaced. Alignment with these two degrees of freedom requires a minimum of two flat mirrors.

In the simplest possible configuration of the two mirrors, a “scanning flat” remains on the focal assembly axis and revolves about it to cause the axis to intercept the primary axis at a point that sat-

isfies the axial spacing requirement, and a “steering flat” that would be located at that intercept and tilted at the proper angle.

FAST STEERING MIRRORS

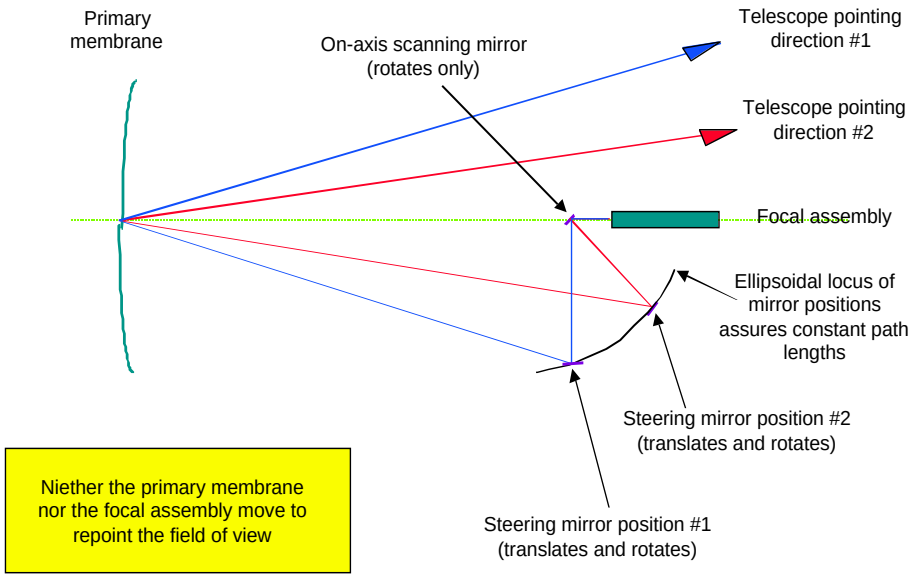

Figure 4.5-1

No system such as this one can be expected to function properly when there is massive misalignment, so it is assumed that external metrology, probably incorporating lasers and small propulsion units, will be used to maintain coarse alignment with millimeter-scale accuracy between the two main subsystems. This capability will be discussed under formation flying and its metrology.

One of the most important aspects of the dynamic module is its ability to be located in the immediate vicinity of a focal point so that the optical elements can be compact and low in mass, but this advantage is rapidly compromised if they need to widely separated.

Such separation is an inherent part of pointing, however, and a half angle Ω requires that the axes be separated by about $R\Omega$ near the focus of the primary mirror, and this means that the largest mirror must have a diameter of at least $D\Omega/2$. Since the telescope has an f/10, and D = 25 meters. the separation of the steering mirror from the focal assembly must be 2 meters and its size 43 cm for steering the telescope field of view Ω by 1^{o}. Of course, the size scales directly with the desired steering: for 1/2 degree a 21 cm mirror suffices, while for 5 degrees the mirror would have to be 2.1 m.

The size of the scanning mirror is unimportant as long it is larger than the entrance aperture of the tertiary at the focus of the primary. A 4 cm. mirror is probably adequate. This mirror rotates only, and is attached to the assembly by a two axis gimbal mount. This is readily manageable, and comparable to the other stationkeeping requirements of the system, particularly in view of the small size and therefore small mass of the steering mirrors to be translated and rotated.

A fundamental shortcoming of the simple two-mirror module is the “blind spot” that arises when the two axes are nearly coincident so that the mirrors try to overlap. This may be avoided by using a third mirror, but it may be shown that an odd number of mirrors will generally introduce image rotation which may create registration difficulties with the liquid crystal corrector reference. Thus is feasible to construct a four mirror system which does not exhibit a blind spot. Such a system is illustrated in Figure 4.5-2.

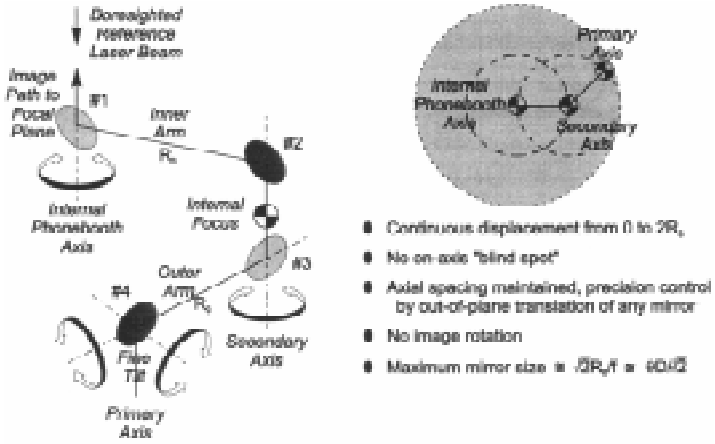

Figure 4.5-2

Even though it is possible to avoid a blind spot by such a three or four-mirror approach, it is not worth the trouble. Most celestial and also terrestrial telescopes can simply avoid the blind spot from a two mirror system, and return to pointing to that precluded direction after the telescope is reoriented. Since reorientations are frequent, there is probably little lost is sticking with a two-mirror steering system.

The fact that the steering and scanning mirrors are very small means that they can be moved rapidly without requiring extremely heavy mirrors, and without introducing disturbances to the primary and to the focal assembly (provided that the scanning flat is dynamically balanced).

Since these mirrors will be required to reorient, and one of them to translate fairly rapidly they may have to be constructed in a conventional manner. Thus, even though they will be small, they will weigh 1-2 Kg for the 43 cm., less than 1 Kg. for the 4 cm. mirror , and another Kg or two for the gimbal. A design for the propulsive means was not done for lack of resources, but this should not prove any more difficult that moving the focal assemble itself, and require a lot less thrust and propellants. It is estimated that these steering mirrors together should not weigh more than 10 Kg total, including all their subsystems.

4.6 Electron beam assembly

The electron beam assembly will stationkeep a few tens of meters behind the primary membrane. It will scan an electron beam over the entire primary surface, varying electron energy and voltage between itself and the membrane in response to commands from the focal assembly central computer.

The size and weight of the electron gun will not control the total weight of the assembly. The electron beam generator is similar to that in cathode ray tubes found in TVs and monitors everywhere. They are small and light, since most of the weight of CRTs is in the glass envelope to maintain vacuum, which of course is not needed in space. Furthermore the gun itself is very small and light, as the deflecting coils and their power supply dominate.

However, there may not be a need to have the 45 degree deflection characteristic of TV display tubes, as the e beam can be positioned as far away from the primary membrane as desired, since there is no truss penalty. This would preclude the need to have deflection coils, which tend to be heavy, and will allow the use of electrode plates which are very light. The power supply weight is probably about the same for both, as the energy requirements are essentially the same.

Nonetheless there will be limits on distance arising from the inability to create as small a crossection of the beam further away due to beam spread from self-repulsion of the electrons. For the purposes of this conceptual design, the e beam assembly is stationkept at twice the primary diameter, or at 50 m, with the understanding that electron beam optimization should be done to choose the best distance. The following discussion refers to the illustration of Figure 4.6-1.

ELECTRON BEAM ASSEMBLY

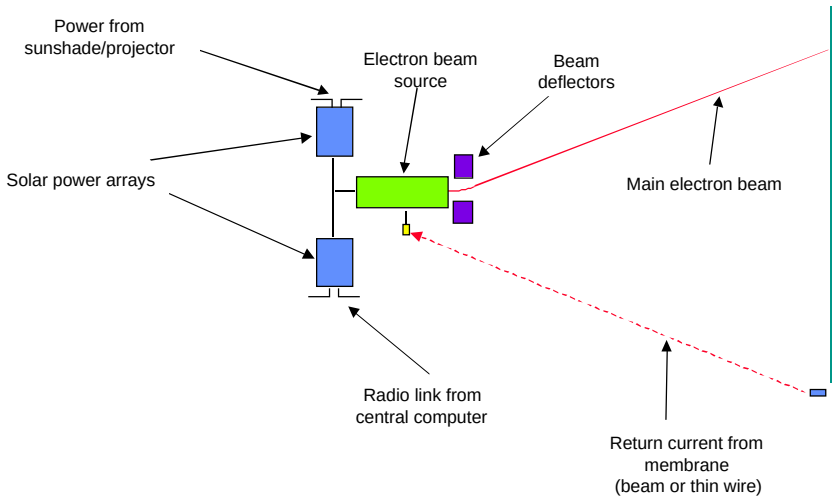

Figure 4.6-1

The energy required for the electron beam is calculated as follows. The primary membrane must be energized sufficiently that it can start flat and bend into a figure whose maximum deviation from planar is about 0.1 m. For sake of conservatism we assume that the primary must be made to bend 10% in any given length along its crossection. Thus any 1 cm portion of the membrane must be able to deflect amount 1 mm. Recalling that the curvature of the film is $C = 1/r = 0.324\,Q/Axt$, where r is the radius of curvature of the bent bimorph portion, Q is the charge deposited by the electron beam in Coulombs, A is the crossectional area of the film, and T is the thickness of the film,, both in meters.

For a patch of membrane 1 cm square, and for a film thickness of 10 microns, $r = 3x10^{-9}/Q$. Now for a film to deform 1 mm in 1 cm of surface in 2 dimensions symmetrically,, its radius of curvature can be calculated to be 1.3 cm, from spherical formulas. Therefore the required charge that must be deposited on the piezoelectric bimorph to produce that radius of curvature is $Q = 3x10^{-9}/r \quad = 3x10^{-7}$ Coulombs. Now since ampere-hours are $AH = Q/3600 = 8.3\times10^{-11}$ we need to inject that many ampere hours into every square cm of surface on the membrane in order to cause the desired worst case of 1 mm deflection per cm of membrane.

If we assume an e beam generator overall efficiency of 10%, which is very conservative and calculate per square m of membrane area, we need about 10^{-5} amp hours per square meter. Since a 25 m diameter

membrane has 480 square meters of area, thus we need $480 \times 10^{-5} = 5 \times 10^{-3}$ ampere hours going into the e beam generator. If we assume that we take 1 hour for the initial shaping of the membrane, since we need to produce electrons at about 800-1000 volts energy (From tests by John Main, U of Kentucky), then we need a current of 5 milliamps. The power required is 5 watts, and the energy input is 5 watt-hours.

This is a very small energy and power level that will be easy to produce at light weight. However we must also calculate the power that will be needed to maintain the shape in the presence of disturbances or commands from the figure sensor, as well as to partially recharge the membrane periodically as the charge bleeds off internally. For that we make some sizing assumptions. We assume that the above conditions require 10% of the charge to be replenished over the entire membrane 10 times per hour, or every 6 minutes. This is not unreasonable based on data obtained by John Main on commercial PVDF film in a vacuum chamber.

We further assume that we have to replenish this charge in 1 minute, every six minutes. While this is an arbitrary number it cannot be much slower or the surface will never get to anything like a steady state, even in the absence of correction commands, and so is not unreasonable at least on the ,.long end. But due to the likely absence of wave dynamic disturbances, it is unlikely that the surface will change so fast as to require more frequent refreshing of the charge. This implies that the response time of the membrane will be in the order of one minute, which is not unreasonable for a 1 hour observation period.

Given the above, a 10% charge administered in 1 minute out of every 6 minutes means that the average current must be $A = \left(5 \times 10^{-3} / 10\right) \times 6 / 1 = 3 \times 10^{-3}$ amps. Since the voltage must be about 1,000 volts, then the average power required is 3 watts. Therefore the power required by the e-beam assembly is 5 watts for the initial hour, and 3 watts steady state average thereafter. This is indeed a very small power requirement.

The power could come from solar cells on the e beam generator, except that the generator will probably be unintentionally shaded by the sunshade for long periods of time. Thus the requirement will also be met by power beaming via a microwave or millimeter wave transmission from the sunshade.

Kimball Physics of Nashua New Hampshire makes a large number of electron guns. A typical laboratory model that produces more than

the required beam current and voltage. This gun is about 14 by 3 cm in size, and weighs 0.15 Kg. The addition of deflection coils of electrodes, plus the power supply to drive them will size the system, not the gun itself, but are unlikely to weigh more than a Kg or two. at most. Those calculations will be done in Phase II.

A functional diagram of the e beam generator is shown in Figure 4.6-2. The e beam generator must be electrically connected to the back electrode of the membrane to have a closed circuit. This connection could be via a thin flexible wire of arbitrary shape, or it could be closed via a small dedicated electron gun carrying the return current flow of about 3 milliamps. Either can be made to work, with the choice not being a driver at this point.

ELECTRON BEAM GENERATOR FUNCTIONAL DIAGRAM

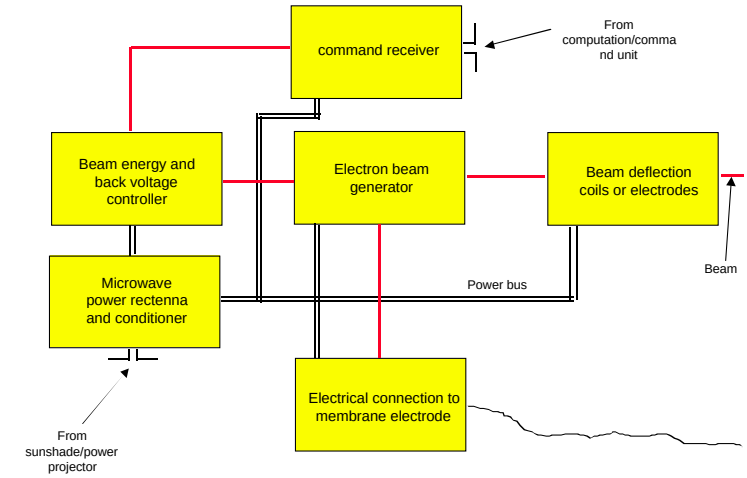

Figure 4.6-2

In addition the assembly must have a command receiver to receive commands from the central computer, in response to the figure sensor. These signals will be used to modulate the beam current and the voltage to the membrane. The entire electron beam assembly will probably weigh less than 5 Kg. on station in space.

4.7 Figure sensor

The adaptive membrane primary as well as the liquid crystal secondary corrector will require a figure sensor to obtain measurements of the actual surfaces, and command the required spatial corrections in 2 dimensions. A number of different figure sensing means exist and are in use. The three main approaches are discussed.

The principal passive technique is in use is one that derives profile errors in the primary from comparison of the phases of the actual image and a slightly defocused image, that is normally obtained at a displacement[from the focal plane. A number of algorithms exist for extraction of the error data, which is obtained in 2 dimensions, some of them proprietary. This technique is known to work for distributed scenes, such as in photography. Though the technique is simple, it is not known how well it would perform for viewing typical astronomical scenes, but is a candidate nonetheless.

A second technique illuminates the primary with a coherent laser with parabolic wavefront. Upon combination of the return with a portion of the laser reference, a hologram of the errors in the primary, compared to the reference parabolic wavefront. This was described in the membrane section as the technique in use by the AFRL researchers. It works well, but since it is interferometric at the laser wavelength, it has a rather small range of surface errors which it can detect because of the large number of fringes that result from those large errors becomes too large to count. It has detected errors of tens of wavelengths, but cannot with the same equipment also measure the surface errors of 0.1-0.2 meters which are expected as the initial conditions of a flat membrane being shaped to parabolic, even at f/10.

A third type of sensor exists which is also is a 2 dimensional interferometric profilometer, but it is driven by a tunable laser. Measurement of the array phase at each detector at each of two laser frequencies synthesizes the heterodyne frequency, which is ideal for measuring highly aberrated surfaces with large surface errors. The principle of operation of this sensor is illustrated in Figure 4.7-1. Small surface errors can be as easily measured by increasing the wavelength separation of the laser beams, thus creating a smaller wavelength better suited for small errors. This heterodyne array figure sensor is being developed by Lenore McMackin of AFRL Albuquerque, and is operating in brassboard.

Figure 4.7-1 also illustrates the synthetic wavelengths being generated, which are the difference between the illuminating wavelengths. Since surface errors whose magnitude approaches the wavelength can be characterized, this sensor clearly can measure features of about 1 mm as well as submicron surface errors. Better yet, the precision of the fine error measurements can be such that the same figure sensor can be used to drive both the coarse corrector (the adaptive membrane), as well as the fine corrector (the liquid crystal).

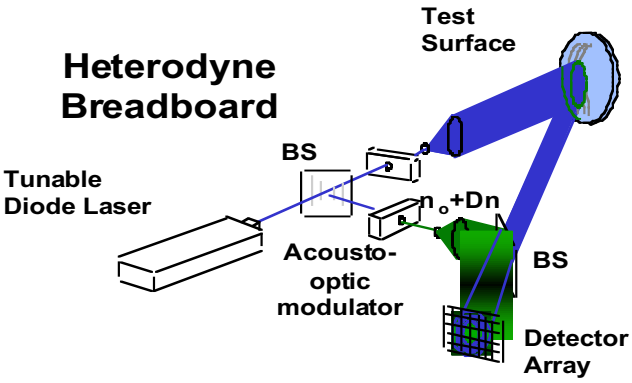

Completely digital wavefront sensing

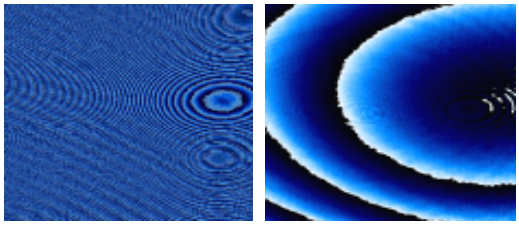

Multi-wavelength system provides variable sensitivity over 3 orders of magnitude

λ_a (μm)	λ_b (μm)	λ_{eq} (μm)
0.792	0.7766	40
0.792	0.7817	60
0.792	0.7842	80
0.792	0.7858	100
0.792	0.7889	200
0.792	0.7910	600
0.792	0.7912	800

Figure 4.7-1

The last two figure sensors are active, and illuminator the primary and analyze the return. They could be located at the focal assembly near the telescope prime focus, however then the primary would have to be blazed in many patch areas with a hologram of a corner reflectors so that the light from the figure sensor returns to it, rather than being sent out into space by the primary. This could be done, but then the figure could only be controlled to the least dimension between patches. Since we are trying to take out errors as small as millimeters on the primary, and smaller if possible, then the entire primary surface would have to be blazed, and of course would not reflect any celestial light into the focal plane at all.

It is for this reason that the figure sensor is located at the center of curvature of the telescope, where a beam will be returned to its source without requiring any patches of any kind on the primary. Foe a spherical primary the center of curvature is a twice the focal

distance from the primary. This is essentially also true for a parabolic primary. Thus the active figure sensor will be located 500 m. from a 25 m. primary with focal length of 250 m.

Stationkeeping this figure sensor will be no different than stationkeeping any other element of the telescope, and will be provided for in the formation flying metrology. The figure sensor will also use FEEP MEMS propulsion thrusters to translate an rotate as required for changing targets and for stationkeeping. Calculations made for rotating and translating the focal assembly can simply be scaled to the weight of the figure sensor, which is expected to be small and lightweight. A total weight of 5 Kg is probably overly generous.

4.8 Sunshade/power projector

In order to minimize thermal disturbances on the primary membrane, the entire primary is shaded from sunlight by a stationkept sunshield. This shield will have attitude and translation control so that it will maintain a position between the sun and the primary at all times. This will also shield the focal assembly, but only when there is coarse axial alignment with the sunward direction. Therefore there may have to be a second sunshield to shade the focal assembly if such is eventually decided upon based on further and more complete analyses.

The Sunshade will therefore have two functions: shielding the primary membrane, and beaming power to it for use by its electronics and propulsion units, which obviously cannot use solar arrays. The functional illustration of the sunshade/power projector is shown in **Figure 4.8-1**. The conceptual design of the sunshade/power projector proceeds as follows.

The sunshade must resist solar pressure with thrust. The force to be resisted is $9x10^{-6}$ N per square meter of area. The total projected area is 488 square meters at normal incidence, thus the peak force to be resisted is $4.3x10^{-3}$ Newtons. However, the average pressure over all configurations is about half that, or $2.15x10^{-3}$ N. The time of action is assumed 5 years, so that the total impulse that must be delivered is Nxs, which is $1.6x10^{8}$ seconds, for an impulse of $3.2x10^{5}$ Ns.

We will use advanced design FEEP propulsion MEMS units throughout this conceptual analysis. Their characteristics were shown in **Figure 4.2-12.** The propellant required to offset the solar flux thrust is

SUNSHADE / POWER PROJECTOR

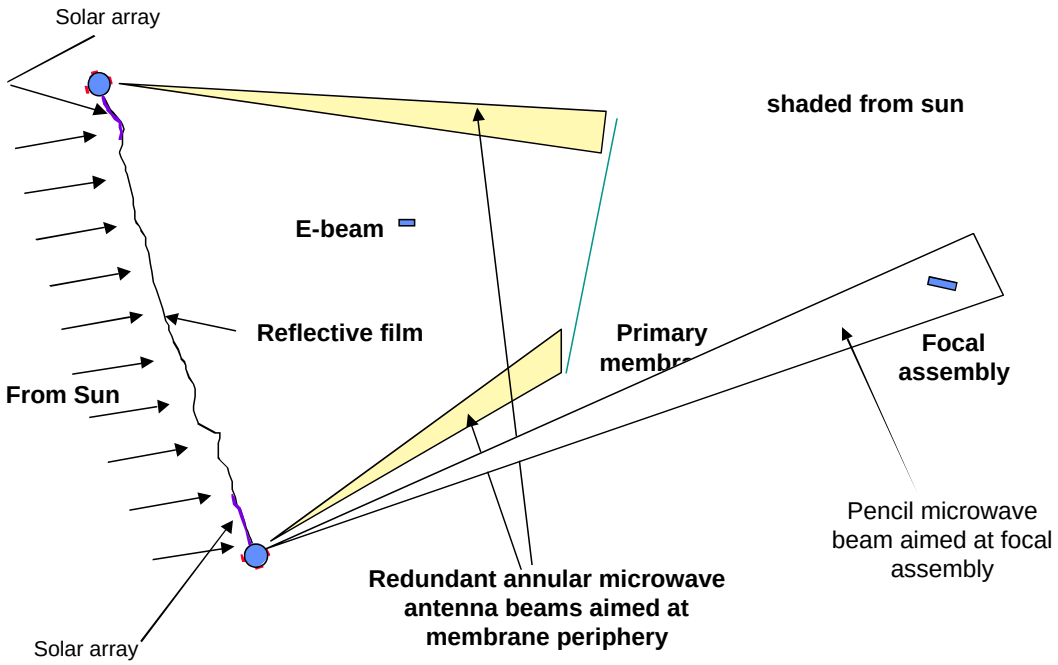

Figure 4.8-1

M = I/Isp x g. Since the Isp is 1000 or more for these FEEPs, then

M = $3.2x10^{5}/1000x10$ = 32 Kg. of propellants for 5 years of operation.

The thruster weight will be W = 77 Kg/N x $2.15x10^{-3}$ N = 0.17 Kg.

The power required to operate the thrusters will be will be given by

$2.15x10^{-3}$N x $6x10^{-5}$ N/w = 35.8 watts.

Since the sunshade will rotate continuously at the solar orbit rate, and it will be a balanced area design, essentially no propellants will be required to maintain its attitude. This will also be true in GEO where, once having attained a rate of one revolution per day, no further major rates are needed.

Thus the propulsive requirements for the sunshade are minimal. To them must be added the stationkeeping from solar and lunar perturbations if the telescope assembly is in GEO, for maintaining E-W position in orbit. This requirement is about 50 m/s per year, for a 250 m/s total. From the rocket equation

$\Delta V = I_{sp}xgx\left(W_i/W_f\right)$, so that the initial to final weight ratio is given by

$W_i/W_f = e^{\left(\Delta V/I_{sp}xg\right)}$ which = 0.025 Thus the initial weight of the sunshade must include 2.5% in propellant to stationkeep in GEO. This is minimal.

The biggest requirement on the sunshade will be to convert sunlight into microwave and transmit it to the primary membrane assembly. The power that is needed by the primary membrane thrusters for the periodic telescope pointing reorientations was determined to be in section 4.2, about 0.1 watts. We determine the required transmission and generation as follows. Assuming conservative numbers for efficiencies: 80% for DC-AC and AC-DC power conversion each, and 10% capture area of the FEEPs on the primary with respect to the transmitter beam we need 0.8x0.8x0.1 = 0.064 efficiency overall. This means that we must generate 0.1/0.064 = 15.6 watts of electricity at the sunshade.

But to this power we have to add the power required to stationkeep the sunshade itself against solar pressure, which was 35.8 watts. Thus we have to generate a total of 51.4 watts. Given a 55% efficient multiple matched bandgap-spectrally split array, the total power received by the array need be only 93.5 watts. Since the solar flux is 1500 w/sq.m., and the array will always be sun-pointing, we only need 0.062 square meters, or less than one square foot, of solar array on the sunshade. This array will weigh, at 50 w/Kg in the time frame, about 1 Kg.

In addition we need to estimate the mass of the RF transmitter and antenna. Given a 0.1 watt output, the solid state transmitter will weigh less than 1 Kg. at Ka band. The antenna can be a simple end-fire line array that creates an annular pattern, which is aimed at the primary membrane, concentrating its power on the periphery where the receivers and propulsion FEEPs are, weighing certainly less than 1 Kg. The transmission function thus weighs 2 Kg.

Thus the sunshade’s power supply function is seen to be relatively easy and lightweight. Its construction would probably be an extremely thin reflecting film, since surface quality is immaterial, and an inflatable torus to tension it. A sunshade diameter of 30 m if made from 1 micron thick aluminized film would weigh 1.4 Kg. It would have to be tensioned loosely, at least initially, by an inflatable torus, which could readily be made of 3 micron film, initially lightly pressurized, and then rigidized with foam or aerogel so as to retain its approximate shape after micrometeorite punctures.

If the torus had a 1 m diameter for reasonable deployment forces, the torus weight would be 1.8 Kg. The foam for rigidization would probably weigh another Kg or so. In addition there has to be some propellant for coarse stationkeeping in addition to that for offsetting the solar pressure. This will be small and is estimated at 1 Kg.

• FEEP thrusters	0.2	Kg
• Reflector	1.4	Kg
• Torus	1.8	Kg
• Foam	1.0	Kg
• Solar cells	1.0	Kg
• Transmitter/antenna	1.0	Kg
• Primary shading stationkeeping propellant	1.0	Kg
• GEO E-W stationkeeping propellant	0.2	Kg
TOTAL WEIGHT IN GEO OR SOLAR ORBIT	7.6	Kg

Thus it is seen that the dual-function sunshade/power projector is a straightforward, if unconventional, development.

4.9 Formation flying metrology and control

4.9.1. FFT Formation Virtual-Truss Architecture

The FFT formation concept is shown in Figure 4.9-1. A distributed sensing and control AFF approach enables a virtual-truss 3D rigidity of the separated telescope elements and maintains the tight tolerances on overall planarity and alignments of the optical system. Relative measurements between linear neighbors and an off-axis observer are depicted. Range, range rate, azimuth and elevation data are obtained and processed both locally on each body and globally by a 'Commander' function, which serves as the formation Navigator and the Command, Control, and Communications Executive. This distribution or sharing of sensing, decision, and control action functions at the Local Level and the Global Level attempts to optimize the division of autonomous management functions for the FFT and future larger formations. A closed-loop architecture diagram later in this report shows these functions more specifically.

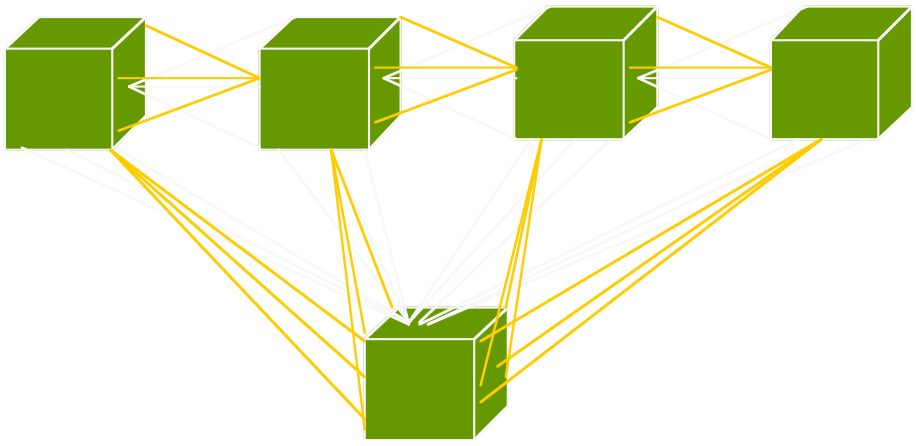

Figure 4.9-1

4.9.1.1 FFT Formation Flying Control Constraints

Two primary FFT Control Challenges: 1) The large Primary Mirror and necessary optical path alignments place constraints on multibody stationkeeping control precision (100 microns composite system error) in science observations; and 2) Diffraction limited imaging creates the requirement for the ultra-fine pointing and line-of-sight stabilization.

The Formation control concept is based on real-time guidance and control autonomy in the form of multi-sensor fusion, distributed intelligence, and multi-level (global-formation to local-spacecraft) placement of control authority in accordance with practical control strategies and derived control laws.

4.9.1.3 FFT Control Requirements and Assumptions

General

. Inertial attitude knowledge is provided by star trackers (et al) and all translational and rotational control to the desired inertial direction is done using the thrusters. This applies to all elements of the formation.

. All other elements of the formation stationkeep (hold relative position) with respect to the Primary Mirror. Relative position knowledge is provided by an RF/Optical metrology system. Because of the large dynamic range between measurement and accuracy/stability, the metrology system may be multi-stage (eg, coarseRF, fineRF, Optical).

. Requirements on the accuracy and stability of the attitude & position knowledge and control are to be derived from the requirements of the on-orbit process of configuring and using the telescope in which

. Absolute accuracy requirements may be less stringent than the stability requirements, and

. Absolute accuracy requirements may be eased if a search strategy is invoked for focal plane imaging acquisition and fine “tuning”.

Telescope Axis

. The axis is defined as the line perpendicular to the ring of the Primary Mirror and is pointed in the desired inertial direction by attitude control of the Primary (2 dof).

Primary Mirror Figure

. The shape of the mirror surface is to be known/controlled, e.g. to be spherical with specified radius of curvature (500m) and center of curvature on the telescope axis.

. The shape is measured by the FigureSensor.

. The Figure Sensor must stationkeep with respect to the Primary at/near the desired center of curvature.
. The Figure Sensor must know/control its attitude to be aligned with respect to the Primary (3 dof).
. The Figure Sensor must measure the shape of the mirror surface.
. The shape actuator is the Electron_ Beam (E_Beam):
. The E_Beam must stationkeep with respect to the Primary at/near an on-axis point behind the Primary (eg 50m).
. The E_Beam must know/control its attitude to be aligned with respect to the Primary (3 dof).
. The E_Beam will irradiate the mirror to correct errors in the shape.
. The final shape of the Primary is measured.

Telescope Line of Sight (LOS) Steering
. Specify the desired telescope inertial LOS, within a limited range of the telescope axis.
. The Primary provides knowledge of its attitude.
. The Primary shape is provided by the Figure Sensor.
. An optical model will determine the required focal point with respect to the Primary (3 pos. & 2 att. dof)

Establish the Telescope Configuation
. Positioning the Focal Plane Assembly (FPA) will establish the correct telescope geometry. The following will ignore the steering mirrors, but it also would apply to the virtual (doubly reflected) FPA with the added mirror degrees of freedom.
. The FPA must stationkeep with respect to the Primary to place the entrance aperture at the focal point (3 dof).
. The FPA must control its attitude (2 dof) to keep its axis in the focal point direction.
. Initial positioning of FPA using RF absolute metrology, followed by a search/fine-tune process using Optical differential (relative) metrology and focal plane image peaking in a positioning closed-loop implementation:
. Search pattern generator directs changes in FPA station until the target is imaged/detected in focal plane
. FPA stationkeeps with respect to relative Optical Metrology
. Realtime image analysis determines translation/rotation needed to center or sharpen the image, and FPA controls its station/attitude to correct.

Science Observation
. Hold the telescope configuration stationary while acquiring science data.

4.9.1.4 Preliminary Error Allocations

Focal point in 10 cm (100 mm) FPA aperture (assumption)
- Allocate error of 10 mm per axis 1-sigma, lateral (2 dof)
- Allocate error of ≥ 10 mm on axis, depth of field assumption
  Further Suballocate Lateral Errors:
- FPA stationkeeping control.....5.0 mm
- Knowledge of focal point.....8.6 mm
  - Optical modeling uncertai.....5.0 mm
  - PrimaryShape knowledge..... 5.0 mm
  - Primary Mirror attitude control..... 5.0 mm (≈2arc-seconds)

Stationkeeping for Dynamic Range of Secondary Adaptive Optics
- Composite Maximum Error of 0.1 mm (100 microns)
- Further Design Suballocations are TBD
  - Capabilities forecast for RF and Optical Metrology
    - Search strategy and focal plane image PSF tuning to obtain calibrated absolute positioning.
    - Heterodyne Laser Interferometry (HLI) to >5 nanometers on-axis relative (differential) accuracy with two off-axis observational platforms if required for adequate lateral error sensitivities.
    - Relative Control of each separated telescope element to ~10 microns translational (3 dof) and ~3 arc-seconds rotational (3 dof) precision.

4.9.2 FFT Measurement & Control Architecture and Methodology

This section develops the overall architecture of measurement and control for the FFT. Following that the formation initialization command sequence and preliminary control logic are derived.

Free Flying Elements Shown in Figure 4.9-2

PMM - Primary mirror membrane (telescope primary)
FPA - Focal plane assembly (telescope secondary)
PFS - Primary figure sensor
SEB - Scanning electron beam
OSS - Orbiting Sun Shade

4.9.2.1 Geometry and Frame Definitions:

F_M - Define the PMM frame F_M by 3 fiducial points at the periphery of the PMM membrane. The z axis is defined normal to the fiducial plane, and in the direction of the nominal LOS of the telescope. The P_M frame is located at the “mechanical center” of the PMM, defined by the mean location of the three fiducial points.

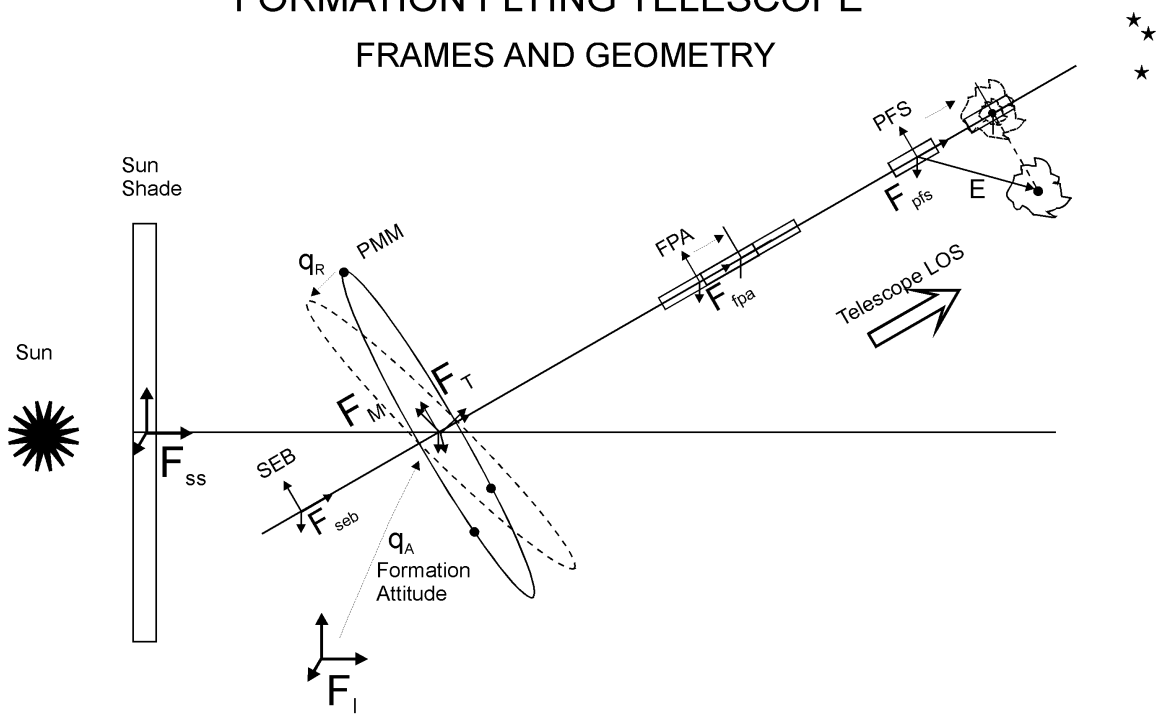

Figure 4.9-2

F_O - Define the Orbital frame F_O of the PMM for a heliocentric orbit. The orbital frame is defined with x_O axis along positive radial vector r from Sun center to the mechanical center of the PMM, and z_O=rXv, where v is the orbital velocity vector. The orbital frame is assumed to be located at the mechanical center of the PMM.

F_I - Inertial Frame F_I taken as J2000

F_T - Telescope Formation Frame F_T, is an inertial frame located at center of PMM, which specifies the desired attitude of the telescope (this points the telescope LOS to a desired J2000 location, and maintains acceptable twist angle of the formation).Thus defined, the z axis of F_T, is labelled as the axis of the desired telescope LOS.

q_A - Define the formation attitude q_A as the quaternion (or equivalent dcos matrix A) which maps the F_I frame into the F_T frame, i.e., F_T= A F_I

q_R - Define the PMM alignment as the quaternion q_R (or equivalent dcos matrix R) which maps the F_T frame into the F_M frame, i.e., F_M=q_R F_T

Define body frames F_fpa, F_pfs, and F_seb for the free flying elements FPA, FPS, SEB, respectively.

4.9.2.2 Assumptions

. The PMM, FPA, PFS, SEB have star trackers, (possibly gyros, TBD), and attitude control thrusters.
. The FPA, PFS, and SEB have thrusters for translation control. Thrusters are assumed to be of the proportional type.
. Since translation control of PMM is not used, the FPA, PFS and SEB formation-fly (translate) to maintain their positions relative to the mechanical frame of the PMM.
. The OSS is attitude controlled to be nominally aligned with the orbital frame, and such that the solar panels face and are normal to the sunline. Position of the sun-shade is station-kept at distance -r_ss meters (TBD) from the center of the PMM along the minus x_O direction of the orbital frame.

4.9.2.3 FFT Guidance & Control Architecture

The brief discussions in this subsection are related to the Architecture Block Diagram shown in Figure 4.9-3. The full integration of 6 dof measurement and control as a closed-loop system is basic to the FFT working as a virtual monolithic optical structure. Structural stiffness and dimensional stability is replaced by the virtual truss and closed-loop control precision. Global (Commander) and Local (each element) Guidance and Control Solutions will be rapidly generated onboard using continuously running factorized Kalman-type filters, enabling real-time knowledge to be determined from propagated element states.

Stationkeeping Control

For the baseline orbit the main dynamic disturbance will be solar radiation producing a “drag” force of magnitude ~ 6 to7 E-6 N/m^2. This disturbance will be essentially uniform, with slight stochastic variations due to solar fluctuations amounting to a few percent of the nominal values. The control system on each illuminated vehicle must cancel these disturbances in order to maintain precise stationkeeping. An important consideration is the noise introduced by the thruster system. This will represents the largest dynamic disturbance, and careful design will be required to ensure that this thrust noise is not excessive.

Attitude Control

Each Optical Element Spacecraft or “Opticraft’s” structure, power, communication, etc., subsystems will be ‘built around the particular optical payload’ using future commercially available components. The

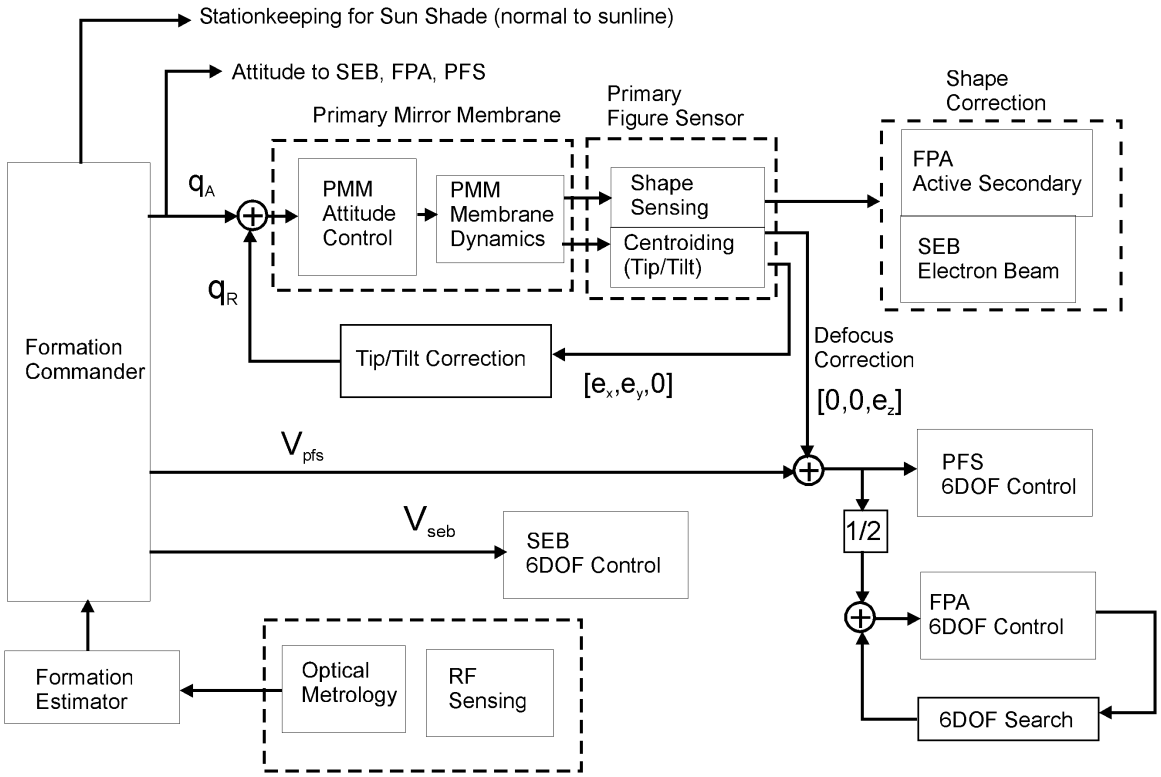

Figure 4.9-3

attitude control system on each comprises sun sensors, star sensors, microgyros and micro-thruster system. Pointing requirements are driven by the need to maintain and maneuver a stellar-pointing orientation of the Line-of-sight (LOS). The pointing stability is tightly controlled by a very high bandwidth focal plane image stabilization system.

4.9.2.4 FFT Control Command Sequence and Logic (Preliminary)

Note: all vectors for this discussion are assumed to be resolved in F_T frame

Coarse Alignment

0) Specify desired attitude F_T of the formation flying telescope.

1) Command F_M to coincide with F_T. This involves full 3-axis attitude control of the PMM using thrusters. Note that this requires that roll about the z_M axis is also controlled, but it will have a less stringent requirement.

2) Command FPA,PFS and SEB to locations specified by nominal vectors V_fpa0=[0,0,250m], V_pfs0=[0,0,500m], V_seb0=[0,0,-50m] (TBD) in the F_T frame (this involves translation control of FPA,PFS and SEB).

3) Command attitudes of FPA,PFS,SEB to coincide with that of F_T (this involves attitude control of FPA,PFS and SEB).

Note: Telescope is now mechanically aligned with respect to fiducials on the primary. Now need to utilize more precise shape sensing information from the PFS to improve optical quality.

4) Take measurements from PFS to determine center of PMM curvature V_center, in the form of a vector offset E=[e_x,e_y,e_z] from the present PFS location, i.e., V_center=V_pfs+E.

5) Command PMM alignment matrix R to null off-axis components (e_x,e_y) of E (this involves attitude control of the PMM using FEEPs)

6) Command PFS to new location V_pfs=V_pfs0+[0,0,e_z] along z axis of F_T to null out on-axis component e_z of E (this involves translation control of the PFS).

7) Take measurements from PFS to determine high-order (beyond focal length and tip/tilt) shape of primary

8) Command SEB to remove high-order abberations of primary to the degree possible within the dynamic range of the electron beam correction.

Note: The control system is architectured so that the focal length (zero’th order) correction is made in step (6) by translating the PFS, while the tip/tilt (first order) correction is made in step (5) by rotating the primary using FEEPs. With this approach the SEB only has to nominally correct for second and higher-order abberations, which is desirable given its limited authority.

After steps 1-8, one has a working telescope. The next steps are to align the FPA secondary and acquire the focus.

9) The FPA is commanded to the position V_fpa=V_pfs/2 (this is TBD, and will be based on an optical model for more precise positioning) which is the best nominal position estimate of where the telescope focal point is, given FPA figure measurements.

10) Command attitude of FPA to align with telescope frame F_T.

11) Search locally using translation control of FPA to place focal point into entrance aperture of FPA. Search in rotation to keep optical axis of secondary in focal point direction.

As a result of Steps 9-11, the focus is acquired and the secondary is aligned. The telescope system is now ready to be Fine Tuned, including correction of higher order wavefront abberations using an adaptive optics secondary.

4.9.2.5 Fine Tuning the Telescope Optics

1) Further tip/tilt error reduction can be done by several mechanisms: FEEPS on the primary (i.e., attitude control), electron beam from SEB, an active secondary on FPA. Or optionally, tip-tilt errors can be treated as LOS errors, and corrected by pointing control as below.

2) Further defocus errors can be taken out by: electron gun, or on-axis translation of FPA

3) Pointing control of the LOS can be accomplished by translating the secondary, or use of a steering mirror at the secondary.

4) Higher-order abberations are taken out using the adaptive optics secondary on the FPA. This is supported by Fine Stationkeeping Control to maintain the limited dynamic range of the Adaptive Optics.

4.9.3 Formation Flying Technologies for Future Exploitation

In this section the identification of and expectations for specific future relevant technologies are provided. The time horizon is within 10 years and forecasts are grounded in the reality of precursors at levels of technology readiness that range from working laboratory models to planned extensions of current SOA capabilities by existing development programs.

4.9.3.1 Field Emission Electrostatic Propulsion (FEEP)

In order to perform the solar radiation drag cancellation, target pointing, and station-keeping to the required precision, the spacecraft thruster system must be proportionally-controllable in the micro-newton regime, and have extremely low quantization and noise.

One of the most promising technology which meets these demanding requirements are ion thrusters known as FEEPs which have been under

development in Europe for many years. As with all ion propulsion systems, the FEEP thrusters operate by accelerating ions in an electric field and ejecting them at high velocity, thereby developing a thrust with very high specific impulse. With the FEEP system, the ions are generated by exposing a free-surface of liquid metal to an electric field. A neutraliser is used to emits electrons into the outgoing ion beam in order to prevent the ions from reacting with spacecraft surfaces, and to prevent spacecraft charging.

There are two types of FEEP systems currently under development. One uses a needle-like emitter geometry with Indium as a propellant, and the other uses a blade-like geometry with Cesium as a propellant. Each technical approach has its advantages and disadvantages, and it is not yet clear which system is optimal.

. For example, Indium has a higher melting point than Cesium but does not require special handling equipment on the ground to avoid contamination (from water, oxygen, etc).

. Cesium, on the other hand, is highly reactive and must be handled with extreme care to avoid contamination. A combination of the two systems, namely blade-type emitters with indium as the propellant, may have advantages.

4.9.3.2 Colloid Electrostatic Propulsion

Another viable proportional microthruster technology candidate, albeit not as mature, is Colloid Electrostatic Propulsion whose basic proof of concept has been laboratory demonstrated but not yet flown. Colloids (glycerol, formamide) may be generally preferred to FEEP liquid metals because of less contamination concerns and the capability to operate at lower voltages.

. Specific impulse is variable with acceleration voltage, with a minimum thrust of < 0.1 micro-N at a voltage of <3 kv and Isp of ~ 500 seconds. Thruster dynamic range up to 20 micro-N may be achievable.

. Such ultra-fine force resolution may have advantages for control of the Sun-shaded Primary Mirror. Trades will be important to investigate in future studies. Development of Colloid thrusters for spacecraft is ongoing at several universities and industry research laboratories.

4.9.3.3 Thruster Sizing and Placement

In further discussions, we will assume the FEEP thrusters are the primary attitude control actuators for telescope pointing, retargeting, and stationkeeping. In order to provide six degrees-of-freedom translation and attitude control, with some redundancy per degree-of-freedom, it is desired to employ 16 thrusters (in clusters of four), distributed around a formation element, with the Sun Shield

having 50 or more units.
. Each of the 16 thruster units will have its own dedicated high voltage generator and heater supply. One neutralizer will be placed on each cluster of four ion emitters. Communication with the space-craft will be handled through a serial RS422 interface.
. Current technology power, *mass, and volume metrics for each FEEP unit are ~ 0.2 W/micro-N ; ~ 0.3 kg/ thruster plus 1 kg electronics; and 250 cc, respectively.
. It is expected there will be a reduction by a factor of 100 in electronics volume by SOAC* technology within 5 years. Mass per unit should then be ~ 0.4 kg including electronics. It is assumed that the power-force relation also may be improved. Specific Impulse (Isp) today is ~ 500 sec. It is assumed that Isp will increase to 1000 sec within 10 years.

4.9.3.4 Thruster Noise

The further development of FEEPs including trade-off studies and ground-based laboratory tests are ongoing, and there is a flight demonstration planned in order to verify the FEEP performance and noise characteristics when used for precision attitude control. Any liquid metal ion source will emit a finite number of macro particles or droplets at some threshold emission current.
. The current at which this occurs is a function of the liquid surface tension and emitter geometry. Charged droplets are a source of thrust “noise” (as well as mass utilization inefficiency) which must be characterized. In particular, understanding the magnitude and repeatability of this noise is important.
. The desired thrust should be smoothly controllable over a range of 1 - 100 micro-N with a minimum control resolution and noise of +/- 0.1 micro-N.

4.9.3.5 Thruster Lifetime and Contamination

The complete thruster system (emitter, accelerator, neutraliser, and power processor) should provide operation within specifications for a 10 year goal. There are some concerns about the lifetime of the thrusters. For example, both Indium and Cesium have small but finite vapor pressure at the temperatures likely to be encountered at the emitter surfaces. Over a 10 year mission life, this raises the possibility of vapor condensation occurring on insulator surfaces creating electrical shorts. Another important consideration with the FEEP system is the possibility of contamination of optical surfaces due to deposited particulates and films. All these issues should be resolved during the ESA FEEP development program.

4.9.3.6 Future Autonomous Formation Flying Metrology

The Autonomous Formation Flying (AFF) Metrology for the Formation Flying Telescope (FFT) consists of a GPS derived Acquisition and Initialization RF (Ka band) metrology system for Coarse (mm) stationkeeping precision, and a Heterodyne Laser Interferometer (HLI) metrology system for Fine (nanometer) stationkeeping precision.
The basic functions of the Autonomous Formation Flying System are:
. Initial formation acquisition of the separated FFT elements using absolute 3-D position sensing by the Autonomous Formation Flying RF receiver/transmitter on each element.
. The RF and Laser Interferometer metrology subsystems both provide relative range, range rate, and azimuth/elevation bearings between spacecraft over the full range of spacecraft separations up to a kilometer for coordinated formation maneuver control during science observations and retargeting.
. Enables six degree-of freedom relative attitude and translation control of each spacecraft using bi-directional arrays of micro-thrusters
. The AFF RF system also handles spacecraft-to-spacecraft communications after launch vehicle deployment.
. Off-axis metrology platforms (one or two) may be needed to provide adequate observability sensitivity transverse to the linear formation axis. Numbers of metrology sets per element will be optimized from future geometric/sensitivity trade studies.

4.9.3.7 Future RF (GPS Derived) Metrology

The innovative new approach for the AFF RF Sensor is modification of the commercially available TurboRogue space receiver so that its internally generated GPS models are used for a 1-way beacon transmission as well as for processing of the received data. Instead of tracking GPS satellites, the TurboRogue space receivers track one another from within a spacecraft formation. Each spacecraft would carry one or more such transceivers for dual one-way tracking. It will use a Ka-band frequency (instead of the usual GPS L-band) to enable more precise tracking.

In order for the separated spacecraft to autonomously self-acquire and maneuver to final formation geometry from arbitrary initial orientations, each spacecraft would have a total of 6 corner-located receive patch antennas and two transmit patch antennas mounted on opposing corners, as illustrated in Figure 4.9-4. This would provide full sky coverage in all directions (4π steradian), assuming hemispherical fields of view for each antenna. Such antennas can be made quite small; for example, GPS “omni” patch antennas flown successfully in space have mass on the order of 100 grams.

The AFF would also enable determination of relative attitudes of the spacecraft in the formation by tracking the relative carrier phase received in each of three antennas mounted on a face of the spacecraft. The relative positions of each spacecraft in the ensemble can be precisely determined from the spacecraft-to-spacecraft phase and range data. Because the transmission and reception of the dual one-way range and phase observables are nearly simultaneous, there will not be a stringent requirement for a stable clock.

Changes in relative positions and orientations of the multiple spacecraft would be sensed automatically by the onboard control systems that initiate corrective maneuvers to maintain the formation geometry.

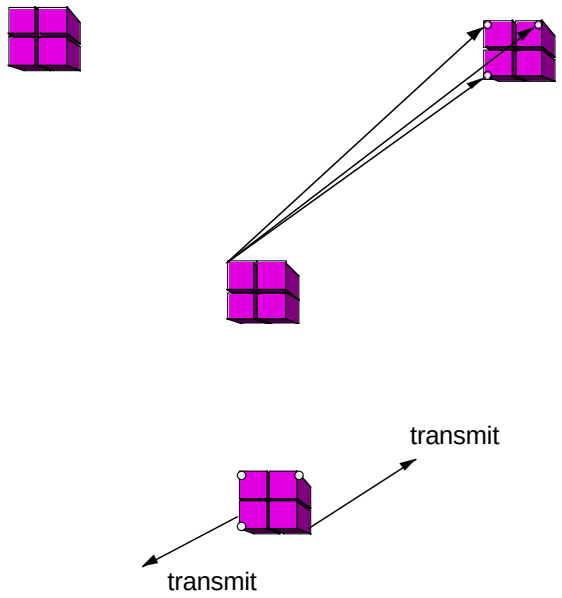

Figure 4.9-4

4.9.3.8 Future Optical Metrology

The concept for the FFT Optical Metrology is based on Heterodyne Interferometery as shown in Figure 4.9-5. Estimates of the in space capability for relative measurements between separated spacecraft as in the New Millenium DS3 mission and the monolithic SIM (Space Interferometry Mission) are shown in the diagram. Methods for self-interference suppression are under development for both missions.

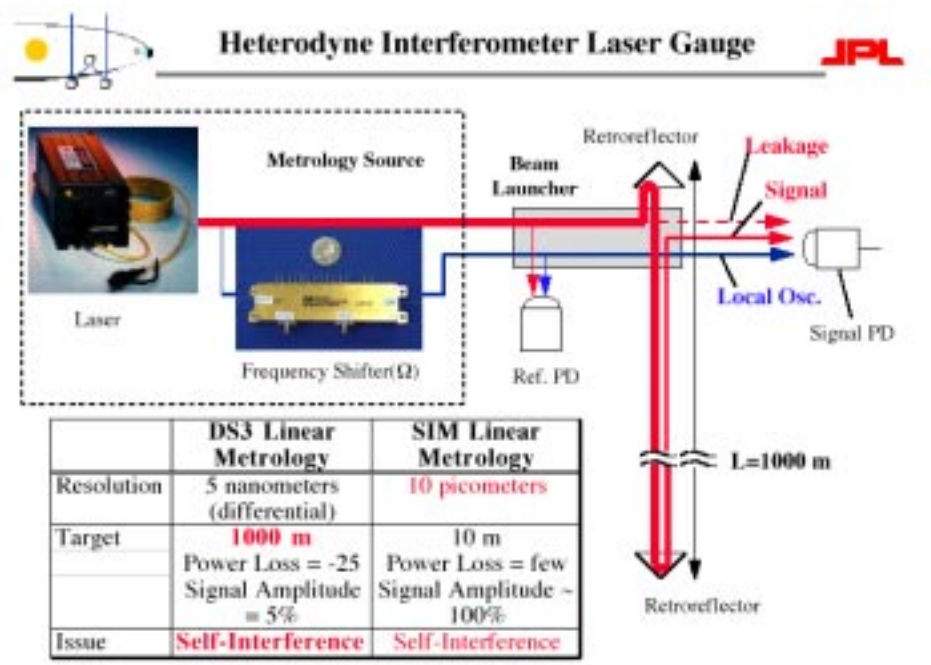

Figure 4.9-5

Pointing requirements

Using analytical expressions describing Gaussian beam propagation, we can estimate the pointing requirements.

A Gaussian beam is emitted from point A and it's phase is detected at point B. See Figure 4.9-6.

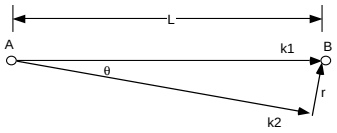

Figure 4.9-6

We need to know the difference in detected phases for the two cases: 1) propagation along k1 and 2) propagation along k2.

The phase difference calculated in units of length, is given as

$$\Delta L = \frac{1}{2} L\theta^2 \left(\frac{z_o^2 / L^2}{1 + z_o^2 / L^2} \right)$$

The first part of the equation, $\frac{1}{2}L\theta^2$, is what we would have for a plane wave and factor $\left(\frac{z_o^2/L^2}{1+z_o^2/L^2}\right)$ is the correction due to a finite radius of curvature of the Gaussian beam.

$z_o = \frac{\pi w_o^2}{\lambda}$ — Rayleigh range, a.k.a. "confocal beam parameter".

w_o =w(z=0) — Gaussian beam waist radius. Above equation assumes that waist occurs at z=0

The Phase Difference equation can be inverted to give pointing, q, needed to keep the pointing-induced phase error, DL, below a specified level.

$$\theta = \sqrt{\frac{2\Delta L}{L}}\frac{L}{z_o}\sqrt{1+\frac{z_o^2}{L^2}}$$

For example, If we want to keep the pointing error below 5 nm for the case of w_o =0.67 cm (A=2cm) and L=1km, i.e. zo=106 m << L, we get

$$\theta \cong \sqrt{\frac{2\Delta L}{L}}\frac{L}{z_o} = \sqrt{\frac{2*5\text{nm}}{1\text{km}}}*\frac{1000}{106} = 30 \text{ urad} = 6.15 \text{ asec}$$

For the L=100 m we get

$$\theta = \sqrt{\frac{2\Delta L}{L}}\frac{L}{z_o}\sqrt{1+\frac{z_o^2}{L^2}} = \sqrt{\frac{2*5\text{nm}}{100\text{m}}}*\frac{100}{106}\sqrt{1+\frac{106^2}{100^2}} = 13.7 \text{ urad} = 2.8 \text{ asec}$$

The above two cases allow us to estimate the FFT optical metrology pointing requirements are in the range of 3 to 5 arcsec for the Heterodyne Interferometry technology between the separated adjacent elements of the telescope. This is compatible with SOA Star Trackers that we plan for each element's attitude determination and pointing control with repect to common star references for both absolute and relative orientation.

4.9.3.9 Future Avionic Sensors

Avionics designs enhanced by cheap negligable mass for internal redundancy on wafer scale integration for all electronics and microsensors. Very high density VLSI micro-electronics packaging

with MCM 3-D methods. Sensors will be constructed of integrated micro-machined silicon technology and on-chip support electronics including self-test and communications interface.

. IMU (inertial measurement unit) built of a SOAC array of gyro and accelerometer chips. Silicon surface-micromachined rate gyros based on the interaction between a coriolis field and a vibrating beam element and using an interferometric or capacitive readout. The commercial precursors for this concept are in place today, with silicon micromachined accelerometer sensing elements fully integrated on-chip with all their support electronics.

Currently, devices like this have low accuracy and sensitivity. However, a microgyro capable of measuring the vibrations of its rate sensing element with the same resolution routinely achieved by scanning tunneling microscopes in measuring the vibrations of their sensing tips (0.01-0.0001 Å/square-root-Hz) could resolve angular displacements on the order of 0.01-1.0 microradian at 1 Hz update. Such Inertial Grade micro-IMU's are feasible within 10 years at the current rate of development.

. Star Trackers and Sun Sensors will use advanced Active Pixel Detectors (APD) integrated with VLSI ASICS and micro-deformable optics to enable "in-flight tuning" of optomechanical precision and the PSF (point spread function). Addressed in much the same way as CIDs, without the penalty of increased read noise, APD's include amplifier elements within each pixel. Combined with lenslet arrays, the APD has high sensitivity, low read noise, high immunity to radiation and the low power of standard CMOS technology. New developments also include lightweight monometallic silicon-carbide reflective optics and optomechanical structures.

4.9.3.10 Future Autonomous Control Developments

. Virtual-Truss Dynamic Stability: AFF Close-loop formation maneuvering and disturbances dynamic modeling; global optical-truss mode shapes and deformation sensitivity analyses; optically-linked multibody simulations and scaled testbed demonstrations.

. Formation Guidance and Control Laws: Synthesis of 3-D guidance and control laws and algorithms for the virtual optical-truss and each of the five to six nodes that will satisfy the optical-truss (formation) linearity and planarity "stiffness" criteria developed in the above modeling/analysis task, and their testbed demonstration.

. Remote Agent Autonomous Formation Control: Guidance and control algorithms for autonomous formation acquisition of five to sixseparated

spacecraft, using the RF and Optical AFF sensors and a Formation Executive Navigator/Commander function with two-way local RF Communication links. This includes Attitude/Translation multi-Sensor Fusion and 6-dof State Estimation technology in testbed demonstrations.

. Fault Protection Methods and Algorithms: Spacecraft collision avoidance fail-safe methods and control algorithms in tight formation flying. FFT will not inherit FFT-unique collision avoidance techniques from DS–3

. DS–3 Planned Mission: Autonomous Formation Flying Proof-Of-Concept space demonstration.

4.9.3.11 Future Hardware Technologies/References

Near Term AdvancedTechnology from other JPL/NASA/ESA programs is identified below as the basis for forecasting FFT feasibility confidence:

. Advanced miniaturized CCD and APD Star Trackers with Ørsted and X2000 Advanced Deep Space Systems Developments (ADSSD) flight heritage
. Autonomous Formation Flying (AFF) Sensor RF System: Transcievers and Antenna for >25 m to 1 Km S/C separations: NMP DS-3, JPL derivative from Turbostar GPS
. Heterodyne Laser Interferometer Gauge from NMP DS3 development
. Laser Radar Integrated Macro-chip AFF: Liquid Crystal Optical Phased-Array Scanner with Passive Q-Switched Diode Pumped Nd:Yag Laser absolute AFF reference: NMP DS-4 (under development by Raytheon E-O Systems)
. Advanced MEMS-based IMU (3-micro-Gyros and 3-micro-Accelerometers derived from X2000/ADSSD and X-33 technology flight experiments
. Helenoid Voice Coil Actuators and Magnetostrictive Actuators for Fast-Steering Mirrors from SIM
. Advanced Low Voltage, Piezoelectric Ceramic Actuators for Optics and Active Vibration Control, using Lead Manganese Niobate (PMN) and Polyvinylidene Flouride (PVDF) in stack and bimorph configurations from BMDO/SDIO research.
. FEEP (Field Emission Electrostatic Propulsion) micro-N thrusters from ESA/ESTEC
. Colloidal Electric Propulsion micro-N thrusters from ongoing research at Yale and MIT
. X2000 Rad-hard, space qualified MCM electronics
. Star Tracker Image Processing and I/O
. Sun Sensor Support Electronics and I/O
. IMU Support Electronics and I/O
. Propulsion Drive Electronics
. Systems On a Chip (SOAC) Research, JPL Center for Space Microelec-

tronics Technology
- Chip size < 100 cc, mass 100 grams
- Ultra Low-Power High-thruput Data/Computing
- Ultra Low-Power integrated power control and magnetics
- RF CMOS digital transciever

3.9.4 Future Error Analysis Items

Attitude Knowledge:
- Alignment of star tracker wrt ReferenceFrame
- Star catalog and aberration correction
- Star tracker systematic bias
- Star tracker random noise
- Gyro (if available, type dependent) noises
- Control actions
- External disturbances
- Attitude Estimator state of convergence

Attitude Control:
- Attitude knowledge errors
- Attitude command dynamics
- Controller bandwidth & type
- Thruster errors, alignment,location,magnitude,etc
- Thruster resolution (eg minimum command)
- Structural flexibility
- External disturbances
- Stationkeeping cross-coupling

Stationkeeping Knowledge:
- Location/alignment of components wrt ReferenceFrames
- Systematic biases
- Measurement noises
- RF/Optical truss geometry
- Relative attitude knowledge errors
- Calibration maneuvers
- Estimator state of convergence
- Multiple-stage estimator

Stationkeeping Control:
- Stationkeeping knowledge errors
- Station command dynamics
- Controller bandwidth & type
- Thruster errors, alignment,location,magnitude,etc
- Thruster resolution (eg minimum command)
- Structural flexibility
- External disturbances
- AttitudeControl cross-coupling

3.9.5 Formation flying conclusions

This section has developed the methodologies and identified the instrumentations with the necessary performance potential to realize precision formation flying the major optical elements of a Very Large Space Telescope by the end of the next decade. The FFT preliminary requirements on the resolution and dynamic range performance of the Field Emission Electrostatic microthrusters, and the identified RF and Optical metrologies are within reach today, and do not present a fundamental barrier. These and other key technologies in optical-truss spatial stability and observability for control, autonomous guidance and control laws, miniaturization of avionics sensors, and Systems-on-a-Chip microelectronics are being advanced by existing research and development programs in the U.S. and Europe. Further more detailed concept definition design, requirements analysis, system modeling, control synthesis and simulations, error analyses, and characterization of identified technologies is needed to enhance our insight and more fully confirm the positive expectations reached from this first order study effort.

4.10 Information/communications

There will be a centralized information processing system that will perform a number of functions, including:

- Image fine tracking
- Formation flying control of all the elements
- Primary membrane shaping and control
- Liquid crystal secondary correction control
- Positioning and attitude of the entire telescope ensemble for coarse pointing of the telescope
- Positioning of the fast scanning mirrors for field of view control
- Control of the sunshade for primary membrane shielding
- Image processing
- Image formatting and data transmission to the ground
- Reception and translation of ground commands from a sequence of telescope functions to a sequence of synchronized element commands

One of the design reference missions involves many separated telescopes, combining their light in phase on one focal plane. In addition, the desire to detect and image earth-sized planets around other stars requires a large number of very widely separated telescopes, operating as a Michaelson interferometer.

The latter case is not analyzed, as it is receiving plenty of attention at JPL. The former case will be analyzed, however, as part of Phase II. For that case the above information processing functions will be reexamined to identify the necessary sequence of actions for the telescope ensemble to function as one coherent whole, and to understand whether there are any driving technology requirements. For this, each individual telescope will go through the alignment steps described in section 5, and then the entire ensemble of telescopes will be slaved to one, thus creating an ensemble of ensembles, all operating as a whole unit as tough connected by a solid stiff truss.

In addition to the information functions that permit formation flying and ensemble operations, there will be needs for specialized image processing functions within each telescope and for coherent image combination from the multiple sources. These functions could include focal array tracking of reference objects, focal plane image processing, alias deconvolution for image formation, processing for correlated interference rejection, pairwise interferometric measurements for the case of multiple widely separated interferometers, or all the above.

This is a complex subject, and way beyond the means of Phase I. However, based on the achievements of optical processors flying today, and on the rapid advancement of processing power (at the rate of Moore’s law), it is clear that this information processing area will not be the “tall pole in the tent” of telescope feasibility.

5. ENSEMBLE OPERATIONS

The entire ensemble of elements will be held together with a “virtual truss” created by the formation flying metrology sensor suite, acting through the thrusters on each element. It is envisioned that once all elements are oriented to a desired direction, the primary membrane will go into a quasi-drift mode, with the other elements doing the active stationkeeping.

Thus during a measurement period, all other elements will in essence be slaved to the primary. During this measurement interval, should the telescope pointing direction change due to drift in the primary axis, it will be measured and maintained by moving the fast steering mirrors as the entire assembly drifts. The steering range of the fast steering mirrors is determined principally by the diameter of the first mirror, with a 43 cm mirror allowing steering within plus or minus 1 degree.

A high level sequence of operations is shown in Figure 5-1. The details are more complicated, of course, and are described to a degree in the formation flying metrology of section 4.9. This entire area requires much more analysis, and will be penetrated more deeply in Phase II. Suffice it to say that a reasonable sequence of operations exists that will allow the various elements of the telescope to act as one, to be moved as an ensemble as though connected by a very still yet weightless truss, and perform the functions of a large yet low weight high quality space telescope.

SETTING UP AND POINTING THE TELESCOPE

- **Rotate the primary slowly (minutes) to within a few degrees of the desired pointing angle**
- **Wait for a period for disturbances to damp out (minutes)**
- **Translate and rotate the E-beam, figure sensor, and focal assemblies to lie on new axis**
- **Translate and rotate the steering and scanning flat mirrors for desired off-axis pointing**
- **Adjust primary shape and correct fine scale errors using E-beam**
- **Correct residual errors using liquid crystal light valve**
- **Start fine scale stationkeeping with all elements slaved to the membrane**
- **Initiate image tracking with the focal plane array**
- **Begin measurements. Track target with fast steering mirrors**
- **Rotate the scanning flat and rotate and translate the steering flat to repoint the telescope**
- **For large reorientation, move the entire ensemble. Repeat this sequence**

Figure 5-1

These are the benefits of “replacing structural webs with information webs”.

6. FEASIBILITY ASSESSMENT

The feasibility of each subsystem/element of the telescope has been assessed and commented on in the individual chapters of section 4. All the subsystems and elements are considered to be feasible, while requiring a lot of work. Nonetheless, some subsystems and technologies are more difficult than others, and this chapter will thus assess all of them in context.

From an overall point of view, the adaptive membrane stationkept elements telescope is certainly felt to be feasible.

The highest risk due to technological uncertainty is the ability to attain an optical quality smoothness on the front side of the very thin adaptive membrane. This is thought by the experts that were consulted to be basically a manufacturing problem, not a fundamental one, and one that could be overcome by both concerted attention and some experimentation.

While setting up a different manufacturing process from one commercially used is doable, it is not inexpensive considering that its total production capacity would be only a few hundred square meters of film. Nonetheless, the overall cost of the new telescope is bound to orders of magnitude less expensive than NGST, and thus the cost to set up a manufacturing capability for what in industry would be only experimental quantities will be extremely inexpensive compared to costs usually associated with space hardware.

The entire concept of this telescope hinges on the membrane surface and its ability to withstand folding and launching, and deployment, and the ability of the formation flying metrology and control/propulsion system to align and stationkeep all the elements to very tight tolerances. The attainment of tolerances in the order of 0.1 millimeters sounds at first blush like a horrific thing to try to attain.

In actuality, however, both the metrology and the algorithms for precision formation flying are under intense attention at JPL for the Separated Spacecraft Interferometry Mission as well as for the more ambitious Terrestrial planet finder and Terrestrial Planet Imager programs. All these programs are funded and underway. The techniques and technology being developed under these programs is exactly the same in principle as needed for this telescope, but less demanding in precision of stationkeeping.

This is not a concern for feasibility assessment, for there is a truism in control systems, which is that if it can be measured, it can be controlled to an accuracy not worse than a few times the measured numbers. Since we need to control the elements being stationkept to about 0.1 mm (100 microns) in location accuracy, we must measure their location to in the order of 30 microns. This is easy, and state of the art with a combination of GPS-like RF rangefinding and laser heterodyne rangefinding, which will at 3-4 orders of magnitude greater measurement accuracy within a couple of years.

Therefore what to people being exposed to the concept for the first time sounds like an extremely difficult undertaking will, in reality, be the straightforward extension of well funded work underway. It will actually not be a very risk development or achievement at all. Difficult? Yes. Feasibility risk? No.

The next riskiest element is the liquid crystal second stage corrector. There is no question that a liquid crystal can be made to work for the telescope application, because it is already working in the laboratory at AFRL. It is clearly feasible. The only element of risk has to do with whether its large correction range can be achieved. This desired range is 1-2 orders of magnitude greater than that being used by AFRL.

The key to attaining this large correction range is to use liquid crystals in a different mode than by AFRL, in which they have inherently small correction range. If the liquid crystal is operated in the laser actuated thermal gradient mode, we have already demonstrated in the laboratory at BEAM engineering over one order of magnitude increase in performance with a crude setup. The theory and some reported papers indicate that another order of magnitude should be readily attainable, without sacrifice in response time or scattering.

The key is to use the right modes, not to plunge blindly ahead trying to squeeze out a marginal improvement in performance in a dead ended mode. Thus it is felt, based on laboratory tests we performed, that the range of correction in a liquid crystal is attainable and that this subsystem is clearly feasible.

The figure sensor is also feasible, as precisely the type of sensor needed is now operating on the bench at the AFRL. This heterodyne sensor is so ideally suited for the mission that it had not already been invented we would have had to invent it for this application.

The sunshade/power projector is also clearly feasible. The only new elements are the FEEP propulsion units, which will be addressed below, and the microwave or millimeter wave power transmission system to send power to the membrane and the electron beam elements.

Microwave power transmission is nothing new. JPL and Raytheon demonstrated transmission of 10 kilowatts of power over one mile in the 1970s as part of the Solar Power Satellite investigations. Thus the transmission of a few watts over distances of a few tens of meters is hardly a daunting task.

The only risk is that the power needs of the using elements will grow, as they probably will. However even if they increase by an order of magnitude the technology for the power transmission is on the shelf today. And it is still hundreds of times less than what has already been done.

The system depends on MEMS scale integrated packages for propulsion as well for command reception, microwave transmission, and for communications as well. The state of the art in all-silicon MEMS fabrication of integrated packages is moving rapidly toward demonstration in a number of areas. There is little question that the packages desired will be routinely obtainable in 10 years time.

The most dramatic and vital such element is an all silicon MEMS fabricated FEEP. Designs and programs are underway at several laboratories in the USA, notably at Aerospace Corporation, that aim to a fabricate such packages in the next 1-2 years as part of its program to develop all-silicon nanosatellites.

There is little question that such packages are feasible, and that they can be constructed I the near term. Experimental FEEP thrusters, tough not MEMS, have been tested for 640 hours on Space Shuttle flights. They are being pursued by ESA as well as by Italy, and are being considered in the US as well. So while a lot of work needs to be done in development and testing of such MEMS thrusters, their feasibility is not in question at all, only how long it will take before they are routinely available on special order.

However, on the timetable that is being pursued for them, they will probably not ne a pacing item for this telescope if a dedicated program is started.

The information processing/command/control subsystem will certainly be feasible by the time the other technologies are sufficiently demonstrated. The only difficult item there will be the processor for the 100 million detectors which will be asked to perform multiple function including image stabilization and fine tracking, image integration, de-aliasing, and other image processing functions. In addition the information processing system will be the heart of the formation flying system, processing metrology information and issuing commands to the FEEPs for controlling the various elements.

This size of focal array is state of the art today, and image processors exist that do similarly daunting image plane processing. Formation flying using similar algorithms will be demonstrated in space in a few years by NASA/JPL, and should be well understood by the time it needs to be applied to this telescope.

Thus this subsystem is also feasible and does not represent undue development risk. Furthermore, since Moore's Law is alive and well, there is no questions that the computing power needed will be there when needed. Given the current pace of computing power, this is zero risk statement.

An additional factor must be discussed, which is that in all the technologies and subsystems discussed above, the impact of not being able to reach most of them is not catastrophic. This is because there is so much give in the self-imposed requirements for the telescope. As an example consider the riskiest element, the membrane. There is little question that bimorphs membranes can work, As the principle has already been demonstrated in the lab. The only question is whether they can have sufficiently smooth surfaces after all is said and done.

The fallback approach is to make the membrane thicker, which will make its surface accuracy more easily attainable. The penalty is mostly in the weight of the telescope. But even if the membrane weigh goes up by an order of magnitude, the 25 m telescope weight will only go up from 125 Kg to a few hundred Kg. Considering that Hubble weighs 12000 Kg and NGST will weigh 1250 Kg, this can hardly be a cause for concern.

Thus in summary the telescope is felt to be unquestionably feasible. That does not mean that we understand all the values of all the parameters. Much work will be needed to be done, for which the Phase II technology investigations will be but an opening gun. However no showstoppers have been found in this Phase I assessment.

7. TECHNOLOGIES REQUIRING DEVELOPMENT/DEMONSTRATION

The foregoing chapters have demonstrated that the development of the telescope concept is feasible. Its development will result in a totally revolutionary capability, resulting inn a 25 meter telescope weighing less than 150 Kg (0.2 Kg/square meter), or a 100 meter telescope weighing under 800 Kg. (0.1 Kg. sq.m.)

The acquisition of such a telescope would dwarf the projected advancement of the NGST over the Hubble Space telescope, at a tiny fraction of its expected cost. In addition this concept would for the first time show a clear concept for implementing both the individual telescopes and the large intefrefometric arrays that NASA has said are necessary to image earth-sized planets around other stars, one of its declared future objectives of the Origins Program.

This report does not in any way suggest that the NGST should not be built, as the concept proposed here will require technology development and demonstration beyond that required for NGST, and thus is probably only a candidate for a later time frame.

The technologies that must be developed and demonstrated have been discussed throughout the above chapters. The most critical are collected here so that a coherent picture emerges of the task ahead. These are the technologies that will be separately proposed for investigation in a Phase II activity.

7.1 Membrane technologies

- Very thin piezoelectric bimorph film manufacture with fine grain non-symmetric surface irregularities
- Nitinol or other shape memory alloy film manufacture with fine grain non-symmetric surface irregularities, and its bonding to the piezoelectric film
- Coating the bonded membrane with a highly reflective coating with optically smooth quality
- Folding the membrane for launch in such a manner as to avoid excessive creases or other surface artifacts which could cause optical performance degradation
- Determination of the static and dynamic properties of large thin membranes in space, provided with “artificial stiffening: via piezoelectric action
- Other technologies as described in the Proprietary Annex.
- Performing an integrated laboratory experiment to demonstrate a number of the technologies operating together.

7.2 Liquid crystal technologies

- Development and demonstration of laser addressed/thermal gradient effect liquid crystals
- Development and demonstration of thick multipass/multilayer liquid cystals with reduced optical anisotropy
- Techniques for their use in spatial or pixellated light modulators in 10 cm sizes.

7.3 Space based electron beam generator

- Development of a focusing and scanning technique capable of focusing an electron bean to a 2 mm spot 10-100 meters away, and sweeping it at 100 million discrete x-y coordinates.

7.4 Formation flying/stationkeeping

- Development of algorithms for coarse/fine acquisition and ensemble repointing without loss of lock

- Development of integrated RF/optical metrology system with 10 micrometer 3 arc second accruacies

7.5 MEMS FEEPs

- Development of FEEP integrated propulsion units in MEMS packages, with integral propellant. Desired characteristics as per **Figure 4.2-12.**

- Integration of power rectenna into some FEEPs

7.6 Software and system integration

Though strictly software and system integration are not technologies, the new telescope concept is a very complex system with many closed loops active in its operation. As many new concept nowadays, it will be totally dependent on software, not by accident or miscalculation but by intent. The attainment of successful integration and operation will require particular attention to rapid yet complex software development and verification.

7.7 Extension technologies

- Technologies and techniques necessary to enable operation of such telescopes in the long wavelength infrared spectrum, as that is where the distant objects of the universe tend to have peak radiance. This involves a host of questions, the biggest being the cooling of the optical membrane by passive or active means. These are mentioned, but are considered beyond the scope of a Phase II follow-on.

8. CONCLUSIONS/RECOMMENDATIONS

The preceding chapters have hopefully made a convincing case that this telescope concept is feasible, both in its subsystems and as a complete space system.

Nonetheless a substantial amount of technology must be developed and demonstrated before all questions are answered to the point that the concept is likely to be accepted by a program office and a funded Phase A industry design study can be undertaken.

The payoff in undertaking these technology investigations would be enormous. The concept promises to attain a 25 m. diameter space telescope weighing less than 150 Kg, and to launch it in a booster smaller than the Pegasus. If adopted as the baseline technique for implementing the Terrestrial Planet Finder of the Origins Program, the 100 telescopes needed would weigh 15,000 Kg and cost about $6 Billion. In contrast if telescopes of the NGST-design were used, they would weigh 1.25 million Kg and cost $450 billion.

In view of the proof of its feasibility and the extraordinary payoff of this revolutionary concept, it is recommended that the technology investigations proposed as Phase II of this investigation be approved and funded.

ACKNOWLEDGEMENTS

The contribution of the following people at JPL to the formation flying section is hereby gratefully acknowledged

Fred Hadaegh (Dept Director)
Edward Mettler, lead
David Bayard
William Breckenridge
Kenneth Lau
Mehran Mesbahi
Samuel Sirlin
Serge Dubovitsky
Eldred Tubbs

The contribution of the following people at The Aerospace Corporation is hereby gratefully acknowledged

Samuel McWaters
Kevin Bell, (overall)
Siegfried Janson (FEEPs)
Richard Boucher (optics)

The help and assistance of Glenn Zeiders of the Sirius Group to the architecture section is gratefully ackowledged.

APPENDICES

Liquid crystal references

1. P.G. de Gennes, *The physics of liquid crystals*, Clarendon Press, Oxford, 1974.
2. L.M. Blionov, V.G. Chigrinov, *Electrooptic effects in liquid crystal materials*, 1994 Springer- Verlag New York, Inc.
3. B. Bahadur (Editor), *Liquid crystals: Applications and Uses*, World Scientific, Singapore, Vol.1-3, 1990.
4. G.B. Love et al., *Adaptive wavefront shaping with liquid crystal*," Opt. & Phot. News 6 (10), 16, 1995.
5. U. Efron (ed), "*Spatial light modulator technology*." Materials, Devices, and Applications, Marcel Dekker, Inc. New York, 1995.
6. A.Yu. Val'kov, L.A. Zubkov, A.P. Kovshik, V.P.Romanov, *Selective scattering of polarized light by an oriented nematic liquid crystal*, Sov. Phys. JETP Lett. 40, 1064-1067, 1984.
7. L.Ts. Adzhemyan, A.N. Vasilyev, M.M. Perekalin, *Angular dependence of extraordinary beam scattering in nematic liquid crystals*, Opt. Spectrosc. 74 (6), 679-684, 1993.
8. B.Ya. Zel'dovich, N.V. Tabiryan, *Fluctuations of the director of a nematic liquid crystal in a cell of finite thickness.* - Sov. Phys. JETP 54(5), 922-926, 1981.
9. K.E. Asatryan, N.V. Tabiryan, *Fast giant nonlinearity of multilayer liquid-crystal cell.* - Sov. Phys. Tech. Phys. 33(8), 934-935, 1988.
10. I.K. Khoo, G.M. Finn, T.H. Liu, R.R. Michael, *Multiple nonlinear film for optical wave mixing*, Technical Digest, Conference on Lasers and Electro-Optics, 1987.
11. T.H. Liu, I.C. Khoo, *Probe beam amplification via degenerate optical wave mixing in a Kerr medium*, IEEE J. Quant. Electron. 23, 2020, 1987.
12. N.V. Tabiryan, B.Ya. Zel'dovich, A.V. Sukhov, *The orientational optical nonlinearity of liquid crystals*. Special Issue of Mol.Cryst. Liquid Cryst., Vol. 136, #1 1986. 140 pages.
13. I.C. Khoo, "*Liquid Crystals: Physical Properties and Nonlinear Optical Phenomena*," Wiley Interscience, NY, 1994.
14. I.C. Khoo, T.H. Liu, P.Y. Yan, *Nonlocal radial dependence of laser induced molecular reorientation in a nematic liquid crystal*, theory and experiment, J. Opt. Soc. Am. B 4, 115-141, 1987.
15. H. Hickmet, B.H. Zwerver, J. Lub, *Anisotropic networks wih tunable optical and mechanical properties*. Makromolecules 27, 6722-6727, 1994.

16. A. Jakli, D.R. Kim, L.C. Chien, A. Saupe, *Effect of a polymer network on the alignment and the rotational viscosity of a nematic liquid crystal*. J. Appl. Phys. 72 (7), 3161-3164, 1992.
17. I.C. Khoo, P.Y. Yan, G.M. Finn, T.H. Liu, R.R. Michael, "*Low-power (10.6-mm) laser-beam amplification by thermal-grating-mediated degenerate four-wave mixing in a nematic-crystal film,"* J. Opt. Soc. Am., B 5 (2), 202-206, 1988
18. S.R. Nersisyan, N.V. Tabiryan, "*Hysteresis of light induced Freedericks transition due to static electric field*," Mol. Cryst. Liquid Cryst. 116 (1-2), 111-114, 1984.
19. S.H. Chen, J.J. Wu, "*Observation of first-order Freedericksz transition in a nematic film induced by electric and optical fields*." Appl. Phys. Let., 52, (23),. 1998-2000, 1988.
20. I.C. Khoo, Liquid Crystal Non-Linear, "*Photorefractive Electro-Optical Storage Device Having a Liquid Crystal Film Including Dopant Species of C_{60} or C_{70} .*" US Patent 5,552,915 (1996).
21. D. Voloshschenko, A. Khyzhnyak, Yu. Reznikov, V. Reshetnyak, Jpn. J. Appl. Phys., 34, 566 (1995)